MWI-ICI Science Plan

A Report From The
MWI-ICI Science Advisory Group

MWI-ICI Science Advisory Group (SAG) Contributors

Dr. William Bell, Met Office
Prof. Stefan Bühler, University of Hamburg
Prof. Susanne Crewell, University of Köln
Prof. Patrick Eriksson, Chalmers University of Technology
Dr. Alan Geer, ECMWF
Dr. Jean-François Mahfouf, Météo-France
Prof. Frank Silvio Marzano, Dept. of Information Eng. “La Sapienza” University of Rome
Dr. Catherine Prigent, Paris Observatory
Dr. Rasmus Tonboe, Danish Meteorological Institute

Version: 3.2
Date: 27/10/2017
Edited for the MWI-ICI Science Advisory Group by EUMETSAT, Eumetsat-Allee 1,
64295 Darmstadt, Germany.

Table of Contents

1 Executive Summary

The Microwave Imager (MWI) and the Ice Cloud Imager (ICI) will be on board of the EPS–SG platforms. EPS-SG is the second generation of the EUMETSAT Polar System (EPS). The MWI instrument has 18 channels whose frequencies range from 18.7 GHz up to 183 GHz. All MWI channels up to 89 GHz measure radiance both in V and H polarisations. The MWI will not only provide continuity of measurements for some heritage microwave imager channels (e.g. SSM/I, AMSR-E) but will also include additional channels such as the 50-55 / 118 GHz bands for temperature sounding in support of precipitation measurements. The ICI will provide unprecedented measurements over the sub-millimetre spectral range contributing to an innovative characterisation of clouds over the whole globe. The ICI has 9 channels measuring radiance at 183 GHz, 325 GHz and 448 GHz with single V polarisation and two channels at 243 GHz and 664 GHz with both V and H polarisation. Fulfilment of the MWI and ICI mission objectives will require detailed knowledge of radiative processes in the microwave and sub-millimetre range, especially considering ICI.

The MWI-ICI Science Plan has been prepared by members of the MWI-ICI Science Advisory Group (SAG), a group established and co-chaired by EUMETSAT and the European Space Agency (ESA) with the aim to support the scientific preparation for the MWI and ICI missions. The Science plan aims to identify the main areas where scientific research and development activities are needed in order to successfully exploit MWI and ICI observations. Thus this document provides a review of the scientific knowledge in several areas related to microwave and sub-millimetre wave imaging, in order to identify where current and future studies may best be directed.

The MWI-ICI Science Plan is divided into five main sections. Section 2 is an introduction to the EPS-SG mission in general and the MWI and ICI missions in particular. Section 3 provides a summary of the main operational and scientific objectives of the MWI and ICI missions. Section 4 provides an overview of the MWI and ICI instruments, together with a description of heritage missions. The need for pre-launch characterization data is highlighted as very important for operational and scientific activities. Section 5 discusses in detail the scientific aspects that need further investigation (spectroscopy, particle scattering, surface properties, radiative transfer, and evaluation tools). Section 6 discusses the retrieval methodologies that can be applied to derive atmospheric and surface variables, and provides also considerations on synergetic use of MWI and ICI with other instruments. Finally the applications of MWI and ICI are discussed.

The main priorities in terms of research activities, identified in Section 5, are listed below. They provide an overview of issues that will require future effort in order to improve the exploitation of MWI and ICI.

1. Problem: In order to quantify current uncertainty, absorption models in particular will need a further development. The continuum water-vapour absorption and the absorption by supercooled liquid water with a focus on higher frequencies need to be considered.
   Approach: Radiative closure studies aiming at consistency across the spectrum employing airborne, ground-based and satellite data.

2. Problem: There is a largely unknown variety of mixed phase and frozen particle size, shape and orientation and associated scattering properties.

Approach: Simulation of realistic particles in line with the developments at NWP centres for ice microphysics schemes to be used for creating single-scattering data bases. Multi-frequency polarimetric active and passive microwave observations can be exploited. This needs to be done on the basis of field measurements including in situ probes and statistical assessment of existing satellite measurements.

3. Problem: Emission and reflection of land and sea ice surfaces needs to be better specified at millimetre and sub-millimetre waves, especially when water vapour content in the atmosphere is low. There is little knowledge on emissivity of frozen surfaces.

Approach: Traceable observations from aircraft are needed with focus on high frequencies over various surfaces, i.e. ocean, land, sea-ice. Development and extension of emissivity models to higher frequencies is necessary.

4. Problem: Accuracy of fast radiative transfer (RT) model for operational NWP and retrieval development needs to be assessed.

Approach: A reference model including the full Stokes vector polarisation information and 3D geometry for assessment can be used. The extension of RTTOV to sub-millimetre range shall be considered and tested.

5. Problem: There is little heritage in Europe with respect to the launch and operation of a microwave or sub-millimetre conical imager. Organisation and infrastructure to calibrate, validate and use data need to be in place at least 2 years before launch for thorough evaluation of instrument performance.

Approach: Establishing a sound Calibration/Validation (Cal/Val) plan is fundamental. The user community shall be involved in the Cal/Val activities.

6. Problem: The full potential of MWI and in particular ICI retrieval products, e.g., clouds, precipitation, surface, volcanic ash, has not been yet explored. The best retrieval technique for each application and the associated uncertainty has still to be established.

Approach: To develop and test retrieval schemes, e.g. variational, ensemble, neuronal networks, by simulation studies and implementation for aircraft observation and thoroughly tests them.

7. Problem: The potential for synergy both between MWI and ICI, with other EPS-SG instruments and other satellite missions needs to be explored. This depends on the different applications, e.g. retrieval of surface properties or precipitation.

Approach: Synthetic studies and/or field campaigns.

8. Problem: Despite long heritage, microwave data is not yet fully exploited in NWP, and there is no experience with ICI. However, the availability of ICI data will provide new opportunities for climate monitoring, nowcasting and reanalysis.

Approach: concerted effort for assimilating radiances in variational approaches and use in ensemble techniques (Ensemble Kalman Filter). Exploiting novel 118 GHz channels – make use of Chinese satellites in order to gather experience (although on microwave sounder configuration and with different spatial resolution).

2 Introduction

The EUMETSAT Polar System – Second Generation (EPS-SG) will provide operational continuity and service enhancements to missions carried by the Metop satellites of the current EUMETSAT Polar System (EPS). The EPS-SG is planned for operation in the 2020- 2040 timeframe and will contribute to the Joint Polar System being jointly set up with NOAA. The satellites will fly, like Metop, in a Sun synchronous, low Earth orbit at around 820 km altitude with an equator crossing time at 09:30 Mean Local Solar Time in descending node. The space segment of the EPS-SG system will consist of a dual satellite configuration with three sounding and imaging satellites (A-series) and three microwave satellites (B-series) to span an operational life time of the programme over 21 years. The EPS-SG satellites will carry the instruments presented in Table 2.1.1.

Metop-SG payload	Metop-SG satellite
IASI-NG: Infrared Atmospheric Sounding Interferometer – New Generation	A
METimage: Visible-Infrared Imager	A
MWS: Microwave Sounder	A
Sentinel-5: UV-VIS-NIR-SWIR Sounder	A
3MI: Multi-viewing, -channel, -polarisation Imager	A
RO: Radio Occultation	A and B
SCA: Scatterometer	B
MWI: Microwave Imager	B
ICI: sub-mm wave Ice Cloud Imager	B
ARGOS A-DCS payload	B

Table 2.1.1. Instruments carried by EPS-SG satellites.

3 Mission Objectives

Among the various missions which are part of EPS-SG, there are the Microwave Imager (MWI) and the Ice Cloud Imager (ICI). The MWI frequencies range from 18 GHz up to 190 GHz. All MWI channels up to 89 GHz measure both V and H polarisations. The primary objective of the MWI mission is to support Numerical Weather Prediction (NWP) at regional and global scales. The MWI will not only provide continuity of measurements for some heritage microwave imager channels (e.g. SSM/I, AMSR-E) but will also include additional channels such as the 50-55 / 118 GHz bands. The combined use of these channels will provide more information on cloud and precipitation over sea and land.

The ICI instrument will provide measurements over the sub-millimetre spectral range contributing to an innovative characterisation of clouds over the whole globe. The ICI has channels at 183 GHz, 325 GHz and 448 GHz with single V polarisation and two channels at 243 GHz and 664 GHz with both V and H polarisation. The ICI's primary objectives are to support climate monitoring and validation of ice cloud models and the parameterisation of ice clouds in weather and climate models through the provision of ice cloud products.

3.1 Operational Objectives

The operational objectives of the EPS-SG missions aim to provide a number of services throughout their operational lifetime, i.e. satisfying precise timeliness and availability requirements. Among the services to the users covered by the EPS-SG missions, the most relevant to this document are:

- Global data acquisition and generation;
- Regional data acquisition and generation;
- Level 1 (L1) Products generation;
- Level 2 (L2) Products generation;
- Near Real Time (NRT) data dissemination;
- Climate Data Records generation.

Specific requirements relevant to all these aspects are specified in the EPS-SG End Users Requirements Document (EURD) which expresses the end user requirements for the various EPS-SG missions in more detail.

3.2 Numerical weather prediction

In the past, NWP has benefited mainly from assimilating radiances sensitive to temperature and humidity in clear-sky conditions, in situations where the surface interaction is not too difficult to model (e.g. channels which do not see the surface, or surface-sensitive channels over ocean). Information on sea-ice and SST has come from externally-generated retrievals such as the Met Office OSTIA product. Information on clouds and precipitation has been used only indirectly, through the use of satellite retrievals to help develop the science that is then encoded in cloud and precipitation parametrisations. However, the picture is now rapidly changing as NWP centres have developed all-sky radiance assimilation (where clear, cloudy and precipitating scenes are all assimilated directly, Geer et al. 2017a, 2017b) and they have increasingly been able to use observations with partial surface sensitivity over sea-ice and land surfaces. Beyond this, NWP centres are starting to incorporate earth-system modelling and assimilation alongside their traditional atmospheric capabilities. Hence, within the lifetime of EPS-SG, it is likely that NWP centres will be assimilating all the geophysical information from MWI and ICI, including atmospheric temperature, humidity, cloud and precipitation, and sea-ice, snow, soil moisture and SST. This data will be directly assimilated as radiances into full earth-system models.

This means that from the NWP perspective, the most important science goals for MWI and ICI are (1) the provision of extremely well calibrated, traceable, and timely level 1b radiance products; (2) the development of physical forward models for (and scientific understanding of) radiation processes in the atmosphere, including cloud and precipitation, as well as the surface (e.g. sea-ice, snowpack, land surface and ocean); (3) the availability of fast forward models for these processes (i.e. computationally efficient, simplified models fitted to more accurate reference geophysical models). As long as variational assimilation remains the dominant data assimilation methodology, these fast models must also supply tangent-linear and adjoint capabilities. Currently, this need is met by the RTTOV package developed by the EUMETSAT NWP-SAF consortium. Section 6.4.1 gives more details on specifically NWP applications, but the majority of scientific developments described in this document will directly support NWP applications of the MWI and ICI level 1b radiances.

3.3 Research

Clouds and precipitation are very active research areas in atmospheric science and climate science. Of particular interest are their radiative and thermodynamic properties, as well as how they interact with the atmospheric dynamics, that is, with circulations on various scales. For example, Rädel et al. (2016) have shown recently that the cloud radiative effect greatly amplifies the El Niño phenomenon. Bony et al. (2015) summarize four ‘grand challenges’ to atmospheric climate research, all grouped around the cloud, precipitation, and dynamics interaction: (1) What role does convection play in cloud feedbacks? (2) What controls the position, strength and variability of storm tracks? (3) What controls the position, strength and variability of the tropical rain belts? (4) What role does convective aggregation play in climate?

MWI/ICI will contribute strongly to address these challenges. Particularly important will be the unprecedented information on cloud ice from the sub-millimetre channels of ICI, an observation that is so far completely absent from the global observing system. Meeting these research objectives imposes slightly different requirements from the operational objectives, particularly on open availability of not only the mission data, but also the pre-launch characterization measurements to the scientific community. This latter point is discussed further in Section 4.4.

3.4 Structural requirements for research applications

Because of the novelty of ICI, it has different structural requirements, if its full potential should be realised. In particular, the international research community should be involved in an appropriate way, in order to leverage its expertise for the development of retrieval algorithm and scientific applications that EUMETSATs satellite application facilities (SAFs) are not supporting. To coordinate this, a dedicated scientific advisory group (SAG) must remain active also during the mission lifetime, in order to participate in the coordination of the MWI/ICI SAG activities with external science and user groups, review the progress and the results of scientific projects initiated in support of MWI and ICI, etc.

A task of the SAG is to advise ESA and EUMETSAT on requirements and methods for instrument calibration and post-launch validation activities.

The SAG is also seen as an appropriate scientific forum to support a decommissioning calibration period near the end of each satellites lifetime, to complement the calibration done in the commissioning period at the beginning. Calibrations could include aircraft campaigns and/or special satellite manoeuvres, for example to look at cold space or at the moon. The decommissioning calibration period would significantly increase the long-term value of the data for climate applications.

Ideally MWI/ICI activities should be coordinated with the Earth Clouds, Aerosol and Radiation Explorer (EarthCARE) from ESA (Illingworth et al. 2015), since there is expected to be a strong synergy. Examples include coordinated aircraft campaigns before launch (with the International Sub-millimetre Airborne Radiometer ISMAR), and collocation/cross-calibration activities after launch.

4 Heritage and Instruments Descriptions

4.1 The MWI instrument

The MWI instrument is a passive conical scanner radiometer capable of measuring thermal radiance emitted by the Earth, at high spatial resolution in specified spectral bands in the microwave region of the electromagnetic spectrum. The MWI has a direct heritage from instruments such as the Special Sensor Microwave/Imager (SSM/I) on the Defence Meteorological Satellite Program (DMSP), its successor the Special Sensor Microwave Imager Sounder (SSMIS), the Tropical Rainfall Measuring Mission (TRMM) Microwave Imager (TMI), the Advanced Microwave Scanning Radiometer-EOS (AMSR-E) and the Global Precipitation Mission Microwave imager (GMI). All these missions have provided, or provide global microwave imaging data useful to retrieve information on precipitating and non-precipitating liquid and frozen hydrometeors, information on water vapour content and relevant surface characteristics (e.g. windspeed over ocean and sea-ice coverage).

MWI will also provide continuity of measurements of key microwave imager channels as observed by SSM/I, TMI, SSMIS, AMSR-E, GMI in support of long-term climate records. Precipitation measurements from passive microwave radiometers support the Global Precipitation Climatology Project (GPCP) as part of the WMO/WCRP GEWEX (World Climate Research Programme Global Energy and Water Cycle Experiment) programme.

The MWI spectral bands are presented in Table 4.1.1, together with other relevant requirements extracted from the EPS-SG EURD.

MWI-1 to MWI-3 and MWI-8 can be considered as SSM/I legacy channels. These channels provide information on total column water vapour, liquid and frozen hydrometeors, sea ice and snow coverage, windspeed information over ocean, land surface emissivity. Channels in the oxygen absorption complexes near 50–60 GHz and 118 GHz are also present (MWI-4 to MWI-7, MWI-9 to MWI-12). These channels are one of the innovative features of MWI, enabling the retrieval of information on weak precipitation and snowfall, typically affecting the weather at high latitudes (Gasiewski et al. 1990, Bauer and Mugnai 2003, Bauer et al. 2005). Channels MWI-13 to MWI-18 can provide information on water vapour profiles and precipitation (Laviola and Levizzani 2011, Laviola et al. 2013).

The instrument collects radiation coming from the Earth by means of a rotating antenna, composed by an offset parabolic reflector antenna and feed-horn cluster rotating together. The rotation of the slanted antenna allows performing the conical scan. The basic scan and viewing geometry is depicted in Figure 4.1.1. The same observation geometry is applicable to ICI; however ICI is counter-rotating with respect to MWI.

The offset angle of the offset parabolic antenna is adjusted in order to have the antenna mechanical boresight pointing in a direction providing an observation zenith angle (OZA) close to 53°±2° (also known as incidence angle). Assuming the nominal EPS-SG orbit altitude of 820 km (ascending node 21:30 Mean Local Solar Time), the offset angle θ (see Figure 4.1) is 44.82°. It must be noted however that the OZA will be different for the various channels due to the different feedhorn position in the focal plane.

The satellite will have yaw steering control. The main impact of yaw steering control on the acquisition geometry is a shift of the scene viewing angle (in azimuth) by a value corresponding to exactly the value of the yaw steering angle, since the axis (Nadir direction) is the same for both rotations (yaw axis of the satellite coincides with the antenna rotation axis, see Figure 4.1.1). The impact of yaw steering is maximum at the equator and minimum near the poles.

The observations are acquired within an angle of ± 65° in azimuth for the fore view, equivalent to a swath of about 1700 km from the altitude of the nominal orbit. Every rotation, two other angular sectors are used to calibrate the receivers. In the initial part of the calibration cycle the horns look at a fixed calibration reflector, collecting the energy coming from the cold sky, and then at a fixed microwave hot calibration target providing the receivers with a known input noise power.

Noise diodes are implemented for channels MWI-1, MWI-2 and MWI-3. The use of noise diodes allows controlling the calibration stability and correcting the transfer function non-linearity. An additional advantage is that it potentially allows having a backup calibration method in case of anomalies on the hot calibration target. The noise diodes will be active every two scan cycles. Hence two consecutive calibration cycles will be needed to perform a continuous computation of the non-linearity for these channels in flight. Additionally, it would be possible to perform a calibration cycle considering the hot calibration with noise diode, and performing the same for the cold calibration.

The MWI-1 channel at 18.7 GHz also includes a radio frequency interference (RFI) resistant receiver to mitigate observed RFI in this spectral region.

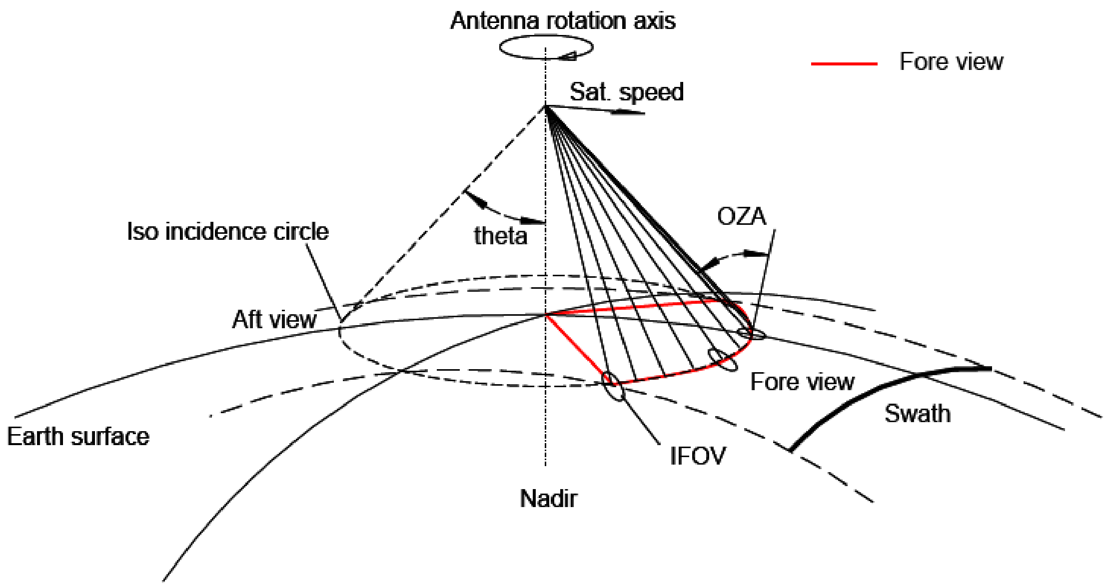

Figure 4.1.1. MWI viewing geometry. ICI has the same viewing geometry; it is however counter-rotating with respect to MWI.

Channel	*Frequency (GHz)*	*Bandwidth (MHz)*	*NEΔT (K)*	*Bias (K)*	*Polarisation*	*Footprint Size at 3dB (km)*
MWI-1	18.7	200	0.8	1.0	V, H	50
MWI-2	23.8	400	0.7	1.0	V, H	50
MWI-3	31.4	200	0.9	1.0	V, H	30
MWI-4	50.3	400	1.1	1.0	V, H	30
MWI-5	52.610	400	1.1	1.0	V, H	30
MWI-6	53.24	400	1.1	1.0	V, H	30
MWI-7	53.750	400	1.1	1.0	V, H	30
MWI-8	89.0	4000	1.1	1.0	V, H	10
MWI-9	118.7503±3.20	2x500	1.3	1.0	V	10
MWI-10	118.7503±2.10	2x400	1.3	1.0	V	10
MWI-11	118.7503±1.40	2x400	1.3	1.0	V	10
MWI-12	118.7503±1.20	2x400	1.3	1.0	V	10
MWI-13	165.5±0.75	2x1350	1.2	1.0	V	10
MWI-14	183.31±7.0	2x2000	1.3	1.0	V	10
MWI-15	183.31±6.1	2x1500	1.2	1.0	V	10
MWI-16	183.31±4.9	2x1500	1.2	1.0	V	10
MWI-17	183.31±3.4	2x1500	1.2	1.0	V	10
MWI-18	183.31±2.0	2x1500	1.3	1.0	V	10

Table 4.1.1. Required MWI performance.

4.2 The ICI instrument

The EPS-SG Ice Cloud Imager (ICI) is a sub-millimetre wave conical imager that will be on board of the EPS-SG satellites. The use of sub-mm frequencies for observation of cloud ice properties was initially investigated and proposed by Evans and Stephens (1995a and b), and Evans et al. (1998), while Buehler et al. (2007, 2012) provided a broad overview and justification for a similar concept proposed as potential ESA Earth Explorer mission.

Numerical weather and climate models are not fully able to represent the radiative and thermodynamic effects of ice clouds, which is especially problematic because these effects couple to the circulation in various ways that are still poorly understood. Clouds and their interaction with the circulation therefore are one of the biggest sources of uncertainty in climate predictions. But it is not only model understanding that is lacking, there is also a lack of ice cloud data with global coverage.

The primary objective of ICI is to support climate research and climate monitoring activities. A particularly important aim of ICI is the provision of measurements related to ice clouds, including bulk microphysical variables, in order to improve the representation of ice clouds in numerical weather and climate models. Furthermore, the availability of ICI data will enhance the ability of NWP centres to initialise global and regional models with more detailed information on clouds. Although their treatment in NWP is important for accurate weather forecasts, clouds are currently not well represented in models.

Further objectives of the ICI mission include the measurement of water-vapour gross profiles and snowfall distributions in support of NWP and nowcasting.

The ICI spectral bands are presented in Table 4.2.1 together with other relevant requirements extracted from the EPS-SG EURD.

The core products of ICI will be data on the bulk mass of ice particles and their size. These can be retrieved as global columns, as described in Jimenez et al. (2007), or as vertical profiles, albeit with a limited vertical resolution. Ice retrieval algorithms will use all ICI channels.

As mentioned earlier, channels ICI-1 to ICI-3 can provide information on water vapour profiles, while Laviola and Levizzani (2011) suggested also the possibility of performing precipitation retrievals using these water vapour sounding channels. These channels are also important to provide information on the upwelling atmospheric emission background, useful to retrieve the cloud properties (e.g. Evans et al. 2002, Rydberg et al. 2007, Evans et al. 2012). Moreover, the use of a combination of sounding channels measurements along the various water vapour lines sensed by ICI allows probing clouds at different heights and with different particle sizes. The availability of channels measuring radiances with both horizontal and vertical polarisation (ICI-4 and ICI-11) allows retrieving information on different ice crystal habits, with polarisation effects increasing with frequency (Evans et al. 2002).

The instrument will be a passive satellite radiometer capable of measuring thermal radiance emitted by the Earth, at high spatial resolution in specified spectral bands in the sub-millimetre wave region of the electromagnetic spectrum. The ICI collects radiation coming from the Earth by means of a rotating antenna, composed by an offset parabolic reflector and a feed-horns cluster rotating together. The rotation of the slanted antenna allows performing the conical scan. ICI scans in clockwise rotation when viewed from the nadir side of the platform, where it is located.

As for MWI, the observations are acquired within an angle of ± 65° in azimuth for the fore view, equivalent to a swath of about 1700 km at nominal orbit altitude. Every rotation, two other angular sectors are used to calibrate the receivers. In the initial part of the calibration cycle the horns look at a fixed calibration reflector, collecting the energy coming from the cold sky, and then at a fixed microwave hot calibration target providing the receivers with a known input noise power.

The basic ICI observation cycle includes the direct observation of the OBCT providing the receivers with a known input noise power, observation of the cold space through the space view reflector and observation of the Earth view. The baseline scan rate is 45 rpm, implying an along-track footprint overlap of at least 40%.

The offset angle of the offset parabolic antenna is adjusted in order to have the antenna mechanical boresight pointing in a direction providing an OZA close to 53°±2°. Assuming the nominal EPS-SG orbit altitude of 820 km (ascending node 21:30 Mean Local Solar Time), the offset angle θ (see Figure 4.1.1) is 44.6°. It must be noted that the OZA will be different for the various channels due to the different feedhorn position in the focal plane.

Channel	***Frequency (GHz)***	***NEΔT (K)***	***Bias (K)***	***Polarisation***	***Footprint Size at 3dB (km)***
ICI-1	183.31±7.0	0.8	1.0	V	16
ICI-2	183.31±3.4	0.8	1.0	V	16
ICI-3	183.31±2.0	0.8	1.0	V	16
ICI-4	243.2±2.5	0.7	1.5	V, H	16
ICI-5	325.15±9.5	1.2	1.5	V	16
ICI-6	325.15±3.5	1.3	1.5	V	16
ICI-7	325.15±1.5	1.5	1.5	V	16
ICI-8	448±7.2	14	1.5	V	16
ICI-9	448±3.0	1.6	1.5	V	16
ICI-10	448±1.4	2.0	1.5	V	16
ICI-11	664±4.2	1.6	1.5	V, H	16

Table 4.2.1. Required ICI performance.

4.3 Prelaunch characteristics and instrument model

Pre-launch measurements of instrument characteristics for current and future EUMETSAT missions shall be made openly available to the users and to the scientific community. The lack of these measurements is a major obstacle for the use of these data for climate applications, which require a traceable calibration based on the best estimate of the true instrument characteristics. Important characteristics that impact the use of the data are:

- Frequency response (spectral response and sideband ratio);
- Antenna pattern and scan characteristics, including radiometric model of instrument and satellite;
- Calibration details, such as thermal characteristics of the hot load and the behaviour of the temperature sensors on the hot load;

- Instrument nonlinearity.

To optimally use the data, all these characteristics must be incorporated into the forward operators that simulate instrument data based on the atmospheric state. This is a strong requirement for climate applications, where even small biases are important because they can lead to spurious trends. But availability of more accurate instrument characteristics is also expected to benefit operational meteorology, because it will reduce the need for complex a-posteriori corrections to the instrument characteristics used in forward models (e.g. Lu and Bell, 2014) and because NWP centres increasingly aspire to identify and correct systematic model errors that in radiance space have signatures of only a few tenths of a Kelvin (Lupu et al., 2016).

It is therefore a strong requirement for scientific applications and a moderately strong requirement for operational applications that all relevant pre-launch instrument characterisation data for MWI and ICI must be made openly available to the users' community. Instrument characterization data should not only be provided without restriction, but also in such a form that they can easily be used. For example, measurement data must include enough documentation for scientists to understand the exact units, meaning, and model assumptions behind the measurement.

4.4 MWI and ICI data processing and products

The sensor Level 1B products obtained from the pre-processing of raw data from MWI and ICI will be calibrated, geo-located, and quality-controlled Earth-view spectral radiances.

The MWI mission can provide, through dedicated retrievals, various geophysical products: cloud and precipitation products including bulk microphysical variables, total column water vapour over ocean, water vapour and temperature gross profiles. Furthermore, it can provide all weather surface imagery including: sea ice coverage (and type), snow coverage and water equivalent, sea surface wind speed (complementary to the scatterometer).

ICI will provide observations related to: cloud-ice content (total column and gross profile), snowfall detection, precipitation content (frozen; total column and gross profile), snowfall rate near the surface, water-vapour profiles. Further variables to which the ICI mission contributes information include the cloud ice effective radius (total column and gross profile).

Considering MWI and ICI, the following products will be produced at the EUMETSAT Central Facilities and delivered in Near Real Time (NRT):

L1B: Spectral radiances from MWI and ICI;
L2: Liquid Water Path (LWP) and Ice Water Path (IWP).

To allow scientific use of the data, EUMETSAT will also provide traceability information for the L1B data, that is, information on how exactly the data are calibrated, what assumptions are used, and which uncertainties enter the calibration.

4.5 References

Bauer, P., and A. Mugnai, 2003: Precipitation profile retrievals using temperature-sounding microwave observations. J. Geophys. Res., Vol. 108, 4730, doi:10.1029/2003JD003572

Bauer, P., E. Moreau, S. Di Michele, 2005: Hydrometeor Retrieval Accuracy Using Microwave Window and Sounding Channel Observations. J. Appl. Meteor., 44, 1016–1032. doi: http://dx.doi.org/10.1175/JAM2257.1

Bony, S. et al., 2015: Clouds, circulation and climate sensivity, Nature Geosci., 8(4), 261–268, doi:10.1038/NGEO2398.

Buehler, S. A., Jimenez, C., Evans, K. F., Eriksson, P., Rydberg, B., Heymsfield, A. J., Stubenrauch, C. J., Lohmann, U., Emde, C., John, V. O., Sreerekha, T. R., and Davis, C. P., 2007: A concept for a satellite mission to measure cloud ice water path, ice particle size, and cloud altitude, Q. J. Roy. Meteorol. Soc., 133, pp. 109–128.

Buehler, S. A., E. Defer, F. Evans, S. Eliasson, J. Mendrok, P. Eriksson, C. Lee, C. Jimenez, C. Prigent, S. Crewell, Y. Kasai, R. Bennartz, and A. J. Gasiewski, 2012: Observing ice clouds in the submillimeter spectral range: the Cloud Ice mission proposal for ESA's Earth Explorer 8, Atmos. Meas. Tech., 5, 1529–1549, www.atmos-meas-tech.net/5/1529/2012/ doi:10.5194/amt-5-1529-2012.

Evans, K. F., Stephens, G. L., 1995a: Microwave radiative transfer through clouds composed of realistically shaped ice crystals. Part I: Single scattering properties", J. Atmos. Sci., 52, 2041–2057.

Evans, K. F., Stephens, G. L., 1995b: Microwave radiative transfer through clouds composed of realistically shaped ice crystals, Part II: Remote sensing of ice clouds", J. Atmos. Sci., 52, 2058–2072.

Evans, K. F., Walter, S. J., Heymsfield, A. J., Deeter, M. N., 1998: Modeling of submillimeter passive remote sensing of cirrus clouds", J. Appl. Meteorol., 37, 184–205.

Evans K. F., Walter S. J., Heymsfield A. J., McFarquhar G. M., 2002. Submillimeter-wave cloud ice radiometer: Simulations of retrieval algorithm performance. J. Geophys. Res. 107: 2.1–2.21.

Evans, K. F., Wang, J. R., O'C Starr, D., Heymsfield, G., Li, L., Tian, L., Lawson, R. P., Heymsfield, A. J., and Bansemer, A., 2012: Ice hydrometeor profile retrieval algorithm for high-frequency microwave radiometers: application to the CoSSIR instrument during TC4, Atmos. Meas. Tech., 5, 2277-2306, doi:10.5194/amt-5-2277-2012.

Feist, D. G., 2004: The Bernese Atmospheric Multiple Catalog Access Tool (BEAMCAT): a tool for users of popular spectral line catalogs, Journal of Quantitative Spectroscopy and Radiative Transfer,85, 57–97, 2004.

Geer, A.J., F. Baordo, N. Bormann, S.J. English, M. Kazumori, H. Lawrence, P. Lean, K. Lonitz and C. Lupu, 2017a: The growing impact of satellite observations sensitive to humidity, cloud and precipitation, Quart. J. Roy. Meteorol. Soc., submitted

Geer, A.J., K. Lonitz, P. Weston, M. Kazumori, K. Okamoto, Y. Zhu, E.H. Liu, A. Collard, W. Bell, S. Migliorini, P. Chambon, N. Fourrié, M.-J. Kim, C. Köpken-Watts and C. Schraff, 2017b: All-sky satellite data assimilation at operational weather forecasting centres, Quart. J. Roy. Meteorol. Soc., submitted

Gasiewski, A. J., J. W. Barrett, P. G. Bonanni, and D. H. Staelin, 1990: Aircraft-based radiometric imaging of tropospheric temperature and precipitation using the 118.75-GHz oxygen resonance. J. Appl. Meteor., 29, 620–632.

llingworth, A., H. Barker, A. Beljaars, M. Ceccaldi, H. Chepfer, N. Clerbaux, J. Cole, J. Delanoë, C. Domenech, D. Donovan, S. Fukuda, M. Hirakata, R. Hogan, A. Huenerbein, P. Kollias, T. Kubota, T. Nakajima, T. Nakajima, T. Nishizawa, Y. Ohno, H. Okamoto, R. Oki, K. Sato, M. Satoh, M. Shephard, A. Velázquez-Blázquez, U. Wandinger, T. Wehr, and G. van Zadelhoff, 2015: The EarthCARE Satellite: The Next Step Forward in Global Measurements of Clouds, Aerosols, Precipitation, and Radiation. *Bull. Amer. Meteor. Soc.*, **96**, 1311–1332, doi: 10.1175/BAMS-D-12-00227.1.

Jiménez, C., S. A. Buehler, B. Rydberg, P. Eriksson, and K. F. Evans, 2007: Performance simulations for a submillimetre wave cloud ice satellite instrument, Q. J. R. Meteorol. Soc., 133(S2), 129–149, doi:10.1002/qj.134.

Laviola, S., and V. Levizzani, 2011: The 183-WSL fast rain rate retrieval algorithm. Part I: Retrieval design. Atmos. Res., 99, 443-461.

Laviola, S., V. Levizzani, E. Cattani, C. Kidd, 2013: The 183-WSL fast rain rate retrieval algorithm. Part II: Validation using ground radar measurements, Atmos. Res., 134, 77-86.

Lu, Q. and W. Bell, 2014. Characterizing channel center frequencies in AMSU-A and MSU microwave sounding instruments. J. Atmos. Ocean. Tech., 31(8), pp.1713-1732.

Lupu, C., A. Geer, N. Bormann and S. English, 2016: An evaluation of radiative transfer modelling errors in AMSU-A data, ECMWF technical memo. 770Rädel, G. et al., 2016: Amplification of El Niño by cloud longwave coupling to atmospheric circulation, Nature Geosci., 9, 106-111, doi: 10.1038/NGEO2630.

Rydberg, B., Eriksson, P. and Buehler, S. A., 2007: Prediction of cloud ice signatures in submillimetre emission spectra by means of ground-based radar and in situ microphysical data. Q.J.R. Meteorol. Soc., 133: 151–162. doi:10.1002/qj.151

5 Underlying Physics

5.1 Spectroscopy

5.1.1 Introduction

For the interpretation of brightness temperature measurements by MWI and ICI, knowledge on the interaction between microwave radiation and atmospheric particles is necessary. To describe the effect of absorption in the radiative transfer (Section 5.4) within the microwave frequency range, absorption coefficients have been derived from theoretical considerations and laboratory studies, though the latter have not been able to cover all the relevant atmospheric temperature and pressure ranges. This section describes the current state of knowledge about absorption characteristics of atmospheric gases and hydrometeors, i.e. cloud droplets, ice particles.

5.1.2 Gaseous absorption

Absorption by atmospheric gases in the microwave range can be separated into contributions by resonant line absorption (i.e., rotational and vibrational transitions by gases like H_2O, O_2, O_3) and non-resonant absorption due to interaction of molecules with each other, i.e. the non-ideality of gas - commonly called continuum absorption (see Figure 5.1.1). A thorough review on microwave spectroscopy relevant for remote sensing of water vapour can be found in Tretyakov (2016).

Under tropospheric conditions the line shape profile for resonant lines is dominated by pressure broadening while Doppler effects can be neglected. The line shape is described by models, i.e. van Vleck and Weisskopf, Voigt, Lorenz models, which require centre frequency, half width at half amplitude and integrated line strength as input. Continuum absorption is less well understood and often simply refers to the absorption observed in window regions that cannot be explained by pure resonant line absorption employing standard line shape models. It mostly originates from bimolecular absorption but also far wings of monomer lines contribute to the continuum as these are neglected in the derivation of line shape models. H_2O, N_2 and O_2 show a significant continuum in the microwave region with water vapour showing the largest uncertainty (Payne et al, 2011). The parameterization of the water vapour continuum absorption includes a component accounting for the broadening by foreign gases (e.g., nitrogen and oxygen) and one accounting for the broadening by water vapour (self-broadening). It is worth noting that only few laboratory studies and under limited atmospheric conditions and spectral ranges have been performed in the past whose analysis reveals spreads in broadening parameters and temperature dependence (Tretyakov et al., 2016). Recently, a Russian – French study found that a strong contribution by the water dimer in the millimetre wave range could be shown (Odintsova et al, 2017).

Two of the most widely used absorption models describing both line and continuum absorption are known as Rosenkranz 98 (Rosenkranz, 1998) with corrections (Turner et al., 2009; Liljegren et al., 2005) and MPM93, the microwave propagation model by Liebe et al. (1993). Note, that Rosenkranz 98 and MPM93 do not include trace gases like O_3, N_2O, or ClO. These trace gases exhibit absorption lines above 100 GHz. Their line parameters are listed in different absorption catalogues, e.g. HITRAN, BEAMCAT (Feist, 2004).Within the ground-based microwave radiometer community also the monochromatic radiative transfer model (MonoRTM, http://rtweb.aer.com) is frequently used. In the radio astronomy community the Atmospheric

Model (AM6.2) by Scott Paine which uses the HITRAN line catalogue (Rothmann et al., 1992) and the Atmospheric Transmission at Microwaves model (ATM, Pardo et al., 2001) which extends into the Terahertz range is widely used.

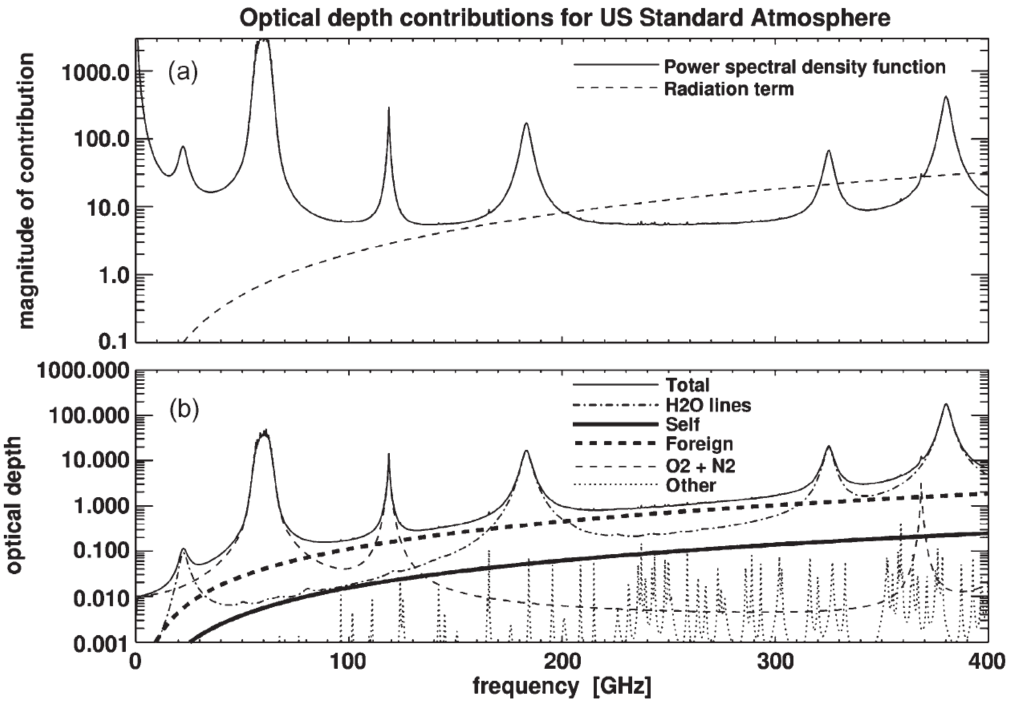

Figure 5.1.1 from Payne et al., 2011. Optical depth contributions from a MonoRTM calculation using the U.S. Standard Atmosphere. (a) Contributions from the power spectral density function and the radiation term. (b) Optical depth contributions from different absorbers.

In order to evaluate the gas absorption models that provide the absorption coefficient α_ν, the relevant meteorological variables for radiative transfer, i.e. from radiosondes, aircraft (Hewison, 2006) or short-term numerical weather prediction (NWP) models, are used to calculate microwave brightness temperatures that are then compared to measured ones. Most frequently, ground-based radiometers are used that measure atmospheric brightness temperatures against the well known cosmic background during clear-sky conditions. By comparisons over various climatological conditions, gas absorption models can be constrained. Various studies have been performed to provide updates for describing resonant, e.g. the half-width of the 22.235 GHz H_2O rotational line (Liljegren et al., 2005), and non-resonant absorption. For the latter Turner et al. (2009) used measurements between 22 and 150 GHz to improve the description of the water vapour continuum. Similar investigations were performed by Payne et al. (2011) using measurements from 22 to 183 GHz leading to an update of the Mlawer, Tobin, Clough, Kneizys, and Davis continuum (MT_CKD). They estimate the uncertainties in the updated continuum coefficients to be 4% for the foreign-broadened water vapour continuum and 4% for the self-broadened water vapour continuum.

Observations at the 183 GHz line by different satellite instruments were thoroughly evaluated using different reference data, e.g. radiosondes, lidar and NWP, revealing a spectrally dependent bias along the wing of the line (Brogniez et al., 2016). In their recommendations they ask for a better coordination between instrument and calibration experts and RTM modelers to ensure that radiative transfer simulations are consistent with the most recent spectroscopy measurements.

5.1.3 Absorption by hydrometeors

The absorption coefficient for liquid hydrometeors like cloud droplets, drizzle, or rain drops which are assumed spherical, are calculated using Mie theory (Mie, 1908) and in general increases with frequency. It depends on the complex permittivity of liquid water, that is traditionally calculated using models like, e.g., Liebe et al. (1991, 1993), Ellison (2006), or Stogryn et al. (1995). While these models predict very similar refractive index properties for liquid water at temperatures higher than 0°C, recent studies have revealed that no refractive index model is currently able to consistently predict the refractive index of supercooled liquid water (i.e., liquid water at temperatures below freezing) over a larger range of frequencies and temperatures (Kneifel et al., 2014; Cadeddu and Turner, 2011). Ground-based microwave radiometer observations of super-cooled liquid clouds have been used in Mätzler et al. (2010) and Kneifel et al. (2014) to derive opacity ratios which provide additional constraints to the super-cooled temperature region, where laboratory data are extremely sparse. Rosenkranz (2015) and Turner et al. (2015) used a combination of these cloud measurements and laboratory datasets to develop improved and more consistent refractive index models. Turner et al. (2015) also provide an error estimate for their refractive index model based on an optimal estimation retrieval technique.

For frozen hydrometeors absorption is mostly negligible compared to scattering (see section 5.2). The refractive index of solid ice is mostly taken from the compilation by Warren and Brandt (2008). More details on temperature dependence etc. can be found in Mätzler et al. (2006).

5.1.4 Summary and recommendations

Improvement of absorption models is an ongoing challenge for the community as discrepancies between observations and modelling still occur. This is particularly true for frequencies observed less frequently, i.e. around the 118 GHz line and at sub-millimetre wavelengths. Specifically, two gaps in our knowledge in respect to absorption characteristics in the frequency range of ICI can be identified.

- First, improving the accuracy of the water continuum absorption. Most evaluations only considered frequencies below 200 GHz and therefore a more detailed assessment for window frequencies at higher frequencies would be beneficial. This might be possible by new laboratory measurements, e.g. Weber et al. (2012) at 400 GHz, Odintsova et al. (2017), or exploitation of field campaigns covering the full spectral range for consistent treatment possibly together with the astronomical community. Here, several interesting data sets exist like the one from RHUBC-II (Radiative Heating in Underexplored Bands Campaign) with observations across the entire terrestrial spectrum (i.e., from 1000 to 3.3 μm) under extremely dry conditions at around 5300 m height above sea level (Turner et al., 2012). However, coordination efforts between spectroscopists, different experimentators including the astronomical community and radiative transfer modellers, including RTTOV, are needed.
- Second, observational data for deriving liquid water refractive index were limited to a maximum frequency of 225 GHz. No data, neither observational nor laboratory, are currently available for temperatures lower than -5°C and for frequencies larger than 225 GHz. This fact leads to potentially large uncertainties of the refractive index predicted by all models at higher frequencies and super-cooled temperatures (Ellison, 2007). Laboratory measurements of the refractive index in the super-cooled region or field campaigns involving radiosondes carrying in situ instrumentation for measurements of

super cooled liquid water for radiative closure studies would therefore be extremely valuable to close this gap particularly at higher frequencies.

5.1.5 References

Brogniez, H., et al., 2016: A review of sources of systematic errors and uncertainties in observations and simulations at 183 GHz, *Atmos. Meas. Tech.*, 9, 2207–2221, doi:10.5194/amt-9-2207-2016.

Cadeddu, M. P. and Turner, D. D, 2011: Evaluation of water permittivity models from ground-based observations of cold clouds at frequencies between 23 and 170 GHz, *IEEE Trans. Geosci. Remote Sensing*, 49, 2999–3008.

Ellison, W.J., 2007: Permittivity of pure water, at standard atmospheric pressure, over the frequency range 0-25 THz and the temperature range 0-100°C. *J. Phys. Chem. Ref. Data*, 36, doi:10.1063/1.2360986.

Ellison, W., 2006: Dielectric properties of natural media, in: Thermal Microwave Radiation: Applications for Remote Sensing, edited by Mätzler, C., pp. 431–455, *The Institution of Engineering and Technology (IET),* London, 2006.

Hewison, T. J., 2006: Aircraft validation of clear air absorption models at millimeter wavelengths (89 – 183 GHz), *J. Geophys. Res*., 111, D14303, doi:10.1029/2005JD006719.

Kneifel, S., Redl, S., Orlandi, E., Löhnert, U., Cadeddu, M. P., Turner, D. D., and Chen, M.-T., 2014: Absorption Properties of Supercooled Liquid Water between 31 and 225 GHz: Evaluation of Absorption Models Using Ground-Based Observations, *J. Appl. Meteor. Climatol*., 53, 1028–1045, doi:10.1175/JAMC-D-13-0214.1.

Liebe, H. J., Hufford, G. A., and Manabe, T., 1991: A model for the complex permittivity of water at frequencies below 1 THz, *J. Infrared Mill. Waves*, 12, 659–675.

Liebe, H. J., Hufford, G. H., and Cotton, M. G., 1993: Propagation modeling of moist air and suspended water/ice particles at frequencies below 1000 GHz, in: *Proc. AGARD*, vol. 542, pp. 1–10.

Liljegren, J. C., S.-A. Boukabara, K. Cady-Pereira, S.A. Clough, 2005: The effect of the half-width of the 22-GHz water vapor line on retrievals of temperature and water vapor profiles with a 12-channel microwave radiometer, *IEEE Trans. Geosci. Remote Sensing*, 10.1109/TGRS.2004.839593

Mätzler, C. , 2006: Microwave dielectric properties of ice, in Thermal Microwave Radiation—Applications for Remote Sensing, Electromagn., Waves Ser., vol. 52, edited by C. Mätzler et al., chap. 5, 455–462, Inst. Eng. Technol., Stevenage, U. K.

Mätzler, C. ,P. W. Rosenkranz, and J. Cermak 2010: Microwave absorption of supercooled clouds and implications for the dielectric properties of water, J. Geophys. Res., 115, D23208, doi:10.1029/2010JD014283.

Mie G. Beiträge zur Optik trüber Medien speziell kolloidaler Goldlösungen (contributions to the optics of diffuse media, especially colloid metal solutions). Ann Phys 1908;25:377–445.

Odintsovaa, T.A., M.Yu. Tretyakova, O. Piralib, P. Roy, 2017: Water vapor continuum in the range of rotational spectrum of H_2O molecule: New experimental data and their comparative analysis, *Journal of Quantitative Spectroscopy and Radiative Transfer*, 187, 116–123, http://dx.doi.org/10.1016/j.jqsrt.2016.09.009.

Pardo, J.R., J. Cernicharo, and E. Serabyn, 2001: Atmospheric transmission at microwaves (ATM): an improved model for millimeter/submillimeter applications, *IEEE Transactions on Antennas and Propagation*, .49(12), 1683-1694.

Payne, V.H., E. J. Mlawer, K. E. Cady-Pereira, and J.-L. Moncet, 2011: Water Vapor Continuum Absorption in the Microwave, *IEEE Transactions on Geoscience and Remote Sensing*, 49(6), 2194-2208.

Rosenkranz, P. W., 1998: Water vapor microwave continuum absorption: A comparison of measurements and models, *Radio Science,* 33, 919–928.

Rosenkranz, P. W., 2015: A Model for the Complex Dielectric Constant of Supercooled Liquid Water at Microwave Frequencies, *IEEE Transactions on Geoscience and Remote Sensing*, 53, 1387–1393, doi:10.1109/TGRS.2014.2339015.

Rothman, L. S., et al., 1992: The HITRAN molecular database: editions of 1991 and 1992, *Journal of Quantitative Spectroscopy and Radiative Transfer*, 48, 469–507.

Stogryn, A. P., Bull, H. T., Rubayi, K., and Iravanchy, S., 1995: The microwave permittivity of sea and freshwater, *Aerojet Internal Report, GenCorp Aerojet*, Azusa, CA.

Tretyakov, M.Yu., 2016: Spectroscopy underlying microwave remote sensing of atmospheric water vapor, *Journal of Molecular Spectroscopy*, 328, 7–26.

Turner, D. D., Cadeddu, M. P., Lohnert, U., Crewell, S., and Vogelmann, A. M., 2009: Modifications to the water vapor continuum in the microwave suggested by ground-based 150-GHz observations, *IEEE Transactions on Geoscience and Remote Sensing*, 47, 3326–3337.

Turner, D.D., S. Kneifel, M.P. Cadeddu: An Improved Liquid Water Absorption Model in the Microwave for Supercooled Liquid Water Clouds, *J. Atmos. Oceanic Tech*., accepted.

Turner, D.D. and E. J. Mlawer, 2010: The Radiative Heating in Underexplored Bands Campaigns. *Bull. Amer. Meteor. Soc*., 91, 911–923.

Turner, D. D. E. J. Mlawer, G. Bianchini, M. P. Cadeddu, S. Crewell, J. S. Delamere, R. O. Knuteson, G. Maschwitz, M. Mlynzcak, S. Paine, L. Palchetti, and D. C. Tobin, 2012: Ground-based high spectral resolution observations of the entire terrestrial spectrum under extremely dry conditions, *Geophys. Res. Lett*. 39, L10801, doi:10.1029/2012GL051542.

Weber, M.J.; Yang, B.B.; Kulie, M.S.; Bennartz, R.; Booske, J.H., 2012: Atmospheric Attenuation of 400 GHz Radiation Due to Water Vapor, IEEE Transactions on Terahertz Science and Technology, 2, 355 - 360.

Warren, S. G., and R. E. Brandt, 2008: Optical constants of ice from the ultraviolet to the microwave: A revised compilation, *J. Geophys. Res*., 113, D14220, doi:10.1029/2007JD009744.

5.2 Particle scattering

5.2.1 Introduction

Our ability to infer cloud and precipitation properties from measured radiation depends on our ability to correctly model the local interaction of the hydrometeor particles and the radiation. The interaction is described by the so-called single scattering properties: absorption vector, extinction matrix, and phase matrix, as defined in Chapter 2 of Mishchenko et al. (2002). These single scattering properties depend on particle refractive index, size, shape, and orientation. They are discussed further in the next subsection, Section 5.2.2.

For remote sensing, we are not interested in the behaviour of individual particles, but in the behaviour of the cloud or precipitation system as a whole. Luckily, atmospheric hydrometeor distributions are sparse enough for the medium to be optically linear, which means that the single scattering properties of a particle ensemble will be described accurately by the ensemble average of the individual particle properties. This greatly simplifies the radiative transfer, since it is sufficient to put the ensemble average single scattering properties into the radiative transfer equation and there is no need to deal with individual particles on that level. However, it opens the big topic of how to correctly describe the particle ensemble. This is discussed further in Section 5.2.3.

Finally, the need to explore the optical properties of volcanic clouds is briefly highlighted in Section 5.2.4.

5.2.2 Individual particles

5.2.2.1 Algorithms and codes

There is a mature and tested hierarchy of algorithms and actual computer codes that can be used to calculate the single scattering properties of individual particles. In order of increasing computational cost and breadth of applicability, the most important ones are Rayleigh theory, Mie theory, the T-Matrix method, and the discrete dipole approximation (DDA) method.

5.2.2.2 Application to cloud and precipitation particles

Rayleigh scattering is not applicable for many hydrometeors at ICI/MWI frequencies. The more general Mie theory is applicable, but restricted to spherical particles, which is suitable for water droplets that are not too large. The T-Matrix method is more general than Mie theory because it can handle spheroidal particles, a more general shape than a sphere. There are no spheroidal hydrometeors, but nevertheless the T-Matrix method has been used extensively for remote sensing of ice particles, for example by Davis et al. (2005). This is based on the hope that the single scattering properties of a spheroid to some extent approximate the ensemble-averaged single scattering properties of more realistically shaped particles. However, Eriksson et al. (2015) in a recent study come to the conclusion that that approach, even though it would work for individual ICI/MWI frequency channels, would not work across different frequency channels. The authors, like the authors of an earlier study (Geer and Baordo 2014), instead suggest that properly selected realistically shaped particles can be a better solution. These particles require the most computationally expensive method to calculate their single scattering properties: the DDA method. Because of the high cost of DDA, several efforts have already been made to precalculate single scattering properties for common shapes and frequencies. These efforts are discussed in the next section. For very large particles, for which DDA is most computationally expensive, geometric optics methods may perhaps be an alternative that can help to reduce computation cost, but we do not discuss this further here, since there is not enough published experience with it.

5.2.2.3 Single scattering databases

Table 5.2.1 presents a summary of available singles scattering databases. As discussed in Eriksson et al. (2015), the most important available databases for ICI/MWI are the ones by Hong et al. (2009) and by Liu (2008). Both databases contain single scattering properties calculated by DDA for a number of different shapes and for a set of frequencies. Liu covers frequencies up to 340 GHz, Hong up to 874 GHz. Both databases only consider randomly oriented particles, which is problematic for the ICI mission, since the polarization signal from ice particles is known to depend strongly on particle orientation.

Hence, none of the available databases fulfils the requirements for ICI/MWI, so that a new single scattering database will have to be created. It should contain single scattering properties for some representative particle shapes at the ICI/MWI frequencies. To allow polarization signatures in the dual-polarization ICI channels to be used operationally and scientifically, the new database has to cover oriented particles, not just randomly oriented particles. More precisely, the case to cover is that of particles that have a defined orientation relative to the zenith direction, but a random azimuthal orientation and a random particle reference frame azimuth orientation. A first step in this direction is currently being taken by a dedicated EUMETSAT study that will establish single scattering properties for selected particles, including some oriented ones (Table 5.2.1).

A further limitation of existing databases also has to be noted, they do not cover mixed phase particles, such as ice particles with a liquid coating. Such particles are present in the melting layer and may have a substantial influence on ICI/MWI measurements. This is therefore also an area that requires further scientific study.

In general, as our knowledge on the distribution of particle habit (shape), size, aspect ratio, and orientation improves, new single scattering property simulations will have to be done in order to cover all needed particles.

Database	General description
Liu (2008)	Only up to 340 GHz; no proper aggregate particle; random orientation.
Hong et al. (2009)	90-874 GHz; based on outdated model of refractive index; one aggregate particle; random orientation.
Smaller datasets	New simulations for example for aggregates and melting, but limited to frequencies below 190 GHz.
ARTS	First version under development, with EUMETSAT support. • For MWI / ICI frequency range • For the first time some oriented particles • Several habits, including aggregates

Table 5.2.1. An overview of single scattering databases most relevant for MWI/ICI.

5.2.3 Particle populations

Here we deal with the question on how to map a known macroscopic atmospheric state to bulk single scattering properties, so that ICI/MWI measurements for that atmospheric state can be simulated. The ability to do this mapping is a prerequisite for any retrieval algorithm.

Since ICI/MWI is an operational mission, we assume that the atmospheric state is taken from an operational NWP model. The state of the art now and likely also at the time of ICI/MWI operation is for such models to have bulk hydrometeor microphysical schemes. That means, there are several hydrometeor species, for example cloud ice, cloud liquid, snow, rain, hail, and graupel. For each species, there are one or more prognostic variables. In the simplest case of a 1-moment bulk scheme that variable simply represents the mass density of the given hydrometeor (the first moment of the particle size distribution (PSD) if the independent variable is particle mass, or the third moment if the independent variable is particle size).

More sophisticated schemes also predict other moments of the PSD; several fairly new operational double-moment schemes use the combination of mass density and number density (Seifert and Beheng, 2006; Morrison, 2005; Milbrandt and Yau, 2005a, 2005b). The Seifert and Beheng scheme is implemented in the German Weather Service's ICON model. The Milbrandt-Yau scheme is implemented in Environment Canada's GEM model, which has been used to generate atmospheric scenes for the EarthCARE mission. One problem that arises with these new schemes when used for remote sensing, is that their particle distributions, although more physics based, are not necessarily more realistic than those of simple one-moment schemes, which are tuned to observations. This research field is currently in rapid development, and it is likely that there will significant progress in the next decade, not the least because of new airborne and satellite sub-millimeter measurements that give new constraints on particle size and habit.

5.2.3.1 Habit distributions

Although a lot of in situ particles observations by aircraft probes exist, the vast majority of these data have not been processed enough to be directly useful for building particle habit distributions, as needed for ICI/MWI. Figure 5.2.1, taken from a recent study by O'Shea et al. (2016) illustrates the problem: There is a complex "zoo" of different particles, and it is hard to extract systematic features from it. Note also that all cirrus clouds are far from equal; the two different flights/clouds in Figure 5.2.1 have very different ice particles even in corresponding temperature bins.

The trend is towards automatic classification of particles and extraction of statistical properties for the different identified habits, and again the O'Shea et al. article provides a good example, shown in Figure 5.2.2. With more digitized data on observed habit distributions we will be able to construct better habit models.

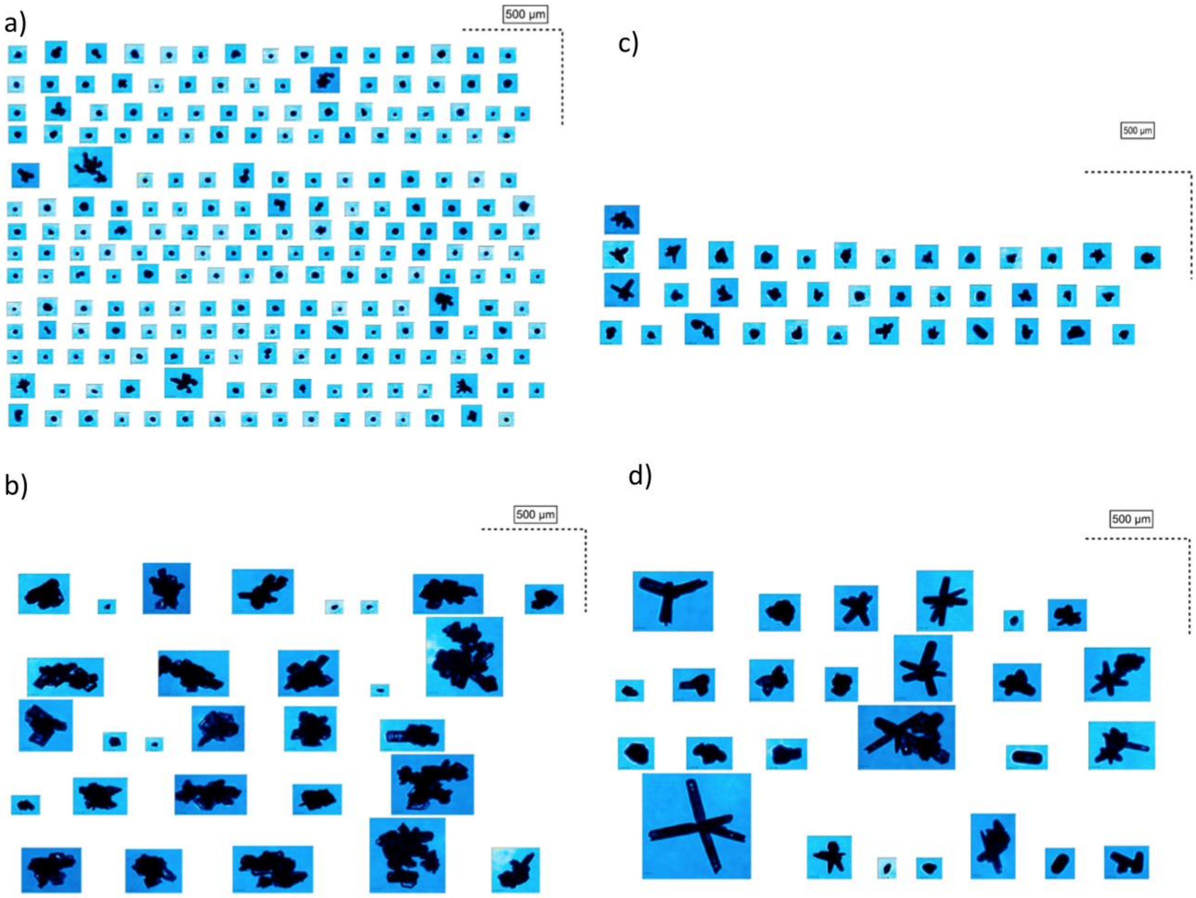

Figure 5.2.1: From O'Shea et al. (2016, Figure 7): Sample Cloud Particle Imager (CPI) images (>50 µm) during (a, b) 11 March 2015 and (c, d) 13 March 2015 for the temperature regions 230 K (a), 239 K (b), 226 K, (c) and 239 K (d). [© 2016, the Authors, reproduced under Creative Commons Attribution License (CCBY)].

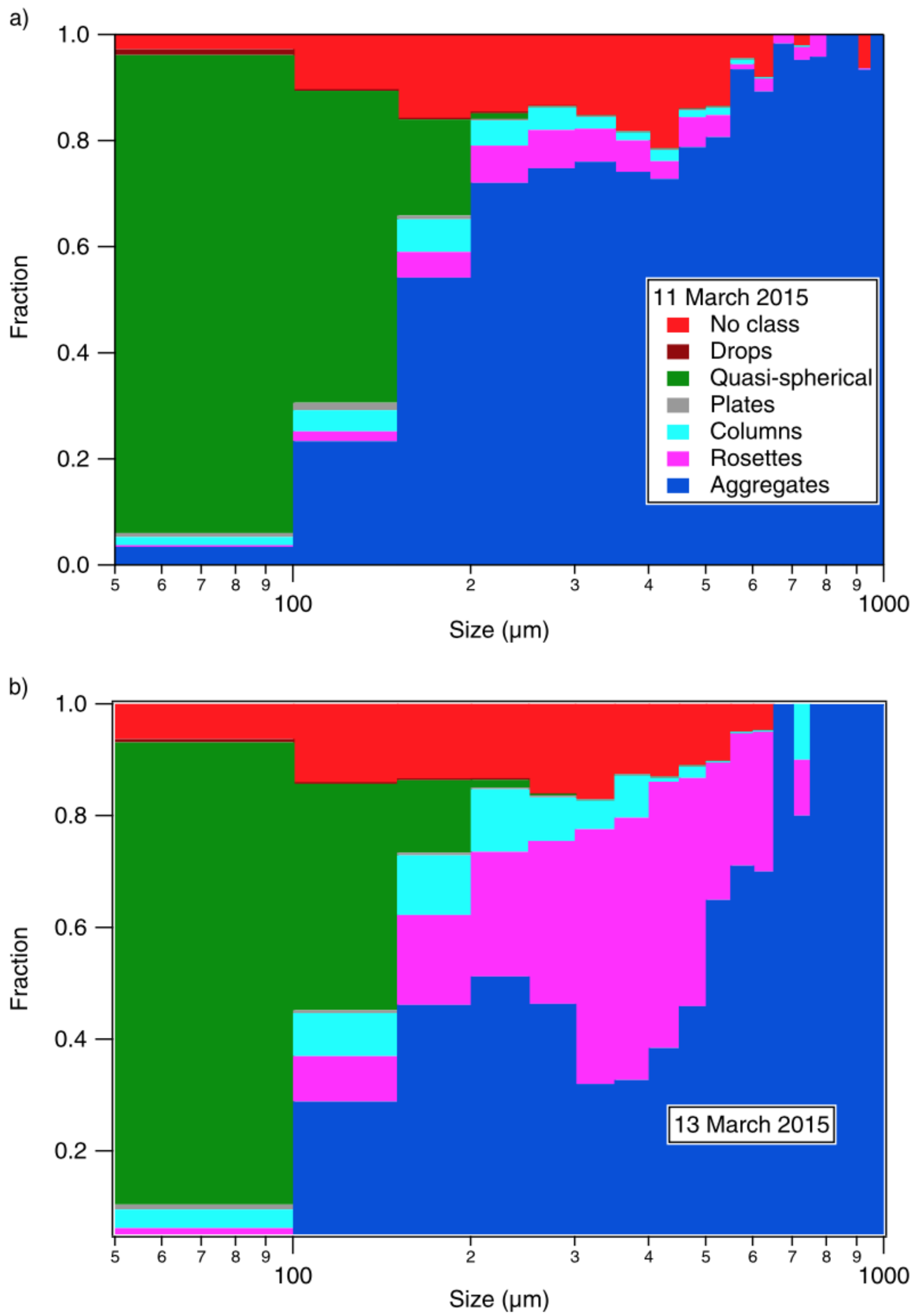

Figure 5.2.2: From O'Shea et al. (2016, Figure 8): Proportion of habits as a function of particle size for the cirrus sampling during flights (a) 11 March 2015 and (b) 13 March 2015. [© 2016, the Authors, reproduced under Creative Commons Attribution License (CCBY)].

5.2.3.2 Size, aspect ratio, and orientation distributions

For computing bulk single scattering properties, a size and orientation distribution has to be created for each particle habit. Once all the distributions have been set up, bulk single scattering properties can be generated by weighted averaging of single scattering properties of an appropriate ensemble or population of particles, taken from a single scattering database. Typically, that distribution depends both on literature results, such as in-situ measured particle size distributions, and on intimate knowledge of assumptions taken in the NWP model microphysics scheme, such as particle fall speed. In other words, the assumed distributions should be as consistent with both the model physics and the real world as possible. To what extent that goal can be achieved likely will depend strongly on the individual NWP model. For multi-moment microphysics schemes there are fewer degrees of freedom for tuning. This makes the task of setting up at least the size distributions easier (there is still no direct model information on shape and orientation, even for those schemes, even though there are broad constraints from the models intrinsic mass-dimension relationship). However, as mentioned above, more complex model microphysics does not necessarily imply better agreement with observations, due to less possibility for tuning.

The mapping of bulk cloud properties to bulk single scattering properties is an active area of research (e.g., Baran et al., 2013). Much more work in this area is needed in order to make full use of the ICI/MWI data.

5.2.4 Volcanic ash

We will not devote much space to it here, but it should at least be mentioned that ICI will be sensitive not only to ice particles, but also to volcanic ash particles (see Section 6.2.2 for further discussion). This could be explored in a dedicated study. The main issue for ash retrieval is that the refractive index is much more poorly known and likely also more variable than for ice particles. Microphysics questions, on the other hand, are likely less important, since the ash particles are comparatively small (at least the most interesting ones that get transported over large distances), and thus can be treated by Rayleigh scattering calculations, where shape is less critical. Quantitative ash mass estimates will depend on good estimates of the particle size distribution.

5.2.5 Summary

Particle scattering is an area that requires significant work for ICI/MWI. Particularly important are two sub areas: The first area is the generation of single scattering databases for realistically shaped and oriented particles. The second area is the selection of appropriate size, shape, and orientation distributions, for given bulk measurement or model data.

The two areas are closely related, since single scattering databases have to contain the right particles, those that occur in the size, shape, and orientation distributions. Which particle shapes form a good basis for representing single scattering properties is the overarching research question here. It is touched on in Geer and Baordo (2014) and Eriksson et al. (2015) but it is far from being finally answered.

Progress on these important questions requires dedicated aircraft campaigns with in-situ probes and radiometers, studies with existing satellite instruments, as well as a considerable effort on radiative transfer modeling, in tight collaboration with circulation model developers. While this can seem daunting at times, the positive side is that our understanding of cirrus clouds in particular will improve tremendously by the process of consolidating circulation models, in-situ, and remote observations. This is one of the main goals of the ICI satellite mission, which is more research driven than most other operational missions, given that it will be the first time that downlooking observations in this frequency range will become available from space.

5.2.6 References

Baran, A. J., Cotton, R., Furtado, K., Havemann, S., Labonnote, L.-C., Marenco, F., et al. (2013), A self-consistent scattering model for cirrus. II: The high and low frequencies, Quarterly Journal of the Royal Meteorological Society, 140(680), 1039–1057. http://doi.org/10.1002/qj.2193

Davis, C. P., D. L. Wu, C. Emde, J. H. Jiang, R. E. Cofield, and R. S. Harwood (2005), Cirrus Induced Polarization in 122 GHz Aura Microwave Limb Sounder radiances, Geophys. Res. Lett., 32, L14806, doi:10.1029/2005GL022681.

Eriksson, P., M. Jamali, J. Mendrok, and S. A. Buehler (2015), On the microwave optical properties of randomly oriented ice hydrometeors, Atmos. Meas. Tech., 1913–1933, doi:10.5194/amt-8-1913-2015.

Geer, A. J. and F. Baordo (2014), Improved scattering radiative transfer for frozen hydrometeors at microwave frequencies, Atmos. Meas. Tech., 7, 1839–1860, doi:10.5194/amt-7-1839-2014.

Hong, G., P. Yang, B. A. Baum, A. J. Heymsfield, F. Weng, Q. Liu, G. Heygster, and S. A. Buehler (2009), Scattering Database in the Millimeter and Submillimeter Wave Range of 100–1000 GHz for Nonspherical Ice Particles, J. Geophys. Res., 114, D06201, doi:10.1029/2008JD010451.

Liu, G. (2008), A Database of Microwave Single-Scattering Properties for Nonspherical Ice Particles, Bull. Amer. Met. Soc., 89(10), 1563–1570, doi:10.1175/2008BAMS2486.1.

Milbrandt, J. A., and M. K. Yau, (2005a), A multi-moment bulk microphysics parameterization. Part I: Analysis of the role of the spectral shape parameter, J. Atmos. Sci., 62, 3051–3064, doi:10.1175/JAS3534.1.

Milbrandt, J. A., and M. K. Yau, (2005b), A multi-moment bulk microphysics parameterization. Part II: A proposed three-moment closure and scheme description, J. Atmos. Sci., 62, 3065–3081, doi:10.1175/JAS3535.1.

Mishchenko, M. I., Travis, L., and Lacis, A. (2002), Scattering, absorption, and emission of light by small particles, Cambridge University Press.

Morrison, H., J. Curry, and V. Khvorostyanov (2005), A New Double-Moment Microphysics Parameterization for Application in Cloud and Climate Models. Part I: Description, J. Atmos. Sci., 62, 1665–1677, doi: 10.1175/JAS3446.1.

O'Shea, S. J., Choularton, T. W., Lloyd, G., Crosier, J., Bower, K. N., Gallagher, M., et al. (2016), Airborne observations of the microphysical structure of two contrasting cirrus clouds, Journal of Geophysical Research Atmospheres, 121(22), 510–536. http://doi.org/10.1002/2016JD025278.

Seifert, A. and Beheng, K. D. (2006). A two-moment cloud microphysics parameterization for mixed-phase clouds. Part 1: Model description. Met. Atm. Phys., 92:45–66.

5.3 Surface properties

MWI and ICI observations will include radiation from the atmosphere but also from the surface for the frequencies that show some atmospheric transmission. The surface contribution will be considered as the information source in the case of surface applications, or as a contamination to the signal in the case of atmospheric applications. In both cases, an accurate estimation of the surface signal is necessary for all channels that are sensitive to the surface contribution. The dryer the atmosphere, the larger the transmission, and significant transmission is observed even at frequencies above 100 GHz, a frequency range where limited studies explored the surface contribution so far. The surface contribution is directly related to its emissivity. The surface emissivity in the microwave varies strongly with the surface type, and several approaches have been developed, depending on the surface type.

5.3.1 The sea surface emissivity (ice-free)

Over open-ocean, the emissivities vary primarily with the surface wind speed, and efficient models have been set up to estimate the emissivity as a function of surface wind speed and direction, sea surface temperature, and salinity. The emissivity of a flat water surface can be calculated from the Fresnel equations for any incidence angle and orthogonal polarization, with the water permittivity calculated as a function of temperature and salinity. When the wind strengthens above the ocean, waves appear and the surface gets rough. The large-scale waves can be treated as an ensemble of facets, for which the Fresnel reflection applies, following geometric optics approach: the total emissivity is the sum of the contribution for each facet, weighted by the slope distribution. Small-scale roughnesses related to ripples have been added and current models include these two scales of roughness. In addition, above a certain wind speed, foam can appear. With an emissivity close to one (as compared to the low emissivity of water), the presence of foam can significantly modify the surface emissivity. Estimating the surface coverage of foam and its emissivity is difficult, and several models exist.

The dielectric properties of sea water depend upon its temperature and salinity. The salt is a good conductor and contributes to the imaginary part of the dielectric constant, for low frequencies. Above 20 GHz, the effect of salinity becomes negligible. Double Debye models have been developed to agree with the observations (Ellison et al., 1998), even at high frequencies up to 410 GHz (Liu et al., 2011).

The large-scale sea surface roughness is related to the surface wind speed. The Cox and Munk (1954) slope distribution, derived from optical measurements of the sun glitter, has been extensively used, in the visible and in the infrared, but also in the microwaves: the slope distribution is Gaussian and the slope variance is a linear function of the surface wind speed. Other more complex ocean roughness spectra have been developed (e.g., Elfouhaily et al., 1997). The geometric optics model that only takes into account the large-scale roughness is a first order approximation. It does not account well for the frequency dependence at low frequencies. The ocean small-scale roughness generated by the capillary waves also needs to be accounted for. Rigorous two-scale surface emissivity models have been developed to include the small-scale waves of the surface roughness (e.g., Yueh et al., 1994). As described in Liu et al. (2011), the two-scale model takes the same facet treatment as the geometric optic model for the large-scale wave but uses the bistatic scattering coefficients instead of the Fresnel reflection coefficients. The capillary waves are driven by the surface tension. It is difficult to separate the small and large scales of roughness in the spectrum. Different cut-off values have been suggested, depending upon the wind speed and the observation wavelength. For large frequencies, the cut-off frequency is large and the small-scale slope variance is not accounted for. It is anticipated that the small-scale roughness will have limited effect at high frequencies.

Calculation of the foam contribution requires the evaluation of the foam cover, as well as the foam emissivity. The foam coverage is usually calculated as a function of the surface wind speed (e.g., Monahan and O'Muircheartaig, 1986). Differences have been evidenced between the various parameterizations, with each parameterization fine-tuned to the specific region, but so far, limited improvement have been evidenced using complex parameterization, and direct retrieval from satellite have not been conclusive. The foam emissivity is known to be high, and is sometimes fixed at 1. Empirical models of foam emissivity have been derived from observations, as a function of frequency, incidence angle, and sea surface temperature (e.g., Stogryn, 1972). The foam emissivity has also been derived from modelling exercises, but they show significant variability (Anguelova, 2008), depending of the hypothesis and their practical application is questioned, especially at frequencies above 50 GHz.

The FAST microwave Emissivity Model (FASTEM) (English and Hewison, 1998; Liu et al., 2011) is adopted in the Radiative Transfer for (A)TOVS (RTTOV) and in the Community Radiative Transfer Model (CRTM). It has undergone several updates (from FASTEM-1 to -6). It corresponds to the parameterized of a two-scale model. The parameterization is optimized for frequencies up to 200 GHz that are currently observed.

Recently, in preparation for the new observations on board EPS-SG and under contract with EUMETSAT, a parameterization of the sea surface emissivity has been proposed from 10 to 700 GHz: TESSEM2 (Tool to Estimate Sea Surface Emissivity from Microwave to sub-Millimetre waves) (Prigent et al., 2016). It is based on the community model FASTEM at frequencies up to 200 GHz where FASTEM has been operationally calibrated and validated. It follows a physical emissivity model at higher frequencies (Prigent and Abba, 1990). A preliminary evaluation of TESSEM2 has been conducted by comparison with airborne International Sub-Millimetre Airborne Radiometer (ISMAR) observations from 118 to 325 GHz, under low wind speed (3 to 5 m/s) off the coast of Scotland. TESSEM2 is a fast parameterization that can easily be implemented in a community radiative transfer model: it is available to the community and will be distributed with the next version of RTTOV.

5.3.2 Generic land surface models

For land surfaces, there are two generic models that cover the full range of land surface environments. The Community Microwave Emission Modeling platform (CMEM) has been developed by ECMWF as the forward operator for the assimilation of low frequency passive microwave brightness temperatures of the surface from 1 to 20 GHz (Holmes et al., 2008). Its physics is based on the parameterizations used in the L-Band (1.4 GHz) and its extension to high microwave frequency should be considered with care. The Community Radiative Transfer Model (CRTM) benefits from up-to-date emissivity models especially in the microwave, with specific developments depending on the environments (Weng et al., 2001). It is a three-layer model characterizing the emission and scattering processes of various land surfaces such as snow cover, deserts, and vegetation. It offers the capability to simulate emissivities from 5 and 150 GHz for most land conditions. A major issue is the need of reliable global input parameters to the models, such as canopy water content, scatterer size, and fractional volume. Figure 5.3.1 presents an example of such CRTM simulations at 89 GHz, at 53° incidence angle and horizontal polarization, for January 2003, as coupled to the NASA Land Information System (LIS).

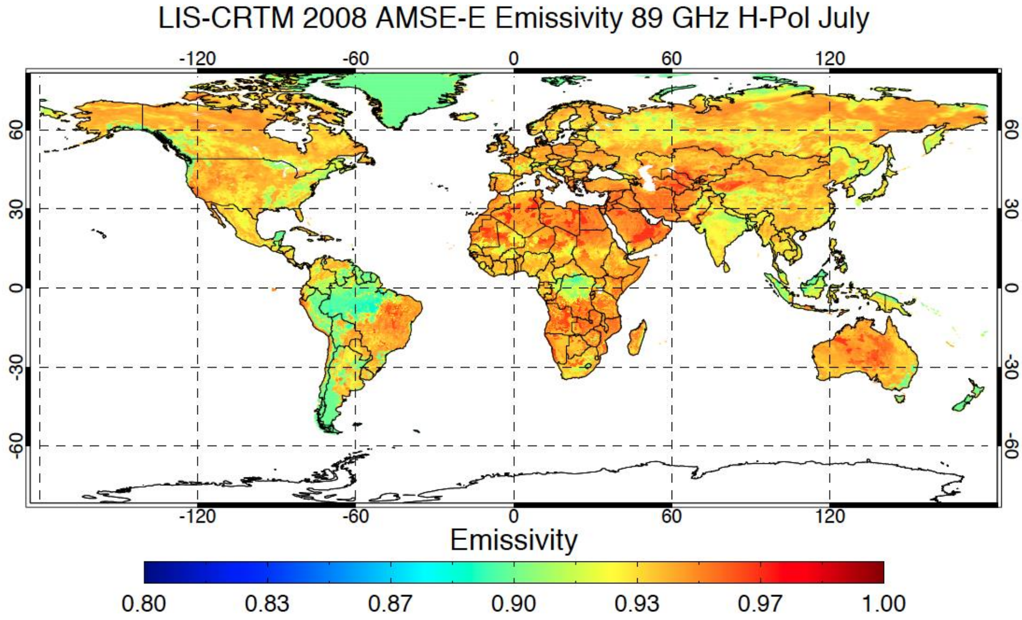

Figure 5.3.1. Land surface emissivity at 89 GHz, 53° incidence and H polarization for July, as modelled by CRTM with LIS as inputs.

5.3.3 Satellite-derived emissivity estimation

Emissivity estimates have also been calculated directly from satellites, subtracting the atmospheric contribution and the modulation from the surface temperature, using ancillary observations. This technique has been applied to conical imagers (e.g., Prigent et al., 1997) as well as to cross-track sounders (e. g., Karbou et al., 2005). The calculation usually assumes that the surface emits at the surface skin temperature (estimated from infrared satellite for instance, under clear sky conditions). However, when volume scattering is involved (such as in sand deserts and in dry snow), the radiation can come from the sub-layers where the temperature can differ from the surface skin temperature.

Analysis of the spectral, angular, and polarization dependences of these satellite-derived emissivities led to the development of the Tool to Estimate the Land Surface Emissivity in the Microwaves (TELSEM) (Aires et al., 2011), to provide a parameterization of the emissivity for all observing conditions and for all continental surfaces, given the surface location and month in the year, for frequency from 19 to 90 GHz. Figure 5.3.2 presents an example of these emissivity estimates at 85 GHz, 53° incidence angle and horizontal polarization for July.

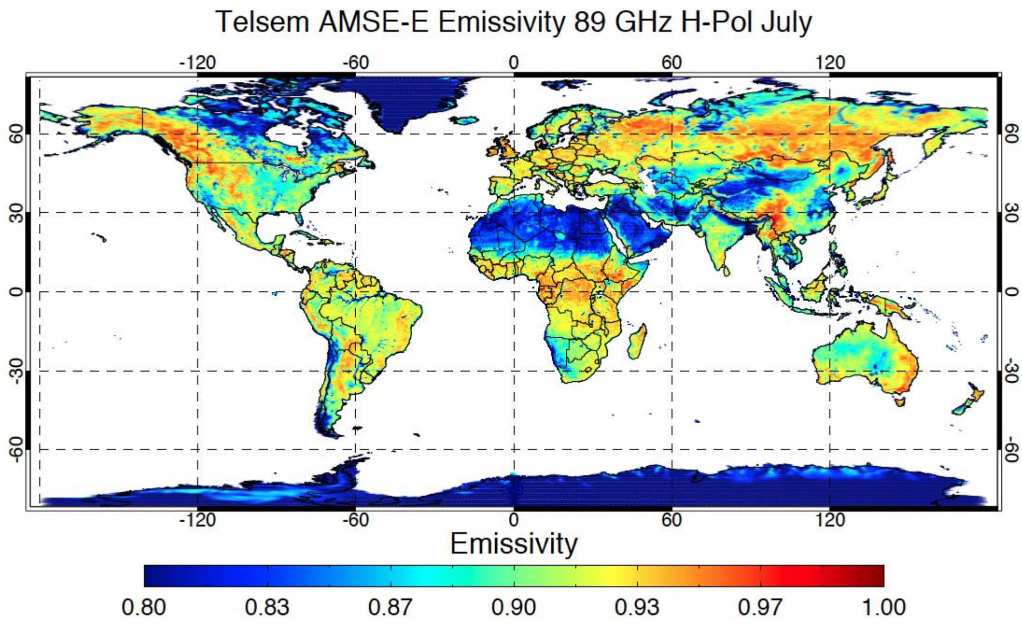

Figure 5.3.2. Land surface emissivity at 89 GHz, 53° incidence angle and H polarization for July, derived from TELSEM.

Significant efforts have been done recently to evaluate and compare different land surface emissivities up to 90 GHz, at local and global scales (e. g., Ferraro et al., 2013; Prigent et al., 2015). Large differences are observed especially over snow and desert where the model suffers from the lack of reliable inputs.

5.3.4 Snow and ice emissivity

Accurate estimation of microwave emissivities of snow and ice is particularly problematic. The variability of snow and ice is very high in space and time, and the interaction between the radiation and the snow / ice is very complex, as it involves both volume and surface scattering within heterogeneous media. Even at a local scale, ground measurements evidenced the difficulty to model the snow emissivity (see for instance Mätzler et al. (1994) measurements in the Alps up to 94 GHz). A variety of physical models have been developed to model the complexity of the snow emissivity, with two main models (besides the CRTM): the single-layer semi-empirical model from Helsinki University of Technology (HUT) (Pulliainen et al., 1999), and the Microwave Emission Model of Layered Snowpack (MEMLS) from University of Bern (Wiesmann and Mätzler, 1999). In MEMLS, the scattering coefficients are determined empirically from measurements whereas the absorption coefficient, the effective permittivity, refraction and reflection at layer interfaces are based on physical models and on measured ice dielectric properties (Mätzler et al., 2006).These models are developed primarily for the 5 to 100 GHz range, for rather small grain size typical of dry winter. A new land-surface community snow radiative transfer model SMRT is also currently under development, funded by ESA, with public release intended in 2017. This package, written in Python, will also likely be extended, in coordination with ESA, to sea-ice modelling, particularly for SMOS. It includes earlier models as plug-in packages and it provides new tools like a discrete ordinates solver, and is valid up to around 150 GHz. However, applications of any of these models at higher frequency is questionable, and alternative approaches have to be tested, or the existing models need to be extended, as evidenced from aircraft experiments up to 183 GHz (Harlow et al., 2012).

5.3.5 Sea-ice emissivity

Depending on its type (new ice, first-year ice, and multi-year ice), sea-ice exhibits different emissivity behaviours, related to differences in dielectric and scattering properties. With age, the ice thickness increases, its salinity decreases, and the potential snow cover changes. Figure 5.3.3 illustrates the variability of the ice emissivity as well as its frequency dependence, from airborne observations (Hewison et al., 2002).

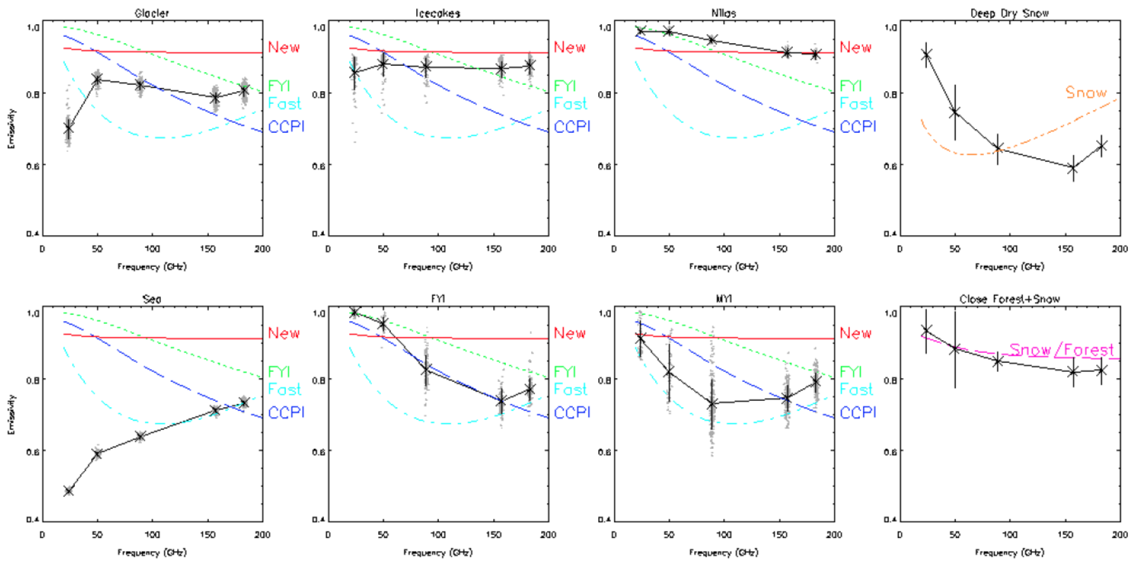

Figure 5.3.3. Sea-ice emissivity close to nadir, observed from instruments on board the UK Met Office aircraft, over the Barents Sea in March (black points and lines). Color lines represent previous estimates of the emissivities. From Hewison and English, 2002.

Based on MEMLS, a sea-ice emissivity model has been derived, modifying the dielectric properties to account for salinity and including possible liquid brine inclusions (e.g., Tonboe, 2010). The inputs of the model are the sequence of layers, their density, the correlation length, the temperature, and the volumetric liquid water content, and the brine volume. With increasing frequencies, the penetration depth in the sea-ice will decrease, and the impact of the sea-ice layering will decrease. However, the relative importance of the scattering by small scatterers will increase, as well as the necessity to properly describe the grain size distribution.

5.3.6 A global land and sea-ice emissivity atlas and parameterization

A parameterization of continental surfaces and sea-ice emissivities has recently been developed for frequencies up to 700 GHz, during a EUMETSAT contract: TELSEM2 (Tool to Estimate the Land Surface Emissivity at Microwaves and Millimetre waves) (Wang et al., under review, JAOT, 2017). It relies upon satellite-derived emissivities up to 200 GHz, and it is anchored to the SSM/I TELSEM monthly climatology dataset (19-85 GHz). Emissivities from Météo-France and NOAA at frequencies up to 190 GHz were used, calculated from SSMIS and AMSU-B observations. TELSEM2 has been evaluated up to 325 GHz with ISMAR observations over Greenland. Above continental snow and ice, TELSEM2 is consistent with the aircraft estimates in spatially homogeneous regions, up to 325 GHz. Over sea ice, the aircraft estimates are very variable spatially and temporally, and the comparisons with the TELSEM2 were not conclusive. TELSEM2 will be distributed in the new version of the RTTOV radiative transfer community code, to be available in 2017.

5.3.7 The way forward?

So far, most efforts in the understanding of the surface emission concentrated on frequencies below 100 GHz, where the atmospheric transmission can be significant. However, the surface contribution can still be observed at millimetre and sub-millimetre frequencies under dry environments and studies are needed to improve our estimation of the surface emissivity, especially for the frozen surfaces.

For the **ice-free ocean surfaces**, FASTEM has been widely used in the NWP community so far. A parameterization of the sea surface emissivity has been recently developed (TESSEM2), to complement FASTEM for frequencies above 200 GHz. Questions about the validity of the models were recently raised in NWP centres, even below 200 GHz, and there is a need for a consolidated reference sea surface physical model, valid over the full frequency range to be used in the Metop-SG area, from 1 to 700 GHz. Aircraft observations, combining measurements from 20 to 664 GHz with the FAAM instrumentation (DEIMOS, MARSS, ISMAR) should be encouraged, for a large variety of conditions, possibly under high wind speed conditions (above 7 m/s).

Over **land and sea-ice**, satellite-derived emissivity estimations have proved valuable up to 100 GHz, as direct inputs to atmospheric radiative transfer models or to assess and improve land surface emissivity models. At MWI frequencies below 100 GHz, observations can provide significant information about the surface characteristics. Modelling efforts should continue for snow and ice surfaces, with a special interest on continental to global applications, combining simple yet efficient parameterizations with realistic and available model inputs. This will lead to more accurate retrieval of the snow and ice characterization from the microwave satellite observations. Land surface temperature is now an essential climate variable and microwave estimates can complement infrared observations under cloudy areas. Additional work is to be done in the analysis of the microwave interaction with dry soil, to increase the accuracy of the land surface temperature in arid and semi-arid regions, under clear and cloudy sky conditions. Above 100 GHz, more work is needed to inter-compare the available satellite-derived estimates and eventually to produce new ones, especially over frozen surfaces where the emissivity frequency dependence is expected to be significant. From these analyses, the parameters that drive the space and time variability should be derived, to help the emissivity model developments. Additional ISMAR observations have to be performed, especially in boreal regions where the atmospheric transmission is low even at high frequencies and where the snow and ice emissivities are particularly variable and difficult to model.

Limited measurements of the dielectric properties of water (sea water and pure water) are available above 100 GHz, for the full range of temperature and salinity conditions. Additional dielectric measurements would help improve the surface emissivity models, but would also be welcome for the estimation of the cloud and rain absorption and scattering. Similarly, measurements of the dielectric properties of ice (pure and saline) should also be encouraged, for both surface and atmospheric applications

5.3.8 References

Aires, F., C. Prigent, F. Bernardo, C. Jimenez, R. Saunders, and P. Brunel (2011), A Tool to Estimate Land-Surface Emissivities at Microwave frequencies (TELSEM) for use in numerical weather prediction, Quart. J. Royal Meteorol. Soc., 137:690-699.

Anguelova, M. D. (2008). Complex dielectric constant of sea foam at microwave frequencies, Journal of Geophysical Research: Oceans, 113(C8), 2008.

Cox, C. and W. Munk (1954), Statistics of the sea surface derived from sun glitter, J. Mar. Res., 13, 198–227.

Elfouhaily, T., B. Chapron, K. Katsaros, and D. Vandemark (1997), A unified directional spectrum for long and short wind-driven waves, J. Geophys. Res., 102, C7, 15 781–15 796.

Ellison, W. J., A. Balana, G. Delbos, K. Lamkaouchi, L. Eymard, C. Guillou, and C. Prigent (1998), New permittivity measurements of seawater, Radio Sci., 33, 3, 639–648.

English, S. J. and Hewison, T. J. (1998). Fast generic millimeter-wave emissivity model. Proc. SPIE, Microwave Remote Sensing of the Atmosphere and Environment, 3508:288-300.

Ferraro, R. et al. (2013), An evaluation of microwave land surface emissivities over the continental United States to benefit GPM−era precipitation algorithms, IEEE Trans. Geo. Remote Sensing, 99, 1−21.

Harlow, R. C., and Essery, R. (2012), Tundra Snow Emissivities at MHS Frequencies: MEMLS Validation Using Airborne Microwave Data Measured During CLPX-II, IEEE Trans. Geosci. Remote Sens., 50, 11.

T.J.Hewison, N.Selbach, G.Heygster, J.P.Taylor and A.J.McGrath, 2002: "Airborne Measurements of Arctic Sea Ice, Glacier and Snow Emissivity at 24-183 GHz," Proceedings of IGARSS 2002.

Hewison, T. J., and S. J. English (1999), Airborne retrievals of snow and ice surface emissivity at millimeter wavelengths, IEEE Trans. Geosci. Remote Sens., 37,1871–1879.

Holmes, T., Drusch M., G, J.-P. Wigneron, S. Lafont, and R. de Jeu (2008), Assimilation of SMOS microwave brightness temperature, IEEE Trans. Geosc. Remote Sens., 46, 3, 846-856.

Karbou, F., C. Prigent, L. Eymard, and J. Pardo (2005), Microwave land emissivity calculations using AMSU measurements, IEEE TGRSE, 43, 5, 948- 959.

Liu, Q., F. Weng, and S. J. English (2011), An Improved Fast Microwave Water Emissivity Model, IEEE Trans. Geosc. Remote Sens., 49, 1238-1250.

Matzler, C. (1994), Passive microwave signatures of landscapes in winter, Meteorol. Atmos. Phys.,5 4, 241-260.

Matzler et al., (Eds.) (2006), Thermal Microwave Radiation -Applications for Remote Sensing, IEE Electromagnetic Waves Series,London, UK.

Monahan, E., and I. G. O'Muircheartaigh (1986), Whitecaps and the passive remote sensing of the ocean surface. International Journal of Remote Sensing, 7(5):627-642.

Prigent, C., and P. Abba (1990), Sea surface equivalent brightness temperature at millimeter wavelength, Ann. Geophys, 8, 627–634.

Prigent C., W. B. Rossow, E. Matthews (1997), Microwave land surface emissivities estimated from SSM/I observations, J. Geophys. Res., 102, 21867-21890.

Prigent, C., P. Liang, Y. Tian, F. Aires, J.-L. Moncet, and S.-A. Boukabara (2015), Evaluating modeled microwave emissivity, J. Geophys. Res, 120, 2706-2718, doi: 10.1002/2014JD021817.

Prigent, C., F. Aires, D. Wang, S. Fox, C. Harlow (2016), Sea surface emissivity parameterization from microwaves to millimeter waves, in press, Quart. J. Royal Meteo. Soc.

Pulliainen, J., J. Grandell, and M. Hallikainen (1999), HUT snow emission model and its applicability to snow water equivalent retrieval, IEEE Trans. Geosc. Remote Sens., 37, 1378-1390.

Stogryn, A., 1972: The emissivity of sea foam at microwave frequencies, J. Geophys. Res., 77, 9, 1658–1666.

Tonboe, R. (2010), The simulated sea ice thermal microwave emission at window and sounding frequencies, Tellus, 62, 333-344.

Wang, D., C. Prigent, L. Kilic, S. Fox, C. Harlow, C. Jimenez, F. Aires, C. Grassotti, and F. Karbou (2017), Surface emissivity at microwaves to millimeter waves over polar regions: parameterization and evaluation with aircraft experiments, under review, J. Atmos. Ocean. Tech.

Weng, F., B. Yan, and N. C. Grody (2001), A microwave land emissivity model, J. Geophys. Res., 106, 20115-20123.

Wiesmann, A., and C. Matzler (1999), Microwave Emission Model of Layered Snowpacks, Remote. Sens. Environ. 70:307-316.

Yueh, S. H., S. V. Nghiem, R. Kwok, W. J. Wilson, F. K. Li, J. T. Johnson, and J. A. Kong (1994), Polarimetric thermal emission from periodic water surfaces, Radio Sci., 29, 1, 87-96.

5.4 Radiative transfer considerations

The previous sections describe local radiative properties of the atmosphere and the surface, while the aim of "radiative transfer" (RT) is to simulate complete measurements. In the case of MWI and ICI, the primary task is to determine radiances at the top of the atmosphere, but when atmospheric scattering is significant, in principle, the complete radiation field inside the atmosphere must be estimated. Finally, various characteristics of the sensor must be considered. Simulations of "clear-sky" situations are discussed in Section 5.1.2, and focus is put on the difficulties raised by atmospheric scattering.

5.4.1 Theory

Local thermodynamic equilibrium can be assumed for microwave RT at least up to 100 km in altitude. For microwaves significant scattering occurs only inside the troposphere, and the scattering can be treated as both elastic and incoherent. Under these conditions, the basic equation to be solved is (Chandrasekhar, 1960; Mishchenko et al., 2002):

$$\frac{dI(\nu,r,\grave{n})}{ds} = -K(\nu,r,\grave{n})I(\nu,r,\grave{n}) + a(\nu,r,\grave{n})B(\nu,r) + \int Z\,(\nu,r,\grave{n},\grave{n}')I(\nu,r,\grave{n}')d\grave{n}' \quad (1)$$

where I is the Stokes vector, ν is frequency, r represents the atmospheric position, $\grave{n}$ is the propagation direction (at r), s is distance along $\grave{n}$, K is the extinction matrix, a is the absorption vector, B is the Planck function and Z is the scattering (or phase) matrix. The first term on the right-hand side represents extinction, the second emission and the third scattering into the line-of-sight. To evaluate the last term, the radiance from all directions must be known, which couples the RT along the $\grave{n}$-direction to RT along all other directions($\grave{n}'$). This results in that the complete radiation field becomes required, a difficult calculation task in the case of multiple scattering.

The complete polarisation state of the radiance is here described by the Stokes formalism. The Stokes vector has four elements. The first element gives the total intensity, while the three last ones express the difference between different specific polarisations (left/right, +45/-45and left-/right-hand circular polarisation, respectively).

5.4.2 Simplifications

If Eq. 1 is followed, and hence the full polarisation state is determined, it can be said that vector RT is made. Frequently only the first element of I is considered, which then corresponds to a scalar RT. At a given moment, the atmosphere exhibits variation in all three dimensions (3D), and to be totally general a RT software must be of 3D character, but horizontal (latitude and longitude) variations are frequently neglected. That is, the atmosphere is assumed to horizontally homogeneous, and only vertical structures are considered. This is denoted as 1D models.

Other geometrical simplifications are to neglect refraction and to operate with a "flat Earth". The latter combined with a 1D view on the atmosphere gives a plane-parallel atmosphere model. An issue related to atmospheric dimensionality is surface topography. A 1D model implies a constant surface altitude, while a 3D model can take topography into account. However, surface roughness can be considered also by 1D models. A general description of surface roughness requires the bidirectional reflectance distribution function (BRDF), but either a perfectly flat (specular) or a perfectly rough (Lambertian) surface, or a combination of the two, is normally used in practice (Mätzler, 2005).

5.4.3 Requirements

A model of spherical type is to prefer, but a flat Earth view should suffice to mimic MWI and ICI observations. The general impact of the ellipsoidal shape of the planet, as well as a small influence of refraction, can be handled separately by performing a ray tracing to determine the geographical position and the incidence angle at surface level, or at some representative altitude in the atmosphere. The found incidence angle is then used to set $\hat{n}$ of Eq. 1.

Polarisation is induced by the surface and non-spherical particles. Without any atmospheric scattering it is possible to apply scalar RT, and treat horizontal (H) and vertical (V) polarisation separately. Atmospheric scattering, already with total random orientation, results in a mixing of polarisations and a complete separation of H and V polarisation is no longer possible. For the same reason, it is not possible to handle oriented particles exactly by making separate H and V calculations. When the separation between H and V breaks down, and hence the limit of scalar RT is reached, should be determined by the degree of multiple scattering, but the exact limit is not known. In any case, multiple scattering occurs even at microwave frequencies, and if a single software shall be capable of handling all relevant situations it must operate with vector RT.

Despite that the real atmosphere is 3D, it is possible for some conditions to apply a 1D model. The demand is, that if a 3D atmosphere is sampled along the line-of-sight (down to the surface) and the obtained atmospheric and surface properties are applied in a 1D model, this should give approximately the same results as a 3D model given the original atmosphere. The combination of a blackbody surface and no atmospheric scattering is the only situation where this demand is fully met. With a reflecting surface, other parts of the atmosphere become influential, and a pure 1D view fails. However, it should in general be atmospheric scattering, and thus cloud and precipitation structures, that govern if 1D modelling can be used or not. If we assume that the surface and atmospheric gases have no horizontal variation, 1D models can be applied for any cloud field in the limit of only first-order (single) scattering, as for this assumption only cloud and precipitation particles along the line-of-sight have an impact.

The requirements depend also on the actual application of the data. In data assimilation for NWP, calculation speed is a main concern, as well as that the tangent linear or the adjoint model must be provided (section 6.2). To meet these criteria, several simplifications must be applied. Usage of most detailed RT tools is so far limited to stand-alone retrievals, based on training databases (section 6.1).

5.4.4 Sensor characteristics

The solution of Eq. 1 gives monochromatic radiances, while any real instrument has finite frequency resolution. Atmospheric properties vary little over each MWI and ICI pass-band and it is relatively straightforward to incorporate the associated frequency response. However, it should be noted that some channel side-bands have high separation, in relative terms. The separation reaches 8 %, that for Rayleigh-type scattering results in a 36 % higher scattering in the upper side-band than the lower one. Accordingly, for some channels, it is necessary to treat lower and upper side-band individually even for relatively rough calculations.

The instrument's antenna pattern causes a sensitivity to radiation from a range of directions, resulting in a "footprint". The angular response is normally not modelled in detail, instead a 1D model pencil beam calculation is used to represent the complete footprint. The limit of this approximation is normally discussed in terms of two effects. One of these effects is the general limitation of 1D RT transfer discussed above. A second effect is present when the relationship between cloud and precipitation properties and the impact on radiances is non-linear. In such non-linear situations the distribution of clouds and precipitation inside the footprint becomes influential, and the effect has accordingly been denoted as beam-filling. A way to overcome beam-filling, without going to 3D simulations, is to use the independent pixel approximation, meaning that a series of 1D calculations is made to incorporate the angular response of the antenna. See Davis et al. (2007) for a more detailed discussion of the topics raised in this paragraph.

5.4.5 Solution approaches and existing code

There exists a large number of RT packages, and a complete review cannot be given here. The scope of this software varies largely, from comprehensive packages to dedicated scattering algorithms. Also the target wavelength region differs, and some are not applicable for MWI and ICI as they are developed for the optical region. The key properties of some scattering solvers are summarised in Table 5.4.1. It is stressed that the table is not meant to be complete, neither that it indicates that this software should be superior to other RT tools. Instead, they are selected to reflect the high variety that exists, and the fact that even a single author (Evans), or community (ARTS), has developed different codes in response to different applications. In-depth comparisons of scattering solvers include Emde et al. (2015).

Several basic approaches to solve the scattering problem exist (see e.g. Thomas and Stamnes, 2002). Two relatively old approaches, both limited to plane-parallel atmospheres, are the Eddington approximation (EA, closely related to the two-stream method) and doubling and adding (DA). Both discrete ordinate (DO) and Monte Carlo (MC) methods are of general nature, but differ strongly in strength and weaknesses, see further Pincus and Evans (2009). Examples on approaches not reflected in Table 5.4.1 are the matrix operator method and successive order of scattering.

Of the solvers included in Table 5.4.1, only RRTOV and SHDOMPPDA support assimilation, and only the two scattering modules of the ARTS forward model combine 3D (column 3) and handling of oriented particles (column 6). The latter scattering solvers are also alone in going beyond a flat Earth approximation (column 4). Inclusion of oriented particles only makes sense if more than the first Stokes element is handled (column 5).

Name	Type	1D/3D	Geoid	Stokes	OP	Main reference
ARTS-DOIT	DO	1D+3D	free	1-4	yes	Emde et al. (2004)
ARTS-MC	MC	3D	free	1-4	yes	Davis et al. (2005)
DISORT	DO	1D	flat	1	no	Stamnes et al. (1988)
RTTOV-SCAT	EA	1D	flat	1	no	Bauer et al. (2006)
RT4	DA	1D	flat	4	yes	Evans and Stephens (1995)
SHDOM	DO	1D+3D	flat	1, 3, 4	no	Evans (1998)
SHDOMPPDA	DO	1D	flat	1	no	Evans (2007)

Table 5.4.1: Characteristics and main reference for some RT software capable of some scattering solvers. The second column gives the basic approach, see text for definition of acronyms. The second to last column indicates if oriented particles (OP) are handled. More comments are given in the text.

5.4.6 Discussion

Atmospheric scattering results in a demanding simulation problem and a RT software that is both fast and general is not yet at hand. Accordingly, basically all practical work is based on scalar plane-parallel models and there exists room for improvements. The impact of the different simplifications applied (mainly 1D and scalar RT) has been given little attention and must be characterised more in detail.

Today, it is likely that uncertainties in microphysical properties dominate over intrinsic RT simplifications, but to make use of the full information content of MWI and ICI further work on RT modelling is still needed. Handling of oriented particles is one example. The models used for data assimilation are of scalar type and they cannot properly model the difference between the dual polarisation channels of ICI. To extend these models to vector RT means both a big development task and a significant increase in calculation time. Although, no NWP atmospheric model actually operates with particle orientation and shape currently, the necessity of providing at least a simplistic representation of the effect of oriented particles on passive microwave radiances, even down to lower MWI frequencies, is becoming increasingly clear. Polarisation differences induced by scattering from oriented particles can easily reach 10 K in, for example, 90 GHz channels (Gong and Wu, 2017). These are not yet handled in fast models like RTTOV-SCATT. Stand-alone retrievals should utilize these polarisation signatures, but software suitable for microwave vector RT is either known to be slow (the ARTS solvers) or has unknown accuracy (RT4).

Beam-filling is a known issue for precipitation retrievals (e.g. Lafont and Guillemet, 2004). This effect can also be present in microwave ice cloud retrievals (Rydberg et al., 2009), but only the “case study” of Davis et al. (2007) provides information directly relevant for ICI. This study considered an extended mid-latitude case, but beam-filling could be more pronounced for other situations. For example, the worst case scenario with respect to beam-filling is likely tropical deep convection, where it should be remembered that MWI and ICI observe these semi-vertical structures in a slant geometry. Beam-filling is especially problematic as it causes a systematic retrieval error, but to consider the effect full 3D simulations, or at least the independent pixel approximation, must be used. It is not known in what circumstances these more advanced calculations options are required, but for example RTTOV-SCAT handles the beamfilling problem to sufficient accuracy for NWP assimilation using an effective cloud fraction approach (Geer et al., 2009)

5.4.7 The way forward

On the research side, the limitations and accuracy of the existing RT approaches should be investigated. Only with this information at hand it is possible to select the best RT tool for a specific application and to set up priorities for further development. The assessment can be divided into two main tasks:

- To determine the limits of pure 1D modelling and the independent pixel approximation. These limits likely vary with frequency and atmospheric conditions. The slant geometry of MWI and ICI is of special concern.
- Increase the understanding of polarisation signatures due to clouds and precipitation. Main issues to resolve are: Do we have a sufficient fast, but still accurate, vector RT tool? What is the limit of separate scalar H and V simulations. To what extent does 3D RT influence polarisation? Is there any way to disentangle degree of orientation and particle axial ratio?

These investigations are most easily performed if several basic scattering solvers are at hand inside a comprehensive RT software (to ensure consistent input and usage of all solvers) and development in this direction should be supported. RTTOV-SCAT (see below), or an equivalent solver (i.e. of 1D EA type), should be given high priority in comparisons of solvers.

Very fast RT tools are needed for a number of applications. In Europe RTTOV is the tool of choice for operational data assimilation and extensions of its scattering part (RTTOV-SCAT) must be made. The main short-term goal is to extend RTTOV-SCAT to also cover the frequency range introduced by ICI. The long-term development is presently a moving target, it depends both on the research studies outlined above and how the atmospheric models used for NWP progress regarding the description of microphysical properties of hydrometeors. Another application of fast RT tools is the “satellite simulators” used around climate models. Passive microwave observations are today scarcely treated by these simulators (then mainly by making use of RTTOV) and it should be considered to develop a general stand-alone RT package to support the usage of passive microwave data for verification of climate models. The combination of MWI and ICI should be especially suited for such studies.

In summary, the main recommendations are

- Support research activities targeting RT aspects, both to improve our general understanding and to make advanced scattering solvers more easily accessible to a broader part of the scientific community.
- Extend the scope of RTTOV to also handle the ICI frequency range.
- Rapidly assess whether there is any way of handling the zero-order effects of oriented particles within the non-vector radiative transfer used by RTTOV, and assess the errors involved compared to reference models such as ARTS. If RTTOV needs to be extended to support vector radiative transfer, this is a major task that needs to start soon.

- Consider if RTTOV is a suitable platform for supporting satellite simulators when it comes to passive microwave observations, or if this task is better handled by a dedicated package.

5.4.8 References

Bauer, P., Moreau, E., Chevallier, F., and O'keeffe, U. (2006). Multiple-scattering microwave radiative transfer for data assimilation applications. Q. J. R. Meteorol. Soc., 132(617):1259–1281.

Chandrasekhar, S. (1960). Radiative Transfer. Dover Publications, New York.

Davis, C., Emde, C., and Harwood, R. (2005). A 3D polarized reversed Monte Carlo radiative transfer model for mm and sub-mm passive remote sensing in cloudy atmospheres. IEEE T. Geosci. Remote, 43(6):1096–1101.

Davis, C. P., Evans, K. F., Buehler, S. A., Wu, D. L., and Pumphrey, H. C. (2007). 3-D polarised simulations of space-borne passive mm/sub-mm midlatitude cirrus observations: A case study. Atmos. Chem. Phys., 7:4149–4158.

Emde, C., Barlakas, V., Cornet, C., Evans, F., Korkin, S., Ota, Y., Labonnote, L. C., Lyapustin, A., Macke, A., Mayer, B., et al. (2015). IPRT polarized radiative transfer model intercomparison project–phase a. J. Quant. Spectrosc. Radiat. Transfer, 164:8–36.

Emde, C., Buehler, S. A., Davis, C., Eriksson, P., Sreerekha, T. R., and Teichmann, C. (2004). A polarized discrete ordinate scattering model for simulations of limb and nadir longwave measurements in 1D/3D spherical atmospheres. J. Geophys. Res., 109(D24):D24207.

Evans, K. F. (1998). The spherical harmonics discrete ordinate method for three-dimensional atmospheric radiative transfer. J. Atmos. Sci., 55(3):429–446.

Evans, K. F. (2007). SHDOMPPDA: A radiative transfer model for cloudy sky data assimilation. J. Atmos. Sci., 64(11):3854–3864.

Evans, K. F. and Stephens, G. L. (1995). Microwave radiative transfer through clouds composed of realistically shaped ice crystals. Part II. Remote sensing of ice clouds. J. Atmos. Sci., 52(11):2058–2072.

Geer, A. J., P. Bauer, and C. W. O'Dell. (2009). A revised cloud overlap scheme for fast microwave radiative transfer in rain and cloud. J. Appl. Meteorol. Clim., 48(11), 2257-2270.

Gong, J., and D. L. Wu., 2017: Microphysical properties of frozen particles inferred from Global Precipitation Measurement (GPM) Microwave Imager (GMI) polarimetric measurements. Atmos. Chem. Phys. 17(4), 2741-2757.

Lafont, D. and Guillemet, B. (2004). Subpixel fractional cloud cover and inhomogeneity effects on microwave beam-filling error. Atmos. Res., 72(1):149–168.

Mätzler, C. (2005). On the determination of surface emissivity from satellite observations. IEEE Geosci. Remote Sens. Let., 2(2):160–163.

Mishchenko, M. I., Travis, L., and Lacis, A. (2002). Scattering, absorption, and emission of light by small particles. Cambridge University Press.

Pincus, R. and Evans, K. F. (2009). Computational cost and accuracy in calculating three-dimensional radiative transfer: Results for new implementations of Monte Carlo and SHDOM. J. Atmos. Sci., 66(10):3131–3146.

Rydberg, B., Eriksson, P., Buehler, S. A., and Murtagh, D. P. (2009). Non-gaussian bayesian retrieval of tropical upper tropospheric cloud ice and water vapour from Odin-SMR measurements. Atmos. Meas. Tech., 2(2):621–637.

Stamnes, K., Tsay, S.-C., Wiscombe, W., Jayaweera, K., et al. (1988). Numerically stable algorithm for discrete-ordinate-method radiative transfer in multiple scattering and emitting layered media. Appl. Opt., 27(12):2502–2509.

Thomas, G. E. and Stamnes, K. (2002). Radiative transfer in the atmosphere and ocean. Cambridge University Press.

5.5 Evaluation tools

5.5.1 **Introduction**

The aim of this section of the science plan is to set out the requirement, and a strategy to meet this requirement, for the evaluation of data from the MWI and ICI missions. Evaluation in this context is taken to mean the characterisation, calibration and validation of data (both Level 1 and Level 2) from both missions. These requirements cover research and development activities to be carried out: pre-launch; in the immediate post-launch phase (to launch + 12 months); as well as longer tem activities to be carried out throughout the lifetime of the mission. The requirements, and activities required to meet these, are set out separately for the MWI and ICI missions in sub-sections 5.5.2 and 5.5.3 respectively.

The strategy for evaluating data from the MWI mission benefits from the experience accrued from similar microwave imaging missions (including SSMI, SSMI/S, TMI, AMSR-E/-2, MWRI and GMI) over the last three decades. The approaches developed through the evaluation and exploitation of data from these missions is summarised in Section 5.5.2.1. Given the maturity of the microwave imager applications base and experienced user community it is envisaged that an efficient and coordinated evaluation of MWI can be set out in this plan.

Analogously, the science and application base for the ICI mission is less mature and, consequently, the strategy for the evaluation of ICI data, although borrowing heavily from the MWI experiences, will require novel approaches.

5.5.2 **Microwave Imager (MWI)**

5.5.2.1 Heritage

The SSMI series of microwave imagers, first launched in 1987, have been widely used for data assimilation in numerical weather prediction (NWP) models (Gerard & Saunders (1999), and more recently Bauer et al (2010)) and for climate trend studies (Trenberth et al, 2005). Colton and Poe (1999) give the first account of a detailed evaluation of SSMI data quality, and present an inter-calibration of SSMI sensors. Ruf et al (2000) describe the use of vicarious calibration targets, including radiometrically cold ocean surfaces and radiometrically stable and homogeneous rainforests, to characterise the long term stability of measured brightness temperatures.

The successor to the SSMI series of instruments, the Special Sensor Microwave Imager/Sounder (SSMI/S) instruments, first launched in 2003, drew upon the SSMI experience, and also benefitted from the inclusion of temperature sounding channels, for which NWP models can be used very effectively to assess instrumental biases (Bell *et al*, 2008). The calibration and validation program for the first SSMIS, outlined in Kunkee *et al* (2008), involved a diverse array of approaches including aircraft underflights, co-located radiosonde launches, as well as NWP-based assessment. The inclusion of temperature sounding channels meant that the NWP-based analyses became the primary tool for the evaluation of subsequent SSMIS missions and several significant instrumental biases were identified, characterised and corrected, including reflector emission effects and solar intrusion effects. The inclusion of temperature sounding channels at 53.75 GHz and the channel suite at 118 GHz, mean that a similar approach can be followed for MWI. This evaluation should play a particularly key role in the early post-launch validation during the satellite in-orbit verification (SIOV) phase of the mission, as well as throughout the subsequent phases of the mission.

Evaluation of data from the TRMM Microwave Imager instrument (TMI) using NWP models revealed biases related to reflector emission (Geer et al, 2010) similar those experienced by SSMIS.

As the accuracy of NWP models, and the sophistication of data assimilation schemes have improved, particularly in the treatment of moist processes and scattering radiative transfer, the value of NWP-based evaluations of microwave radiometer data has steadily improved (see Lu *et al* (2011a,b), Bormann *et al* (2013)). In the most recent example from the assessment of data from GCOM-W AMSR-2 (Kazumori *et al*, 2015) subtle biases resulting from incorrect treatment of ocean surface emissivity, and the particular choice of scattering RT parametrisation were elucidated. Further improvements in the general use of NWP-based evaluations of microwave imager data are expected over the next 5-10 years, as work continues on the evaluation of data from the China's FY-3 microwave imager (MWRI) missions (Dong *et al* (2009)), GPM-GMI, Russia's Meteor-M MTVZA instruments and AMSR-2. The EU's GAIA-CLIM project (2014-2017) aims to perform a two NWP centre (ECMWF and Met Office) coordinated evaluation of data from GCOM AMSR-2.

The inter-calibration of microwave imager data is a central focus of the X-Cal group, under the auspices of GSICS, and the techniques developed here should be considered for the evaluation of MWI data. Post-launch activities should be coordinated where possible.

In summary, it is envisaged that NWP-based evaluation will play a central role in the evaluation of L1 data from the MWI mission from the SIOV phase onwards and from this requirement follows a set of activities to enable this to happen in an efficient way (Sections 5.5.2.2 - 5.5.2.4), coordinated across NWP centres. The use of reference quality data from radiosondes will also play a role in determining absolute radiometric uncertainties, and aircraft underflights will have a role in characterising observations at 118 GHz, which, even by 2021, will remain relatively new. These aspects are covered in more detail below.

5.5.2.2 MWI: pre-launch activities

An overarching principle of evaluation activities should be *coordination* in order to achieve effective and timely coverage of all critical scientific aspects of MWI data exploitation, whilst minimising cost and inappropriate redundancy. The activities outlined here are therefore some of the key elements of a Cal/Val plan for MWI.

The key activities pre-launch to support a timely and efficient NWP-based analysis of MWI data include:

- Establishing effective coordination between Cal/Val teams in the user community, and the instrument teams leading the SIOV and Cal/Val phase (launch to launch +6 months) of the MWI mission, including;

- Exchange of relevant measured instrument parameters (including channel centre frequencies, pass band forms, NEDT, antenna corrections and uncertainties, cross polarisation parameters, etc), by launch -18 months.
- Generation and distribution of sample L1 data sets in appropriate formats, to facilitate preparation of DA systems, by launch – 18 months.
- Consolidation of best available spectroscopy, surface parametrisations, scattering parametrisations & radiative transfer modelling into fast RT models to support NWP-based assessment of the data quality. This is covered in more detail in Sections 5.1 - 5.4.

Relating to the planning of aircraft-based Cal/Val activities:

- Review outstanding scientific issues (at launch – 24 months) relating to the exploitation of MWI data that cannot be addressed using NWP-based evaluation, to provide a focus for aircraft campaigns. Likely key areas include: radiative transfer at 118 GHz, surface emissivity over snow, ice and land; and the absolute radiometric calibration of MWI;
- Coordination, where possible, of aircraft campaigns by available facilities (including ISMAR, MARSS, DEIMOS, and HAMP in Europe, and others as appropriate).

Relating to the coordination of ground-based validation activities:

- Engagement with GRUAN community to establish the value of GRUAN data for MWI validation, and mechanisms for engagement (see Immler *et al* (2010), Calbet *et al* (2011)). Likely areas include validation of L1 measurements at 50, 118 & 183 GHz sounding channels – through forward modelling based on GRUAN measurements.

Regarding coordination with wider GSICS / Cross-Calibration activities:
- Engagement to ensure evaluation of MWI data is coordinated with Cross-Calibration /GSICS planning.

Many of these activities are closely related to, and dependent on, the evaluation of underlying spectroscopy and radiative transfer models, already covered in Sections 5.1 - 5.4 of this Science Plan.

5.5.2.3 MWI: early post-launch phase (SIOV) and Cal/Val

In common with other Metop-SG instruments, it is anticipated that the early in-orbit validation phase (‘Satellite In-Orbit Verification’, or SIOV) will be led by the industrial consortia instrument teams. Previous experience (from SSMIS and FY-3, for example) shows that this phase of the mission benefits from the early engagement with the extended Cal/Val team, in order that issues related to the instrument or ground processing system performance can be identified and rectified at the earliest opportunity. This has also proved successful in the early post-phases of the Metop IASI and ATOVS instruments.

Key activities are therefore:

- Earliest possible distribution of real data post-launch to extended Cal/Val team, timetable to be set-out at launch-12 months.

- Establish mechanisms for exchange of information during SIOV and Cal/Val, and feedback to instrument teams, to include launch + 2 months review of data quality involving Cal/Val teams.
- Early validation activities to include: generation of first guess departures for all MWI channels from designated lead NWP centres, within T+1 week of first data receipt; comparison of GRUAN equivalent radiances, within 1 month of data receipt; initial SNO comparisons (within 1 month of first data receipt).

5.5.2.4 MWI longer term post-launch evaluation

This will encompass evaluations from a range of applications, including global and regional NWP and nowcasting, sea-ice analysis, reanalysis and climate science. Major outputs from these activities are expected to be:

- Detailed evaluation of (consolidated, operational, NRT) data quality from the perspective of global and regional NWP-users, coordinated across European NWP centres through the EUMETSAT NWPSAF. Based on first guess departure based analysis and initial observing system experiments (launch+12 months).
- Detailed evaluation of the impact of MWI data in global NWP systems through extended observing system experiments, and through comparisons of impacts from similar microwave imagers (beyond launch + 12 months).
- Detailed assessment of the impact of MWI data in nowcasting systems and convective scale NWP systems, with a particular focus on the analysis and forecasting of the hydrological cycle, including extreme precipitation events.
- Evaluation of sea-ice products generated from MWI data, relative to existing state-of-the-art.
- Assessment of, and preparation of, MWI data as a fundamental climate data record (FCDR), to include comparisons & homogenisation with long term records from other microwave imagers, as well as an assessment of long-term radiometric stability.
- Assessment of MWI data in global and regional reanalyses.

5.5.3 **Ice Cloud Imager (ICI)**

5.5.3.1 Heritage

Unlike MWI, ICI is a completely novel operational instrument and therefore the strategy for evaluating ICI data - although borrowing some elements from that for MWI – will have to be *bespoke.*

Some aspects of the capability of ICI are familiar. The suite of channels at 183 GHz are common to the MWS and the MWI instruments on Metop-SG, as well as a large group of *on-orbit* operational sounders which, by 2021, are likely to include MHS (N-18, N-19, Metop-B and Metop-C), ATMS (S-NPP, JPSS-1 and JPSS-2), SSMIS (F-19 and F-20) and FY-3 (-C, -D and -E) MWHS-2. As outlined in Section 5.5.2.1 global NWP models will be a key tool for the evaluation of these channels. Model background errors, expressed in *observation space* (through $[\mathbf{HBH^T}]^{0.5}$), are currently around 1 K for these channels, and in the 2021-2025 timeframe will most likely be in the range 0.5-1.0 K, as a result of further improvements in NWP. This represents the model error for a single simulated radiance. Improved sensitivity can be achieved through spatial averaging, and therefore it's a reasonable expectation that NWP models will be able to detect instrumental biases at several tenths of a Kelvin for these channels.

For channels in the range 243-664 GHz the accuracy of radiances simulated from NWP models has yet to be established and is clearly dependent on both the models representation of ice cloud, as well as the ability of current RT models to represent atmospheric absorption/emission and scattering in this frequency range. Consequently, targeted pre-launch activities should focus on the validation of NWP-based simulations of TOA radiances in the 243-664 GHz spectral region. A large component of this will be the validation of radiative transfer models, and specifically the accurate treatment of spectroscopy (5.1), scattering parametrisation (5.2) and solutions to the radiative transfer equation (5.4).

Notwithstanding this, and anticipating that NWP based-simulations, even by 2021, will not be of sufficient accuracy to validate the radiometric performance of ICI it is expected that (ISMAR) aircraft campaigns will pay a central role in the development of the science base to exploit ICI data as well as post-launch validation of ICI.

5.5.3.2 Pre-launch activities

Similar considerations outlined for MWI in Section 5.5.2.2 apply here to ICI: an overarching principle of planned evaluation activities should be *coordination* in order to achieve effective and timely coverage of all critical scientific aspects of ICI data exploitation, whilst minimising cost and inappropriate redundancy. Some of the activities outlined below are key elements of a Cal/Val plan for ICI.

The key activities pre-launch to support timely and efficient *NWP-based* evaluation of ICI data include:

- Consolidation of best available spectroscopy, scattering parametrisations & radiative transfer modelling into fast RT models to support NWP-based assessment of the data quality. This will remain a rapidly developing area over the next 5 years and efficient exchange of findings will be critical to the effectiveness of new scientific developments. Key channels for this exchange will be: the Science Advisory Group (SAG); the ISMAR community & workshops; and the RTTOV & ARTS communities.

- Establishing effective coordination between Cal/Val teams in the user community, and the instrument teams leading the SIOV and Cal/Val phase (launch to launch + 6 months) of the ICI mission, including;

- Exchange of relevant measured instrument parameters (including channel centre frequencies, pass band forms, NEDT, antenna corrections & uncertainties, cross polarisation parameters, etc.), by launch -18 months.

- Generation and distribution of sample L1 data sets in appropriate formats, to facilitate preparation of DA systems, by launch – 18 months.

Relating to the planning of aircraft-based Cal/Val activities:

- Review outstanding scientific issues (at launch – 24 months) relating to the exploitation of ICI data, that cannot be addressed using NWP-based evaluation, to provide a focus for aircraft campaigns. Likely key areas include: gas phase spectroscopy 243-664 GHz; the accuracy of scattering parametrisations – especially fast parameterisations; RT modelling; assessment and validation of ice representation in NWP models.

- Coordination, where possible, of aircraft campaigns using available facilities (including ISMAR in Europe, and others as appropriate).

Relating to the coordination of ground-based validation activities:

- Engagement with GRUAN community to establish the value of GRUAN data for ICI validation, and mechanisms for engagement.

Many of these activities are closely related to, and dependent on, the evaluation of underlying spectroscopy and radiative transfer models, already covered in Sections 5.1 - 5.4 of this Science Plan.

5.5.3.3 ICI: early post-launch phase (SIOV) and Cal/Val

As noted in 5.5.2.3, in common with other Metop-SG instruments, it is anticipated that the early in-orbit validation phase (SIOV) will be led by the industrial consortia instrument teams. Previous experience shows that this phase of the mission benefits from the early engagement with the extended Cal/Val team, in order that issues related to the instrument or ground processing system performance can be identified and rectified at the earliest opportunity. This has also proved successful in the early post-launch phases of the Metop IASI and ATOVS instruments.

Key activities are therefore:

- Earliest possible distribution of real ICI data post-launch to extended Cal/Val team, timetable to be set-out at launch-12 months.
- Establish mechanisms for exchange of information during SIOV and Cal/Val, and feedback to instrument teams, to include launch + 2 months review of data quality involving Cal/Val teams.
- Early validation activities to include: generation of first guess departures for all ICI channels from designated lead NWP centres, within T+1 week of first data receipt; and comparison of GRUAN equivalent radiances (for 183 GHz radiances), within 1 month of data receipt.

5.5.2.4 ICI longer term post-launch evaluation

This will encompass evaluations from a range of applications, including global and regional NWP, reanalysis and climate science. Major outputs from these activities are expected to be:

- Detailed evaluation of (consolidated, operational, NRT) data quality from the perspective of global NWP-users, coordinated across European NWP centres through the EUMETSAT NWPSAF. Based on first guess departure-based analysis and initial observing system experiments (launch+12 months).
- Detailed evaluation of the impact of ICI data in global NWP systems through extended observing system experiments, and through comparisons of impacts from similar microwave imagers (beyond launch + 12 months).
- Detailed assessment of the impact of ICI data in nowcasting systems and convective scale NWP systems, with a particular focus on the analysis and forecasting of ice cloud;
- Assessment of, and preparation of, ICI data as a fundamental climate data record (FCDR).
- Assessment of ICI data in global and regional reanalyses.

5.5.4 **References**

Bauer P., A. Geer, P. Lopez, D. Salmond, Direct 4D-Var assimilation of all-sky radiances. Part I: Implementation, QJRMS, 12 October 2010, DOI: 10.1002/qj.659View/save citation

Bell, W., et al., 2008: The Assimilation of SSMIS Radiances in Numerical Weather Prediction Models. IEEE Transactions on Geoscience and Remote Sensing, 46, 884–900.

Bormann, N., et al, 2013, Evaluation and assimilation of ATMS data in the ECMWF system, Journal of Geophysical Research: Atmospheres, Volume 118, Issue 23, pages 12,970–12,980, 16 December 2013.

Calbet, X. et al, 2011, Matching radiative transfer models and radiosonde data from the EPS / Metop Sodankyla campaign to IASI measurements, Atmos. Meas. Tech., 4, 1177–1189, 2011, www.atmos-meas-tech.net/4/1177/2011/doi:10.5194/amt-4-1177-2011

Colton, M.C. and G. A. Poe, “Intersensor calibration of DMSP SSM/I’s:F-8 to F-14, 1987–1997,”IEEE Trans. Geosci. Remote Sensing, vol. 37,pp. 418–439, Jan. 1999.

Dong, C., et al., 2009: An Overview of Chinese New Weather Satellite FY-3A. Bulletin of The American Meteorological Society, 90, 1531–1544.

Geer, A. J., P. Bauer and N. Bormann , Solar Biases in Microwave Imager Observations Assimilated at ECMWF, IEEE Transactions on Geoscience and Remote Sensing - IEEE TRANS GEOSCI REMOT SEN , vol. 48, no. 6, pp. 2660-2669, 2010DOI: 10.1109/TGRS.2010.2040186

Gerard, E. And R. Saunders, Four-dimensional variational assimilation of special sensor microwave/imager total column water vapour in the ECMWF model, Q.J.R.M.S., October 1999, DOI: 10.1002/qj.49712556014.

Immler, F. J. et al, 2010,Reference Quality Upper-Air Measurements: guidance for developing GRUAN data products; H Atmos. Meas. Tech., 3, 1217-1231,doi:10.5194/amt-3-1217-2010, 2010

Kazumori, M., A.J. Geer, S.J. English, Effects of all-sky assimilation of GCOM-W/AMSR2 radiances in the ECMWF numerical weather prediction system, QJRMS, 11 November 2015, DOI: 10.1002/qj.2669

Kunkee, D. B. et al., 2008, Design and Evaluation of the First Special Sensor Microwave Imager/ Sounder, IEEE Tran. Geosci. Remote Sens., 46, 863-883, 2008.

Lu, Q., et al, 2011a, Characterizing the FY-3A microwave temperature sounder using the ECMWF model. J. Atmospheric and Oceanic Technology, 28.

Lu, Q., et al , 2011b, Improved assimilation of data from china’s FY-3A microwave temperature sounder. Atmospheric Science Letters, 13.

Ruf, C., 2000, Detection of Calibration Drifts in Spaceborne Microwave Radiometers Using a Vicarious Cold Reference, IEEE Transactions on Geoscience and Remote Sensing , Vol. 38, No. 1, January 2000.

Trenberth K.E. , J. Fasullo, L. Smith, Trends and variability in column-integrated atmospheric water vapour, Climate Dynamics (2005) 24: 741–758, DOI 10.1007/s00382-005-0017-4

6 Retrieval of geophysical variables

6.1 Retrieval theory

The main goal of retrieval techniques is to extract the geophysical information (atmospheric profiles and surface properties) contained in the set of brightness temperatures (radiances) to be measured by the MWI and ICI radiometers. Before describing the specific retrieval techniques to be developed for these two instruments, this section provides an overview of the most widely used retrieval methodologies. The retrieval theory is an inversion problem that is schematically presented in Figure 6.1.1. The direct problem is to simulate, with an appropriate numerical operator (noted *H* in the following), measured quantities (described by a vector y° of dimension N_y) from a number of geophysical quantities (described by a vector x of dimension N_x) The inverse problem is to retrieve the geophysical quantities x, knowing the measured quantities y. The fact that in general $N_x >> N_y$, makes the inversion an ill-posed problem (the solution is not unique). A direct consequence is that additional information is required to make the problem invertible. Such *a priori* information (obtained independently from the observations) is noted x_b (Figure 6.1.1). Most of the differences between retrieval methodologies are associated with the choice of this *a priori* information. Another type of differences lies in the capacity of accounting for non-linearities that are generally present in the operator *H*, that relates the x and y° quantities. An important aspect to be considered in the retrieval theory is the definition of an optimality criteria that is generally fulfilled in a statistical sense.

6.1.1 Retrieval methodologies

6.1.1.1 Importance of training databases

Most inversion techniques rely on databases of geophysical quantities x (atmospheric profiles) that have been used to simulate the observed quantities y (radiances at the top of the atmosphere). An important requirement is that the database samples a wide variety of atmospheric conditions in order to have a high probability to contain the situation of interest during the inversion process. The database needs to be large enough to fulfil this property. On the other hand, it cannot be too large in order to make the simulation of y affordable and also, when necessary, to make the search in the database during the inversion process not too costly. Inversions that are performed within cloud systems need to sample a wide range of situations, which were for a long time provided by cloud resolving models over specific case studies (tropical cyclones, squall lines, isolated storms, frontal systems, etc.). Inversions in clear sky conditions can rely on a smaller sample of profiles representing the Earth climate (from dry/cold conditions to warm/humid ones). Databases were originally built from radiosoundings such as the Thermodynamic Initial Guess Retrieval (TIGR) database (Chedin et al., 1985) but they tend to be superseded by atmospheric reanalyses (e.g. Uppala et al., 2005; Dee et al., 2011) that contain more profiles and additional physical quantities that are not measured by radiosondes. In particular, the description of clouds and precipitation in NWP models has increased in realism during the last ten years with higher spatial resolutions, making their short-range forecasts very convenient and rather accurate databases for the retrieval of geophysical parameters from remote-sensing data. The database of Chevallier et al. (2006) generated from the European Centre for Medium range Weather Forecasts (ECMWF) global Numerical Weather Prediction (NWP) model proposes a reduced set of atmospheric profiles having maximum variability for various meteorological parameters (temperature, water vapour, ozone, cloud hydrometeors, precipitating hydrometeors). A consequence is that the Probability

Distribution Functions (PDFs) of these profiles are not representative of the actual PDFs of the corresponding atmospheric variables over the globe. Even though it is less used nowadays, a number of databases have been built from the collocation of atmospheric profiles (radiosoundings) with actual satellite measurements (e.g. Alishouse et al., 1990). This approach does not require the simulation of the measurements. The spatial-temporal constraint for coincident (x, y°) values generally limits considerably the size of the database. In a classical manner in statistics, the database sample is divided in two sets, with a training database where the retrieval algorithm is built and a validation database where the accuracy of the retrieval is evaluated.

6.1.1.2 Statistical approaches

The simplest retrieval methods are based on multi-linear regression solutions where, from the knowledge of a training data set composed of M atmospheric profiles x coincident with observed (or simulated) radiances y°, a matrix **C** is searched such that:

$$x-\langle x\rangle = \mathbf{C}\,(y^\circ - \langle y^\circ\rangle)$$

where the symbol $\langle x\rangle$ represents the element-by-element average of the vector x.

The matrix **C** which minimizes errors in the above equation from in a least-square sense is:

$$\mathbf{C}=\mathbf{X}\mathbf{Y}^T(\mathbf{Y}\mathbf{Y}^T)^{-1}$$

X is a N_x x M matrix whose columns are the vectors $x-\langle x\rangle$ and **Y** is a N_y x M matrix whose columns are the vectors $y^\circ-\langle y^\circ\rangle$.

One problem with this regression solution is that no "filtering" of noise from the input profiles or radiances is done. As, a result, the **C** matrix can be unstable, that is small radiance errors can produce unacceptably large errors in the retrieved profiles. Such statistical schemes can be improved by filtering noise using statistical eigenvectors (Smith and Woolf, 1976) or through a singular value decomposition (Thompson, 1992).

More sophisticated linear methods account for the availability of an *a priori* information and for the uncertainties both in the observations and in the *a priori*. They are usually expressed in terms of *a posteriori* PDF: the mean or the maximum likelihood of this function gives the most likely state of the geophysical variables of interest (that is called an analysis in the NWP context). Indeed, from the Bayes theorem, it is possible to write this PDF as:

$$p(x|y) = p(y|x)p(x)/p(y)$$

where p(x) is the *a priori* probability density, p(y|x) is the likelihood function of x, and p(y) can be considered as a normalisation factor (independent of x). With Gaussian and unbiased error statistics for the *a priori* information and for the observations, expressed as covariance matrices **B** and **R** respectively, one can write:

$$p(y^\circ|x) = \exp(-0.5\,(y^\circ-H(x))^T\mathbf{R}^{-1}(y^\circ-H(x))) \text{ and } p(x)=\exp(-0.5(x-x_b)^T\mathbf{B}^{-1}(x-x_b))$$

Maximizing the PDF is equivalent to a minimisation of the opposite of its logarithm:

$$J(x) = 0.5(x-x_b)^T\mathbf{B}^{-1}(x-x_b) + 0.5(y^\circ-H(x))^T\mathbf{R}^{-1}(y^\circ-H(x))$$

In a linear context, one can write: $\mathbf{H}(x) = \mathbf{H}(x_b) + H(x-x_b)$, where $\mathbf{H}$ is the Jacobian matrix of H. Therefore, the solution (minimum of the above cost-function) can be estimated analytically as:

$$x_a = x_b + \mathbf{BH}^T(\mathbf{HBH}^T+\mathbf{R})^{-1} (y°-H(x))$$

and the associated covariance matrix of analysis error is : $\mathbf{A}^{-1}=(\mathbf{B}^{-1} + \mathbf{H}^T\mathbf{R}^{-1}\mathbf{H})^{-1}$.

In other situations (non-linear cases), the inversion problem is solved by a variational method, called 1D-Var for atmospheric profiles. The cost-function J(x) is minimized through an iterative process where its gradient is needed in order to find a new solution closer to the minimum (with classical algorithms such as conjugate gradient or quasi-Newton). The gradient of J is $\mathbf{B}^{-1}(x-x_b) + \mathbf{H}^T\mathbf{R}^{-1}(y°-H(x))$, which means that $\mathbf{H}^T$ the transpose of the Jacobian matrix of the operator H (also called adjoint operator) is necessary. The operator $\mathbf{H}^T$ can be rather costly to estimate either through a finite difference approach or through an analytical derivation of the non-linear code represented by the operator H.

In situations where the estimation of the **B** matrix can be rather difficult (for the retrieval of hydrometeors or other cloud properties), the solution of the Bayes theorem can be obtained by examining profiles in a pre-computed database and providing the mean value of the *a posteriori* PDF through a weighted average of the profiles according to their distance to the observations y°.

$$x_a = \Sigma\, x_i \exp(y°-H(x_i))\mathbf{R}^{-1}(y°-H(x_i)) \;/\; \Sigma \exp(y°-H(x_i))\mathbf{R}^{-1}(y°-H(x_i))$$

This method, called a priori database (APD) inversion scheme, has been widely used for the retrieval of precipitation profiles from microwave radiances (Smith et al., 1992; Mugnai et al., 1993; Kummerow et al., 1996, 2001; Olson et al., 1996; Marzano et al., 1999, 2010; Bauer, 2001; Di Michele et al., 2005; Viltard et al., 2006; Mugnai et al., 2013).

To address the ill-posed nature of the problem, the retrieval can be also performed in a reduced space so that empirical orthogonal functions (EOFs) are computed for the geophysical background covariance matrix to diagonalize it (e.g., Boukabara et al., 2011). Only a limited number of eigenvectors/eigenvalues are kept in this reduced space. The selection of how many EOFs to use for each parameter is somehow subjective, but it depends on the number of channels available that are sensitive to that parameter. The EOF transformation matrix (set of eigenvectors) is then used to project back and forth between the original and reduced spaces

Practical aspects regarding the specification of **B** and **R** matrices are given in the following sections.

6.1.1.3 Parametric approaches (neural networks)

In order to better handle the non-linear relationships between the observed quantities y and the geophysical variables x to be retrieved, artificial neural network (ANN) methods have been used. The most popular one is the "Multi Layer Perceptron" model proposed by Rumelhart et al. (1986). Once a database is available, the architecture (topology) of the network can be defined according to the complexity of the inverse problem of interest (number of hidden layers, number of neural in each hidden layer). In the learning phase, the optimal weights of the neural network are estimated. In practice, in order to avoid convergence problems, various regularizations are necessary such as linear transforms of the inputs (standardized variables) or a reduction of their dimension (e.g. principal component analysis). Moreover, the use of an *a priori* information and of noisy measurements can also help the convergence of the weights in the learning phase. The performances of the neural network are examined in terms of bias and variance. The bias identifies the inability of the neural network to fit the operator H with the training database. A too large bias indicates that there are too few degrees of freedom in the neural network that leads to a under-parameterization. When the complexity of the neural network is too large with respect to the operator H to be described (over-parameterization), the variance increases. The larger the dimension of the problem, the larger the training database should be.

6.1.1.4 Information content

The information content of a set of observations y° on geophysical quantities x can be obtained from linear optimal estimation theory. It is provided by comparing the *a priori* errors on x against *a posteriori* errors once the observations y° have been used to improve its estimation. A quantitative estimation is given by the Degrees of Freedom for Signal (*DFS*) or the Entropy Reduction (*ER*). The *DFS* represents the number of independent pieces of information from a measurement vector relative to noise. The *ER* represents the probabilities of possible states, it is maximum if all states have equal probability and it is minimum if all states except one have zero probabilities (Rogers, 2000). The *DFS* corresponds to the expectation value of the normalized difference between *a posteriori* state x_a and the *a priori* state x_b :

$$DFS = \mathrm{E}(x_a - x_b)^T \mathbf{B}^{-1}(x_a - x_b)) = \mathrm{Tr}(\mathbf{I} - \mathbf{AB}^{-1})$$

The *ER* is defined as the difference between the entropy *S* of the *a priori* probability distribution p(x) and the one of the *a posteriori* probability distribution p(x|y):

$$ER = S(\mathrm{p}(x)) - S(\mathrm{p}(x|y)) = 0.5\log_2(|\mathbf{B}|/|\mathbf{A}|)$$

Such method has been successfully used for the channel selection of hyperspectral infra-red instruments in order to consider only the most informative ones for assimilation in NWP models (e.g. Rabier et al., 2002; Collard, 2007). It has been mostly used for channel selection informative on clear sky conditions (temperature, water vapour, ozone, …) since the underlying linearity assumption is valid and the specification of background covariance errors **B** can be taken from operational NWP data assimilation systems (Holm and Kral, 2012). Despite having been applied for the information content of satellite radiances on clouds and precipitation (Di Michele and Bauer, 2006; Martinet et al., 2014) this method is more questionable since the operator H is strongly non-linear and the specification of a **B**-matrix for hydrometeors is more difficult (statistical description of errors that are very much situation-dependent).

6.1.2 Specific considerations for retrieval schemes

6.1.2.1 Detection of clouds and aerosols

In the situation where atmospheric quantities such as temperature and water vapour are to be retrieved in clear sky conditions (e.g. assuming the training database has been obtained in such conditions), the possible contamination of pixels by clouds and aerosols need to be identified in a pre-processing step in order to avoid biases in the retrievals. The availability of window channels on the instrument can provide useful information on clouds such as the cloud liquid water path (Grody et al., 2001) and the pixel can be declared cloudy when the quantity is above a prescribed threshold. Another method is to compare the clear sky simulated radiance with the observed one and to declare the pixel cloudy when the difference is above a given threshold. This technique has been refined by McNally and Watts (2003) for hyperspectral infra-red sounders, such that for each pixel, channels having most of their weighting functions above cloud top can be considered as clear-sky. When the payload of the satellite is such that additional instruments are available (e.g. visible and infra-red imagers at higher resolution) and pixels can be co-localized, sub-grid information on clouds can be provided within the scene of interest, and again thresholds can be applied in order to identify and reject cloudy pixels (Martinet et al., 2013). On the other hand, cloud identification can also be used to select pixels where to apply specific retrieval algorithms for the inversion of hydrometeor properties.

6.1.2.2 Surface characteristics

An accurate estimation of the surface contribution to the top-of-the-atmosphere radiance is essential in order to retrieve the signal from the atmospheric constituents (gases, hydrometeors, aerosols). Over oceans, fast and accurate surface emissivity models are available such as FASTEM (Deblonde and English, 2000) that is mostly dependent upon the surface wind, but is currently limited to frequencies below 200 GHz. The recent work of Prigent et al. (2016) have proposed an extension of the FASTEM model to microwave frequencies up to 700 GHz. Over other surfaces (land, sea-ice), a number of emissivity atlases are available (Karbou et al., 2006; Aires et al., 2011), with a recent extension of the TELSEM atlas to frequencies above 200 GHz (Wang et al., 2017). Another approach that can be considered is a direct inversion of surface emissivity in window channels through an inversion of the radiative transfer equation assuming that the surface temperature, and the atmospheric profiles from the *a priori* information are accurate enough. This approach has been applied successfully at Météo-France to assimilate microwave channels sensitive to the surface over land (Karbou et al., 2010) and sea-ice (Karbou et al., 2014).

6.1.2.3 Radiative biases computation: main causes and possible schemes

The retrieval techniques are optimal when the model and the observations are biased free. It is known that the systematic comparison of model and observations can display significant biases that arise from issues with cloud clearing, radiative transfer modelling (instrumental spectral response, assumptions on line shapes and on the water vapour continuum), or instrument geometry. A recent workshop was dedicated to examine the various origins of biases present in the simulation of channels in the 183 GHz water vapour absorption band (Brogniez et al., 2016). Biases can be removed by setting up multiple linear regressions with relevant predictors using a training database containing observed and simulated radiances. The proposal of Harris and Kelly (2001) has been widely used in the NWP context. It is now superseded by a dynamical approach (adaptive scheme) where the coefficients of the multiple linear regressions are estimated within the data assimilation system, allowing slow drifts of instruments to be corrected on the fly. This approach, named "variational bias correction" (Dee, 2005, Auligné et al., 2007), is only efficient if the data assimilation system is anchored by a number of unbiased observing systems (such as radiosoundings or GNSS-radio-occultation measurements).

6.1.2.4 Observation errors: instrument and forward model

The estimation of observation error should consider in addition to the instrumental noise (radiometric noise defined by NeΔT), the errors in the forward model, which can be rather large when considering the simulation of cloudy atmospheres (uncertainties in particles shapes, sizes and densities leading to uncertainties in radiative properties). The uncertainties in the specification of surface emissivity have also to be accounted for. Recently Aires et al. (2015) have proposed a pragmatic approach that accounts for atmospheric opacity in order to increase observations errors for rather transparent channels to reflect uncertainties in the specification of surface emissivity. Finally, representativeness errors have to be considered. They are associated with scale differences between the ones resolved by the profiles used to simulate the observations and the observations themselves. Within data assimilation systems, under optimality assumptions, it is possible to diagnose *a posteriori* errors from the comparison of observations with the background and the analysis states projected into the observation space (Desroziers et al., 2005). Such diagnostics are also useful to estimate error correlations (between channels), and the historical practice of neglecting them for convenience is currently changing in operational NWP centres (Weston et al., 2014). When a geophysical quantity can be estimated by three independent ways (e.g. two observing systems and a model simulation), the triple-collocation analysis (Stoffelen, 1998) can be used to derive the error of each system through the statistics of the differences between them.

6.1.2.5 A priori error characteristics

The *a priori* error characteristics are generally obtained through an ensemble of realisations. If a training database of profiles x is available a covariance matrix of a priori errors can be built from:

$$\mathbf{B} = E((x-\langle x\rangle)(x-\langle x\rangle)^T)$$

In the NWP context, *a priori* profiles are built from an ensemble of short-range forecasts that are issued from an ensemble of analyses from a set of data assimilation systems. Given the cost of NWP data assimilation systems, the statistics can only be generated with a small number of members, which leads to noisy results that need to be filtered in a suitable manner in order to extract the useful signal (Raynaud et al., 2009, Ménétrier et al., 2014). Holm and Kral (2012) have proposed *a priori* statistics from the ECMWF NWP system for single column retrievals of temperature, water vapour and ozone. When considering hydrometeors, a priori error statistics are more difficult to estimate from NWP systems, but solutions have been proposed with linearized physical parametrization schemes for clouds and precipitation (Bauer et al., 2005).

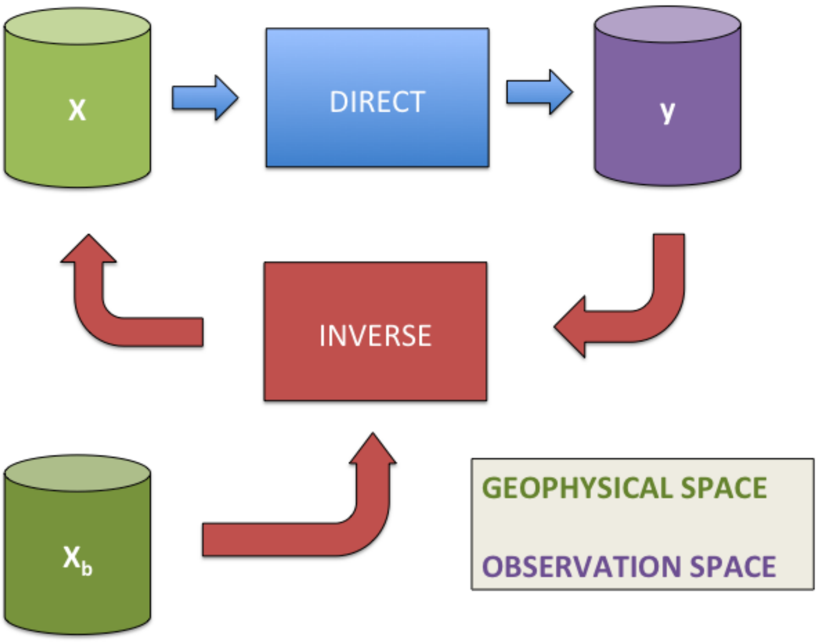

Figure 6.1.1. Schematic description of the retrieval technique of geophysical quantities (x) from observations (y) and using an a priori knowledge (x_b) of the geophysical quantities. The direct problem is represented by the blue box and arrows and the inverse problem is described by the red box and arrows.

6.1.3 References

Aires, F. C. Prigent, F. Bernardo, C. Jimenez, R. Saunders, and P. Brunel, 2011: A Tool to Estimate Land-Surface Emissivities at Microwave frequencies (TELSEM) for use in Numerical Weather Prediction. Quart. J. Roy. Meteor. Soc., 137, 690-699.

Aires, F., C. Prigent, E. Orlandi, M. Milz, P. Eriksson, S. Crewell; C.-C. Lin, and V. Kangas, 2015: Microwave hyper-spectral measurements for temperature and humidity atmospheric profiling from satellite: the clear-sky case. J. Geophys. Res., doi:10.1002/2015JD023331

Alishouse, J. C., Snyder, S. A., Vongsathorn, J., and R.R. Ferraro, 1990: Determination of oceanic total precipitable water from the SSM/I. IEEE Trans. Geosci. Remote Sens. , 28, 811-816

Auligné, T., A. P., McNally, and D.P. Dee, 2007: Adaptive bias correction for satellite data in a Numerical Weather Prediction system. Quart. J. Roy. Meteor. Soc., 133, 631-642.

Bauer, P.: Over-ocean rainfall retrieval from multisensory data or the Tropical Rainfall Measuring Mission, Part I: Design and evaluation of inversion databases, J. Atmos. Ocean. Techn., 18, 1315–1330, 2001.

Bauer, P., E. Moreau, and S. Di Michele, 2005: Hydrometeor retrieval accuracy using microwave window and sounding channel observations. J. Appl. Meteor., 44, 1016-1032

Boukabara S.-A., K. Garrett, W. Chen, F. Iturbide-Sanchez, C. Grassotti, C. Kongoli, R. Chen, Q. Liu, B. Yan, F. Weng, R. Ferraro, T.J. Kleespies, H. Meng: MiRS: An All-Weather 1D-Var Satellite Data Assimilation and Retrieval System, IEEE T. Geosci. Remote, 49(9):3249-3272, 2011

Brogniez, H., S. English, J.-F. Mahfouf, A. Behrendt, S. Boukabara, S. Buelher, P. Chambon, A. Gambacorta, W. Ingram, M. Matricardi, V. Payne, P. Thorne, J. Wang and W. Berg, 2016: A bias in observations in the 183 GHz water vapour absorption line: a mini-review.

Chedin, A., N. A., Scott, C. Wahiche, and P. Moulinier, 1985: The improved initialization inversion method: A high resolution physical method for temperature retrievals from satellites of the TIROS-N series. J. Clim. Appl. Meteor., 24, 128-143

Chevallier, F., S. Di Michele, and A. P. McNally, 2006: Diverse profile datasets from the ECMWF 91-level short range forecasts. NWP SAF Report.

Collard, A., 2007: Selection of IASI channels for use in Numerical Weather Prediction. Quart. J. Roy. Meteor. Soc., 122, 1977-1992

Deblonde, G., and S. English, 2000: Evaluation of FASTEM and FASTEM2 fast microwave oceanic surface emissivity model. Proc 11th Int. ATOVS Study Conf., Budapest, Hungary, WMO, 67-78.

Dee, D. P., 2005: Bias and data assimilation. Quart. J. Roy. Meteor. Soc., 131, 3323-3343.

Dee, D. P., et al., 2011: The ERA-Intermin reanalysis: configuration and performance of the data assimilation system. Quart. J. Roy. Meteor. Soc., 137, 553-597. Doi: 10.1002/qj.828

Desroziers , G., P. Brousseau, and B. Chapnik, 2005: Use of randomization to diagnose the impact of observations on analyses and forecasts. Quart. J. Roy. Meteor. Soc., 131, 2821-2837

Di Michele S., A. Tassa, A. Mugnai, F.S. Marzano, P. Bauer and J.P.V. Poiares Baptista: Bayesian Algorithm for Microwave based Precipitation Retrieval: description and application to TMI measurements over ocean, IEEE Trans. Geosci. Rem. Sens., ISSN: 0196-2892, vol. 43, pp. 778-791, 2005.

Di Michele S. and P. Bauer, 2006: Passive microwave radiometer channel selection based on cloud and precipitation information content. Quart. J. Roy. Meteor. Soc., 132, 199-1323

Grody, N., J. Zhao, R. Ferraro, F. Weng, and R. Boers, 2001: Determination of precipitable water and cloud liquid water over oceans from the NOAA-15 Advanced Microwave Sounding Unit. J. Geophys. Res., 106, D3, 2943-2953.

Harris B.A., and G. Kelly, 2001: A satellite radiance-bias correction scheme for data assimilation. Quart. J. Roy. Meteor. Soc., 127, 1453-1468.

Holm, E. V., and T. Kral, 2012: Flow dependent, geographically varying background error covariances for 1D-Var applications in MTG-IRS L2 processing. ECMWF Technical Memorandum N°XXX

Karbou F., E. Gérard, and F. Rabier, 2006: Microwave land emissivity and skin temperature for AMSU-A and –B assimilation over land. Quart. J. Roy. Meteor. Soc., 132, 2333-2355, doi:10.1256/qj.05.216

Karbou, F., E. Gérard, and F. Rabier, 2010: Global 4DVAR assimilation and forecast experiments using AMSU observations over land. Part I: impact of various land surface emissivity parameterizations. Wea. Forecasting., 25, 5-19

Karbou, F., F. Rabier, and C. Prigent, 2014: The assimilation of observations from the Advanced Microwave Sounding Unit over sea-ice in the French global Numerical Weather Prediction system. Mon. Wea. Rev., 142, 125-140.

Kummerow C., W. S. Olson, and L. Giglio: A simplified scheme for obtaining precipitation and vertical hydrometeor profiles from passive microwave sensors, IEEE Tran. Geosci. Remote Sensing, vol. 34, pp. 1213–1232, Sept. 1996.

Kummerow, C., Hong, H., Olson, W. S., Yang, S., Adler, R. F., Mc-Collum, J., Ferraro, R., Petty, G., Shin, D.-B., and Wilheit, T. T.: The evolution of the Goddard Profiling Algorithm (GPROF) for rainfall estimation from passive microwave sensors, J. Appl. Meteor., 40, 1801–1820, 2001

Martinet, P., N. Fourrié, V. Guidard, F. Rabier, T. Montmerle and P. Brunel, 2013: Towards the use of microphysical variables for the assimilation of cloud-affected infrared radiances. Quart. J. Roy. Meteor. Soc., 139, 1402-1416. Doi: 10.1002/qj.2046

Martinet, P., L. Lavanant, N. Fourrié, F. Rabier and A. Gambacorta, 2014: Evaluation of a revised IASI channel selection for cloudy retrievals with a focus on the Mediterranean basin. Quart. J. Roy. Meteor. Soc., 140, 1563-1577

Marzano, F. S., Mugnai, A., Panegrossi, G., Pierdicca, N., Smith, E. A., and Turk, F. J.: Bayesian estimation of precipitating cloud parameters from combined measurements of spaceborne microwave radiometer and radar, IEEE Trans. Geosci. Remote Sens., 37, 596–613, 1999.

Marzano F.S., D. Cimini, T. Rossi, D. Mortari, S. Di Michele and P. Bauer: High-repetition Millimeter-wave Passive Remote Sensing of Humidity and Hydrometeor Profiles from Elliptical Orbit Constellations, J. Appl. Meteor and Climat., ISSN: 1558-8424, DOI: 10.1175/2010JAMC2329.1, vol. 49, pp. 1454–1476, 2010

McNally, A. P. and P. D., Watts, 2003: A cloud detection algorithm for high-spectral-resolution infrared sounders. Quart. J. Roy. Meteor. Soc., 129, 3411-3423.

Ménétrier , B., T. Montmerle, Y. Michel, and L. Berre, 2014: Linear filtering of sample covariances for ensemble-based data assimilation. Part I: optimality criteria and application to variance filtering and covariance localization. Mon. Wea. Rev., 143, 1622-1643

Mugnai, A., Smith, E. A., and Tripoli, G. J.: Foundations for statistical – physical precipitation retrieval from passive microwave satellite measurements, Part II: Emission source and generalized weighting function properties of a time dependent cloud – radiation model, J. Appl. Meteor., 32, 17–39, 1993

Mugnai A., E.A. Smith, G. J. Tripoli, B. Bizzarri, D. Casella, S. Dietrich, F. Di Paola, G. Panegrossi, and P. Sanò: CDRD and PNPR satellite passive microwave precipitation retrieval algorithms: EuroTRMM/EURAINSAT origins and H-SAF operations, Nat. Hazards Earth Syst. Sci., 13, 887–912, 2013.

Olson, W.S., C.D. Kummerow, G.M. Heymsfield, and L. Giglio, 1996: A method for combined passive-active microwave retrievals of cloud and precipitation parameters. J. Appl. Meteor., 35, 1763-1789.

Prigent, C., F. Aires, D. Wang, S. Fox, and C. Harlow, 2016: Sea-surface emissivity parameterization from microwaves to millimetre waves. Quart. J. Roy. Meteor. Soc.,, doi:10.1002/qj.2953

Rabier, F., N. Fourrié, D. Chafaï, and P. Prunet, 2002: Channel selection for the Infrared Amospheric Sounding Interferometer. Quart. J. Roy. Meteor. Soc., 128, 1011-1027.

Raynaud, L., L. Berre, and G. Desroziers, 2009: Objective filtering of ensemble-based background-error variances. Quart. J. Roy. Meteor. Soc., 135, 1177-1199.

Rogers, C. D., 2000: Inverse methods for atmospheric sounding: theory and practice. World Scientific Publishing, London

Rumelhart , D. E., G. E., Hinton, and R. J. Williams, 1986: Learning internal representations by error propagation. pp. 318-362, in Parallel distributed processing: Explorations in the macrostructure of cognition 1. Eds. Rumelhart and McClelland. MIT Press

Smith, W. L. and H. M., Woolf, 1976: The use of eigenvectors of statistical covariance matrices for interpreting satellite sounding radiometer observations. J. Atmos. Sci., 33, 1127-1140

Smith, E. A., Mugnai, A., Cooper, H. J., Tripoli, G. J., and Xiang, X.: Foundations for statistical – physical precipitation retrieval from passive microwave satellite measurements, Part I: Brightness temperature properties of a time dependent cloud – radiation model, J. Appl. Meteor., 31, 506–531, 1992.

Stoffelen, A., 1998: Towards the true near-surface wind speed: Error modelling and calibration using triple collocation. J. Geophys. Res., 103, 7755-7766, doi:10.1029/97JC03180

Thompson, O.E.,1992: Regularizing the satellite temperature-retrieval problem through Singular-Value Decomposition of the radiative transfer physics. Mon. Wea. Rev., 120, 2314-2328.

Uppala, S.M. et al., 2005: The ERA-40 re-analysis. Quart. J. Roy. Meteor. Soc., 131, 2961-3012

Viltard, N., Burlaud, C., and Kummerow, C. D.: Rain retrieval from TMI brightness temperature measurements using a TRMM PR– based database, J. Appl. Meteorol. Climatol., 45, 455–466, 2006.

Wang, D., C. Prigent, L., Kilic, S. Fox, C. Harlow, C. Jimenez, F. Aires, C. Grassoti and F. Karbou, 2017: Surface emissivity at microwaves to millimetre waves over polar regions: parameterization and evaluation with aircraft experiments. J. Atmos. Ocean Tech. (accepted for publication)

Weston, P. P., W. Bell, and J. R. Eyre, 2014: Accounting for correlated error in the assimilation of high-resolution sounder data. Quart. J. Roy. Meteor. Soc., 140, 2420-2429. Doi: 10.1002/qj.2306

6.2 Retrievals of atmospheric and surface variables

Atmospheric monitoring is a major goal of current and future operational space missions. In this context spaceborne microwave radiometry plays a relevant role due to its capability to sound through clouds and to detect precipitation due to its well established spaceborne testing since late seventies (Wilheit et al., 1977; Barrett and Martin, 1981; Levizzani et al., 2007).

Satellite microwave radiometric imagers have demonstrated in the past and current space missions that surface and atmospheric variables can be fruitfully derived even in terms of gross vertical profiles of hydrometeors if spectral diversity and weighting-function concepts are exploited. The role of microwave radiometric missions is nowadays well established and recognized essential for any environmental analysis (Kidd and Levizzani, 2011; Reed et al., 2014).

As mentioned in Section 4, microwave imagers are focused on window frequencies with a typical suite of channels around 18/21 GHz, 30/40 GHz, 85/95 GHz, 155/165 GHz, but also absorption bands around 183 GHz (e.g., Ulaby and Long, 2014). MWI complements this frequency set by ingesting also channels around 50/53 GHz and 118 GHz, the latter for the first time operated in space. Indeed, the novelty of the EPS-SG microwave imagers is also related to ICI frequency bands which are set in the windows around 243 and 664 GHz plus the water-vapour absorption bands around 325 and 448, never exploited for atmospheric parameter retrieval from space by any EO mission so far. There is a clear complementarity of MWI with the frequency allocation of MWS, focussed on the exploitation of water vapour absorption bands around 23 and 183 GHz and oxygen absorption complex band around 53/60 GHz together with window frequency bands around 30/40 GHz, 50-52 GHz, 85/95 GHz and a new promising channel around 229 GHz.

6.2.1 Clouds, precipitation and thermodynamic variables

Satellite microwave radiometry has been used for temperature retrieval since the 1970s. Indeed, for this purposes microwave passive sounders are best suited due to their channel packages which are preferentially designed for gas-absorbing frequencies such as 50-60 GHz in the O_2 spectral complex (e.g., Marzano and Visconti, 2002). However, the new generation of microwave imagers, such as MWI and ICI, will provide profiling channels in the 50-60 GHz band and new channels in the 118-GHz O_2 band (apart from those conventionally around 22-GHz and 183 GHz due to atmospheric water vapour absorption). In this respect, MWI and ICI should have a significant added value for retrieving the clear-air scenario embedded within clouds and precipitation (e.g., Di Michele and Bauer, 2006). Clear-air and cloudy temperature and water vapour profiles should be heavily attached to the capability of the cross-track sounder MWS with its 24 channels in the frequency range of 23.8-229.0 GHz.

Objectives of microwave radiometric retrieval from space should be to perform the retrieval in all-weather conditions and over all-surface types using a physically-based approach which guarantees rigorous foundations, flexible modularity, and upgradable configurations to current and future space missions within a common framework. The various approaches described in Section 6.1 (1D-Var, APD, ANN) are well established, and can be adapted to MWI and ICI channels in a relatively straightforward manner. However, a number of specific challenges need to be addressed: the radiative transfer model for non-spherical ice particles, the handling of the polarization diversity and the characterization of surface emissivity for frequencies higher than 200 GHz.

6.2.1.1 Variational iterative Bayesian inversion scheme

The 1D-Var inversion scheme, introduced in section 6.1, employs a radiative transfer model (RTM) as the forward model together with its adjoint operator (e.g., Lorenc, 1995; Rodgers, 2000; Boukabara et al., 2007, 2011). The 1D-Var typically solves for the surface and the atmospheric parameters simultaneously, including hydrometeors. The surface can be represented by its temperature and emissivity spectrum, whereas the atmosphere is represented by the temperature, moisture, non-precipitating cloud, and precipitation profiles in both liquid and frozen phases. Besides these primary parameters, other products can be derived either by performing a vertical integration as in the case of the total precipitable water (TPW), cloud liquid water (CLW), ice water path (IWP), and rain water path (RWP), or by performing a more elaborate post-processing as in the case of the surface rainfall rate (RR) based on the hydrometeor parameters, for example, or the snow and ice properties based on the emissivity vector.

Note that the geophysical parameters of water vapour, cloud, rain, and ice are typically transformed into the logarithmic space before the retrieval for the twofold purpose of: i) avoiding the negative values; ii) making the geophysical parameter distributions more Gaussian distributed, which is a necessary condition for an optimal variational inversion.

Using all channels to retrieve all parameters simultaneously maximizes the information content available and accounts for the impacts from the multitude of parameters that affect the channels as much as possible, assuming that the sensor data is of high quality and that the RTM can simulate the measurements with low uncertainty. Lower-atmospheric temperature sounding channels, for instance, are sensitive to the surface, cloud, and tropospheric humidity, whereas water vapour sounding channels also have non-negligible sensitivity to temperature, ice, cloud, and rain. Surface-sensitive channels are also sensitive to the presence of cloud, rain, and water vapour. Therefore, this approach is adopted in 1D-Var to solve for all parameters simultaneously to benefit from their sensitivity to multiple channels and intercorrelations. Another important reason to use all channels is that the solution must fit all of the radiances measured simultaneously. This is not a sufficient condition to obtain the correct solution, but it is a necessary one: if the state vector retrieved is not satisfying the condition of fitting all measurements at the same time, the retrieval is not the solution (otherwise, the measurements are assumed wrong).

6.2.1.2 A priori database Bayesian inversion scheme

The input information of the APD inversion scheme, introduced in section 6.1, is tuned to the specific spaceborne radiometric system to handle and can include: off-nadir viewing angles, Earth-viewing incidence angles, across-scan sweep angles, scan track lengths, beam sizes according to channel frequencies, beam-to-beam separation lengths and the down-track/along-track instantaneous-field-of-view (IFOV) spatial resolutions. All of these system and geometric factors are a function of satellite height.

In addition to the multispectral brightness temperatures (TBs) measured by available satellite-borne radiometers, dynamical-thermodynamical-hydrological (DTH) parameter constraints can be used in the APD inversion algorithm (e.g., Mugnai et al., 2013).

6.2.1.3 A priori database neural-network inversion scheme

The ANN inversion schemes, introduced in section 6.1, have been used extensively for precipitation remote sensing which is characterized by a highly nonlinear response (e.g., Hsu et al., 1997; Chen and Staelin, 2003; Tapiador et al., 2004a, 2004b; Marzano et al., 2007; Surussavadee and Staelin, 2008; Mugnai et al., 2013).

Typical inputs of an ANN are the measured brightness temperatures and some ancillary data, such as latitude, longitude, surface height, the background surface type, season, pixel number and the secant of the zenith angle along the cross-track scan if needed. Geographical and meteorological parameters can be also introduced in order to mitigate against the ambiguity intrinsic to the precipitation retrieval process (e.g., Tapiador et al., 2004a, 2004b; Surussavadee and Staelin, 2008). Pixel number and secant of the zenith angle are also needed to determine the correction of the limb smearing on the TBs for cross-track scanning, an effect produced by the changing atmospheric path length along the scan. EOFs can be performed on radiometer channels to explore the possibility of decreasing the number of inputs, of reducing the effect of surface emission variability on the measured TBs and consequently of improving the network performance in retrieving surface precipitation (Mugnai et al., 2013). Canonical correlation analysis (CCA) can be also carried out to find the linear combination of the TBs (canonical variable) of the various channels with maximum correlation with the surface precipitation.

6.2.1.4 Precipitation screening and surface masking

Precipitation retrieval algorithms are typically organized into 2 steps: i) detection of precipitating cloud signatures (screening); ii) estimation of precipitating cloud parameters (extraction). The latter step has been discussed in the previous sections and can be accomplished using established approaches as 1D-Var, APD, ANN with their advantages and disadvantages (Ferraro et al., 1998). The first step about precipitation screening is actually essential before applying APD and ANN techniques, but in a full 1D-Var inversion is not needed as the emissivity spectrum is part of the state vector to be predicted. This means that the 1D-Var algorithm, as already mentioned, consistently estimates a surface emissivity compatible with the atmospheric state, background scenario and measured TBs. On the other hand, this means that the overall estimation accuracy of APD and ANN approaches is strongly dependent on the correctness of the preliminary precipitation screening.

The rainfall screening test for APD and ANN techniques can be linked to the type of surface involved (water, land or coast), depending on which type of channel frequency set is being used (e.g., Ferraro et al., 1998; Behrangi et al., 2009; Casella et al., 2015). The low-end channel frequency screening (between 18 and 95 GHz) typically requires knowledge of the type of surface within view whereas high-end channel frequency screening (above 150 GHz) does not require such knowledge. Detection-of-rainfall screening can involve emission-based tests, scattering-based tests, or both. For low-end screening over water, which has a relatively low and invariant emissivity, screening is not complex and an emission-based test using the lower frequencies of the low-end frequency set are used to determine if rainfall is present in the atmospheric column. For land, surface emissivities are much more variable and generally larger, all of which tend to obscure the emission signature of the water content in an atmospheric column – which is directly related to rainfall – creating a more complex screening process. Over coasts, a measurement involves a mixture of a radiometrically cold water surface and a radiometrically warm land surface, producing even more complexities than associated with land. In essence, rainfall screening for either land or coastal surfaces is designed to detect TB depressions due to scattering in the upper portions of the clouds, requiring use of the higher frequencies within the low-end frequency set in conjunction with a mix of emission and scattering-based tests. Schematically, a water surface emissivity is generally between 0.4–0.5. Thus, any precipitation over water generally augments the total radiation stream by emission and thus rain appears warm against a cold background. Each channel frequency responds differently to cloud liquid water depending on the droplet size. The complexity in detecting the presence of rainfall over land is due to the large and variable emissivity of the surface, with dependence on the type of surface, e.g., vegetation, snow, ice, desert, semi-arid soil, etc. Typically, these surfaces exhibit relatively large emissivities, ranging from 0.6 to 0.95 depending on their water content. Such elevated emissivities tend to obscure emission signatures stemming from liquid water in the atmospheric column, consequently requiring the use of scattering-based tests for the detection of rainfall. TBs at a given polarization or vertical–horizontal (V–H) TB polarization differences are dependent on channel frequency and surface type. In general, the scattering signature of rain is identified by a decrease in the V-polarized TB with an increase in frequency, although a snow surface may also indicate this property. Alternatively, for most surfaces, V–H TB polarization differences are greater at lower than at higher frequencies, whereas precipitation exhibits a somewhat flat V–H TB polarization difference with respect to frequency. Desert surfaces generally indicate the greatest V–H TB polarization differences when considering all land surfaces, although certain snow surfaces can exhibit such large differences. Because coastal measurement footprints represent a mixture of radiometrically cold water surfaces and radiometrically warm land surfaces, the associated screening schemes are, by nature, more complex than for either surface independently. The main problem originates from the fact that by combining opposite surfaces, a result is generated akin to adding the effects of rainfall whether rainfall is present or not. In essence, when land is in a footprint, the combining of surface water reduces the TB similar to how rainfall scattering creates a TB depression. Alternatively, when surface water is in a footprint, the combining of land increases the TB, similar to how rainfall emission creates a TB warming. Thus, detecting the presence of rain can involve ambiguities without a carefully designed sequence of emission-based and scattering-based tests.

6.2.1.5 Retrieval uncertainty, performance assessment and validation

After rejecting telemetry errors that result in nonphysical antenna temperatures (e.g., outside the 50–310 K interval), MWI-ICI data quality evaluation can be part of the algorithm design and aims at providing an intrinsic relative variance of the parameter estimate (e.g., Kummerow et al., 2001; Boukabara et al., 2011). The optimal estimation theory provides several quality assessment parameters associated to the retrievals such as the covariance matrix of retrieval errors, the contribution function, the average Kernel, as well as the *DFS* and the *ER* (Rodgers, 2000). These parameters are extremely relevant for NWP applications and blending techniques since they provide objective information about the uncertainties of the retrievals and the radiometric information content used on a point-to-point basis.

There are different types of performance assessments that can be carried out on MWI-ICI spaceborne microwave radiometer products on an instantaneous, daily or monthly basis: 1) The first one is the routine assessment of the retrieval algorithm with respect to other algorithms (e.g., 1D-Var, APD, ANN, regression), to NWP analyses (e.g., ECMWF, NCEP, GDAS) or to other spaceborne sensors (e.g., aboard NOAA, NASA, JAXA, CNES, CSA satellites). This assessment generally offers a global coverage of the comparisons, as well as robust statistics, given the abundance of points. Stratification of the performances (by angle, by scan position, by latitude, etc.) can also be done in this type of assessment. 2) The second type of assessment uses highly valued references to assess the performances and is the closest to the process of validation. Although the main advantage is the use of high-quality data (e.g., radar network data and raingauge network data for the rainrate assessment and radiosondes or dropsondes for the temperature and moisture profile assessment), it generally suffers from other limitations such as the geographical distribution of the reference data sources, the intra-variability of the reference data quality, and the representativeness of the footprint cell (w.r.t. the point measurement of the reference source). 3) The third type of reference assessment is simply a qualitative assessment of the behaviour of atmospheric retrieval products. The objective in this case is to ensure that the products behave individually and collectively in a physically and meteorologically consistent fashion.

Validation of microwave radiometric measurements and products is a complex activity (Ebert et al., 2007; Levizzani et al., 2007). It can be related to the routine monitoring of MWI-ICI inversion algorithm performances (computed against NWP analyses for instance), but indeed it is more focused either on a posteriori analyses of large datasets (eventually collected during routine monitoring) or on field campaigns including coordinated ground-based instrumentation and airborne instruments. Again, the goal of the validation should be directed toward the intercomparison of temperature and moisture sounding retrievals, concurrent surface parameters (emissivity, snow water equivalent, sea ice concentration) and clouds and hydrometeor parameters (cloud water profile, rain water profile, ice water profile, surface rainrate). These hydrometeor parameters are notoriously difficult to assess because of the multitude of unknowns in the cloud physical processes. They are also difficult to assess because of the difficulty to measure or estimate these quantities (from either ground-based or airborne sensors). The easiest quantity to assess among these hydrometeor parameters is the surface RR, which can be compared to both ground-based meteorological radars as well as to other algorithms (and other sensors) and surface-based rain gauges.

6.2.2 Volcanic ash clouds

Volcanic eruptions can cause serious threats to human life on local to regional and even global scales (Prata et al., 1991). Threats include health issues due to ash aspiration, the interruption of the air traffic due to the potential airplane engine failure, and climate changes induced by ash and sulfate aerosols dispersed in the stratosphere. The synergy of models and remote sensing tools is probably the best way to fulfil the main requirements suggested by the civil authorities and scientific communities (Rose et al., 2000; Zehner, 2010). Requirements can be divided into the following: 1) issuing timely warnings; 2) monitoring the ash plume during its evolution; and 3) quantitatively estimating the tephra, i.e., the fragmented material produced by a volcanic eruption. Due to the inherent limitations of individual measurements and methods, the characterization of the spatial and temporal scale dynamics of volcanic eruptions requires the combination of different types of observations (Sparks et al., 1997).

When the observation is close to the volcano vent, remote sensing instruments can be used to estimate the so-called near-source eruption parameters (Zehner, 2010; Marzano et al., 2013). The most common near-source parameters are the plume height, the tephra eruption rate, and mass. The retrieval of these parameters is crucial as an input for dispersion models that are designed to quantitatively predict geographical areas likely to be affected by specific levels of ash concentrations. Remote sensing measurements of tephra can also be used for model validation purposes. On the other hand, similarly to what is often done for water clouds, volcanic plume models can provide the physical basis to build model-based estimators of ash cloud parameters from remote sensors.

6.2.2.1 Evidences of volcanic ash cloud microwave signatures

Radar-derived retrievals cannot be compared with ground ash samples and drills due to unavailability of the latter till now (Marzano et al., 2011). Most volcanoes are very often out of range of operational radar systems for meteorological monitoring. Satellite-based ultraviolet and infrared sensors are used to study volcanic gas clouds and infrared sensors are used to track and characterize volcanic ash clouds in the atmosphere for up to several days after an eruption (Rose et al., 2000). However, near the volcanic vent, most of volcanic ash clouds are opaque in the ultraviolet to infrared region and appear as thick as meteorological clouds. As a result, visible-infrared (VIS-IR) sensors aboard LEO and GEO satellites are of limited use in determining the particle size distribution and mass of these opaque volcanic ash clouds. In this respect, passive observations from microwave (MW) radiometers on LEO satellites can offer useful complementary information due to the relatively low microwave extinction and high thermal emission of ash clouds (Delene et al., 1996; Marzano et al., 2013; Montopoli et al., 2013). This means that microwave brightness temperature is sensitive to the whole ash column and not only to the upper part as typical for VIS-IR radiometers both on LEO and GEO satellites. The major disadvantage of LEO microwave radiometers is the relatively poor spatial resolution which is of the order of few kilometers around 180 GHz up to tens of kilometers around 30 GHz. It is worth mentioning that the remote sensing principle of MW radiometers is completely different from that of MW radars, the latter being an active sensor based on backscattering response whereas the first a passive sensor detecting the thermal emission and multiple scattering.

Recent works have clearly shown the potential of spaceborne microwave radiometers for volcanic ash detection and estimation (Marzano et al., 2013). In order to examine the sensitivity of MW TBs to the presence and intensity of ash clouds, the considered Icelandic sub-glacial Grímsvötn 2011 eruption case study has been analysed and discussed by using data from SSMIS. Referring to horizontal and vertical polarization by H and V, respectively, Fig. 6.2.1 shows TB images (in K) at 37V, 91V, 150H and 183±6H GHz acquired by SSMIS aboard the F-16 DMSP satellite overpassing Iceland on May 21, 2011 at 08:46 UTC during the eruption of the Grímsvötn volcano. The TB depression, which is evident in all images around the volcano vent in terms of lower values with respect to the surrounding pixels, is the signature of the plume due to ash (and, if present, ice) particle scattering of the MW radiation emitted by the land/ocean background. The MW TB of this scene is clearly frequency and surface dependent: for example, the sea is relatively “cold” at 37 GHz due to the effect of quasi-specular surface low emissivity and “warm” above 100 GHz due to the effect of atmospheric water vapour whose contribution is not anymore negligible at these frequencies. Note that the surface features can be misinterpreted: ice glaciers have a signature which can be ambiguous with respect to ash clouds, especially below 100 GHz due to the fact that both targets are relatively efficient scatters with a low emissivity. Surface TB effects are more evident below 100 GHz with a radiometric signature of the cloud-free ice cap (especially in north-west area with respect to the vent where the ash plume was not dispersed), whereas around 183 GHz the strong emission of water vapour tends to mask the surface itself, as evident in the figure.

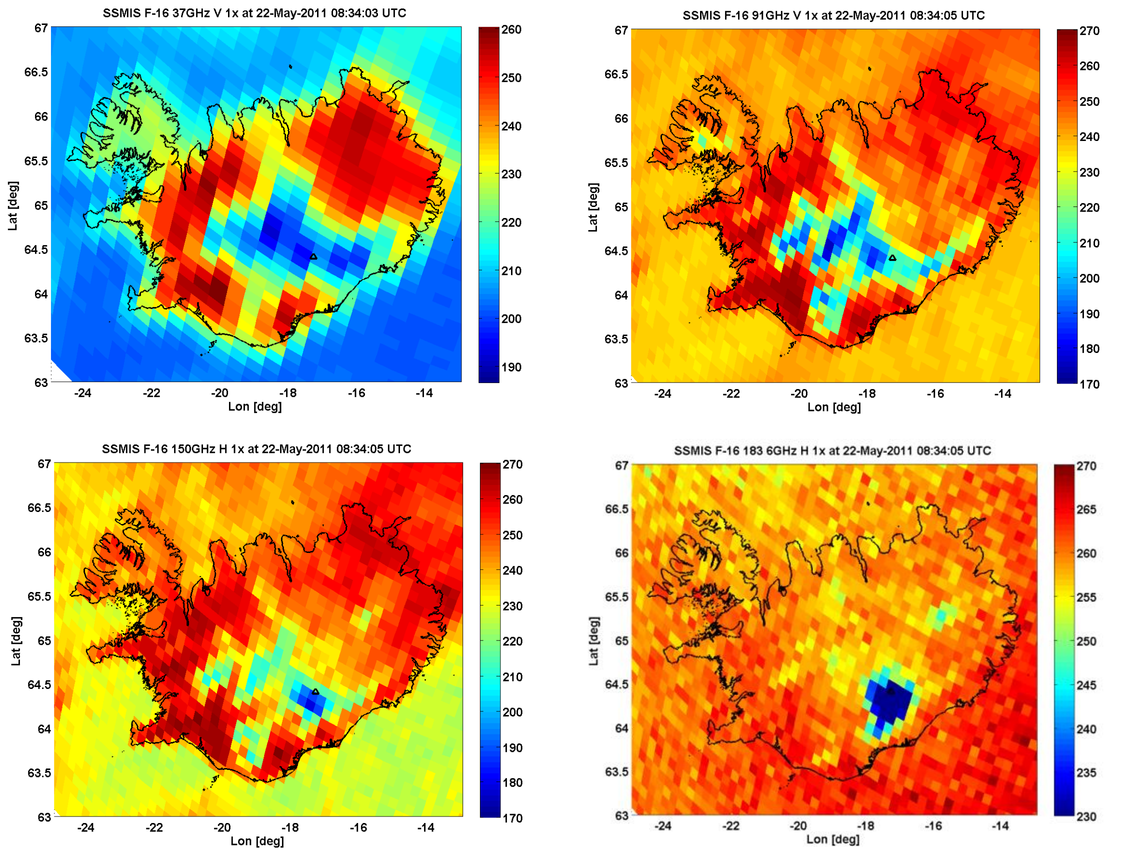

Figure 6.2.1. Brightness temperature (TB, K) images at 37, 91, 150 and 183±6 GHz at vertical polarization, acquired by SSMIS (Special Microwave Imager Special) aboard the DMSP satellite on May 22, 2011 at 8:34 UTC during the eruption of the Grímsvötn volcano. The signature of the ash cloud is evident in all images around the volcano vent (indicated by a black triangle) as a depression of the measured TB with respect to the land TB due to tephra (and possible ice particles) scattering of land emitted radiation (adapted from Marzano et al., 2013).

6.2.2.2 Remote sensing of volcanic ash cloud parameters

The potential of satellite passive microwave sensors to provide quantitative information about near-source volcanic ash cloud parameters has been recently assessed (Montopoli et al., 2013). To this aim, ground-based microwave weather radar and spaceborne microwave radiometer observations have been used together with forward-model simulations. The latter are based on 2-D simulations with the numerical plume model Active Tracer High-Resolution Atmospheric Model (ATHAM), in conjunction with a radiative transfer model, based on the delta-Eddington approximation and includes Mie scattering. The study area has been the same of Fig. 6.2.4, the Icelandic subarctic volcanic region of the Grímsvötn eruption in May 2011. ATHAM input parameters have been adjusted using available ground data, and sensitivity tests have been conducted to investigate the observed brightness temperatures and their variance. The tests have been based on the variation of environmental conditions like the terrain emissivity, water vapour, and ice in the volcanic plume. Quantitative correlation analysis between ATHAM/SDSU forward-model columnar content simulations and available microwave radiometric brightness temperature measurements, derived from SSMIS, have shown encouraging results in terms of both dynamic range and correlation coefficient. The correlation coefficients have been found to vary from −0.37 to −0.63 for SSMIS channels from 91 to 183±1 GHz, respectively. The larger sensitivity of the brightness temperature at 183 ± 1 GHz to the columnar content, with respect to other channels, has allowed to consider this channel as the basis for a model-based polynomial relationship of volcanic plume height as a function of the measured brightness temperature. These results suggest that MWI-ICI observations can be fruitfully exploited to detect ash clouds by using channel frequencies above 90 GHz and properly analysing the ICI response to ash layer particles up to 664 GHz.

6.2.3 Scientific priorities for MWI-ICI atmospheric parameter retrieval

The frequency allocation of MWI complements the conventional frequency set of SSMIS by ingesting also channels around 50/53 GHz and 118 GHz, the latter for the first time operated in space. Indeed, the novelty of the EPS-SG MW imagers is also related to ICI frequency bands which are set in the windows around 243 and 664 GHz plus the water-vapour absorption bands around 325 and 448, never exploited for atmospheric parameter retrieval from space by any EO mission so far.

Some basic issues are supposed to better handled with the use MWI-ICI : i) accuracy of the extracted vertical profile of cloud and precipitation particles with a given vertical and horizontal spatial resolution due to the inherent broad sounding of microwave channels, limited degree of freedom of the available measurements and beam-filling inhomogeneity; ii) opportunity to perform a separate retrieval of atmospheric and surface variables whose signatures are strongly coupled and tend to bias the retrieval if not taken into account with its variability; iii) effectiveness to use an a priori database for retrieving hydrometeor vertical profiles in terms of its representativeness and assumptions behind their building either they are derived from meteorological numerical models or from combined multisensor measurements. The physically-based retrieval approaches, quite well established, can be adapted to MWI and ICI channels in a relatively straightforward manner, being the radiative transfer model for non-spherical ice particles, the handling of the polarization diversity and the characterization of surface emissivity for frequencies higher than 200 GHz the criticalities to be faced.

On the basis of the previous sections and the above considerations, a science plan for improving MWI-ICI atmospheric products should be focused on:

1. RETRIEVAL. Development of a generalized retrieval algorithm able to ingest both MWI and ICI channels and to retrieve cloud and precipitation profile together with temperature and humidity profiles and surface parameters. An extension of such MWI-ICI algorithm to volcanic ash clouds could be envisaged considering the societal importance of this topic.

   The development of an inversion approach should carefully deal with the characterization of the estimation uncertainty of complete state vector, the measurement and/or modelling error covariance matrix and the establishment of robust forward model operator (together with its Jacobian) with respect to complete state vector. Precipitation screening, as a standalone approach, might be worth considering and eventually coupled within the inversion technique as an a priori information. The setup of a suite of inversion algorithms (e.g., 1D-Var, APD, ANN) can be envisaged for intercomparison purposes and to evaluate their spread together with ad hoc validation strategies using synthetic validation datasets.

2. MODELLING. Set up of an efficient and relatively refined forward model able to feed a MWI-ICI physically-based retrieval algorithm. This radiative transfer model should be able to simulate channel frequencies from 18.7 up to 664 GHz possibly in presence of non-spherical particles. The latter issue should be carefully evaluated since the significant uncertainty in the ice particle microphysics and large variability of satellite observation geometry may introduce a noise floor into the inversion process.

Moreover, any implementation of the forward model should demonstrate to be computationally efficient since the iterative inversion algorithms and a-priori global-scale simulation efforts are heavily affected by computation time. Surface emissivity database, at least as a background or first guess, should be available across the MWI-ICI frequency range. If ash clouds are considered as targets, their radiative transfer modelling should be also taken into account especially including ICI channel response which may resemble the thermal infrared radiometric response.

3. VALIDATION. The validation of MWI-ICI retrieval products should be carried by different perspectives, as already mentioned. First of all, we should separate the development and implementation stage before the satellite launch, from the operational and monitoring stage after the satellite launch. In the development stage, the design of the retrieval algorithm is expected to be tested on a similar satellite instrument. So far the closest spaceborne imager is the GMI aboard GPM and SSMIS board DMSP since even the new generation ATMS aboard S-NPP is a cross scanner. However, all these imagers lack of 118-GHz frequency band and ICI channels above 200 GHz. This means that the only to test these channels is to resort to airborne field campaigns using ad hoc instruments such as ISMAR (International Sub-Millimetre Airborne Radiometer). ISMAR is a new passive remote-sensing radiometer which has been jointly funded by the UK Met Office and the European Space Agency (ESA). It contains a number of heterodyne receivers operating at frequencies between 118 and 664 GHz, some with dual polarisation. Indeed, it is the first time in space mission planning that an operational instrument, such as ICI, is not anticipated by a prototype small mission in order to test its scientific concept and actual performances (apart from the technology readiness). This unusual scenario poses several unknowns, but also many opportunities to exploit ICI data.

   Thus, at least one or more field campaigns involving ground-based instrumentation and airborne observations not limited to ISMAR (e.g., as the recent IOP of HyMEx) are envisaged. On the other hand, the developed MWI retrieval algorithm should be applied to GMI and SSMIS and tested against their operational algorithms following a strategy (possibly stratified by angle, latitude, season, surface) which can involve: i) NWP analysis (e.g., ECMWF, NCEP, GDAS) and radiosonde for temperature/humidity profiles; ii) radar network data and raingauge network data for the rainrate assessment; iii) comparable retrieval products from other meteorological centres using the same satellite data, such as NASA Goddard centre, NOAA STAR (Satellite application and research centre) and EUMETSAT HSAF (Hydrology Satellite Application Facility); iv) daily or monthly global datasets such as those from EUMETSAT MPE (Multi-sensor Precipitation Estimate), NASA MPA (Multisatellite Precipitation Analysis), and JAXA GSMap (Global Satellite Mapping).

   In the operational stage, a MWI-ICI retrieval algorithm should be continuously monitored by using the same approach as in the development stage, but now employing its own measurement set and dedicated campaigns possibly in synergy with other space agencies (for example, within the GPM constellation concept).

4. INTERCALIBRATION. The use of MWI-ICI is envisaged to be within the GPM constellation concept and contributing to the essential climate record (ECR) variable time series for what concerns the hydrometeorological cycle. In this respect it is fundamental that MWI-ICI Level 1 TB data are properly calibrated by external targets (e.g., by using the vicarious cold calibration over sea surfaces) and intercalibrated with respect to the other current spaceborne radiometers. This step is of critical importance for the widespread usage

of MWI-ICI datasets for climate studies, but also for merging and assimilating retrieval products into environmental models.

6.2.4 Surface variables

The EUMETSAT SAF's are producing operationally a number of surface products based on satellite data. These include e.g. land surface temperature, sea ice concentration, and sea surface temperature. The primary stakeholders are the numerical modelling community running atmospheric and ocean forecast models operationally.

6.2.4.1 The retrieval of surface variables

Today the retrieval of surface variables such as sea ice is done at frequencies which are comparable to the window channels on MWI, in particular the 18.7-19, 31-37 and 89-91 GHz horizontal and vertical polarization channels. However, because of significant penetration through the atmosphere to the surface at the tropospheric sounding channels and even at the ICI suite of channels over deserts and in polar regions it will also be necessary to retrieve surface parameters such as the surface emissivity and the effective temperature for atmospheric sounding applications also at the sounding frequencies on EPS-SG. These applications are yet to be developed and the estimation of emissivity and effective temperature for frequencies above 100 GHz is indeed an open research topic (see section 5.3).

Water surface temperature and emissivity
The retrieval of surface temperature and surface emissivity are intimately linked. When measuring the upwelling brightness temperature onboard the satellite there are contributions from the atmosphere, galactic and atmospheric reflected emission and then the product of the emissivity and the effective temperature of the surface. The relative contribution from the surface compared to the atmosphere is depending on the composition of the atmosphere and the electromagnetic wavelength and the surface emission itself whether that being land, sea ice or open ocean (Ulaby et al., 1986). At sounding frequencies and at ICI frequencies the atmosphere is virtually opaque and the entire signal stems from atmospheric emission except in polar and in desert regions where the atmosphere is very dry and there is a contribution from the surface.

The ocean surface brightness temperature is a function of surface effective temperature, wind speed and direction, and for frequencies less than about 10 GHz also the sea surface salinity (salinity is not applicable to MWI-ICI) (Ulaby et al., 1986; Meissner and Wentz, 2012; Saunders et al., 1999). Both in the microwave and in the infrared the penetration depth into the water is very shallow (in the order of a millimeter or less) which means that the effective temperature is very close to the skin temperature or the sea surface temperature (SST) and temperature gradients caused by evaporation within the upper millimeters of the ocean can be simulated to match up measurements in the infrared, microwave and on drifting buoys (e.g. Donlon et al., 2002). Cloud detection schemes for measurement of SST using infrared channels are effective over open water which means that the global SST is measured accurately by both polar orbiting and geostationary infrared satellites. This will also be the case with e.g. the IASI NG and the Metimage instruments on Metop-SG A. In addition, the cloud penetrating microwave 6 GHz AMSR-2 radiometer measuring SST has complete global coverage at coarser spatial resolution. The brightness temperature is proportional to SST near 6 GHz. Having an accurate estimate of SST constrains the estimation of the sea surface emissivity (English, 2008).

The emissivity is a key element in humidity and temperature sounding applications using microwave radiometers like MSU and eventually MWI and MWS. The sea surface emissivity can therefore be simulated accurately at both sounding and window frequencies because of the accurate SST estimates and the mature emission models for the ocean surface and the atmosphere.

Land surface information

Microwave observations can provide Land Surface Temperature (LST), regardless of the cloud cover, contrarily to the infrared measurements that are only possible under clear sky conditions. Land surface temperature information is attracting more and more attention, even in Numerical Weather Prediction (NWP) centres. The best frequencies to estimate the LST from microwave are between 18 and 40 GHz: at lower frequencies, the signal sensitivity to the subsurface increases and at higher frequencies the atmospheric contribution is larger. Direct physical retrieval of surface skin temperature using observations at 19 and 22 GHz was developed by Weng and Grody (1998). Holmes et al. (2009) proposed a simple land surface temperature algorithm, based on a single-frequency channel (37 GHz in vertical polarization). It is shown to yield realistic estimates of LST, for a large range of surfaces. Using window frequencies from 19 to 85 GHz, as will be available with MWI, can provide LST with good accuracy as compared to in situ measurements under all sky conditions and to IR satellite estimates under clear sky conditions (Jimenez et al., 2017). Results are less satisfactory in very arid regions, due to the potential penetration depth of the microwave signal (Prigent et al., 1999), and over snow due to the complexity of the interaction between the radiation and the snow. Efforts have to be conducted in the understanding and modelling of the microwave signal and the medium in these scattering media (snow and sand).

The ideal frequencies to estimate the soil moisture information are around 1.4 GHz, as confirmed by the success of the SMOS and SMAP missions. However, relevant soil moisture estimates have been extracted from imagers between 18 and 90 GHz. Owe et al. (2008) for instance combined the results from different imagers to obtain a 30 year soil moisture database. MWI can be considered as an extra source of soil moisture information, especially if the lower frequency observations from 1.4 to 10 GHz are not available in the future.

Surface wind speed over the oceans

Gravity waves, foam on the surface from wind speeds greater than about 7 m/s, and the small scale roughness of capillary waves caused by surface wind shear over the ocean are affecting the water surface emissivity at all microwave frequencies (Meissner and Wentz, 2012). The sensitivity to wind speed increases with frequency for the MWI window channels from 18.7 to 89 GHz. The brightness temperature sensitivity to wind is highest looking upwind and smaller looking downwind while the wind sensitivity is at a minimum when the radiometer is looking perpendicular to the wind direction at the surface (Ulaby et al., 1986). However, in order to retrieve the surface wind direction unambiguously from just one single radiometer measurement it is necessary to have the full stokes vector including the 3rd and 4th stokes components which is not available on MWI. 10 m wind speeds less than about 3 m/s is not forming the small scale roughness which is sensed by the radiometer and there is no wind sensitivity at these low wind speeds. Wind speed is just one of a number of physical parameters affecting the brightness temperature over the open ocean, these including the SST, the atmospheric water vapour, liquid water and temperature profiles and composition of clouds. All of these are retrieved simultaneously together with the wind speed using an emission model and for example optimal estimation (Wentz et al., 2000; 2007).

Snow and ice coverage over both land and ocean

At MWI microwave frequencies between 18.7 and 89 GHz mature sea ice is a warm target dominated by diffuse scattering while water is a cold target dominated by specular reflection because of the water/snow/ice differences in the permittivity, surface and volume scattering magnitude and the emissivity (Tonboe, 2010). The contrast between sea ice and open water is very high not only in terms of brightness temperature but also in terms of the polarisation difference and the spectral gradient when several frequencies at different channels are available (Comiso et al., 1997). This contrast between sea ice and open water is exploited when mapping the sea ice concentration and the sea ice edge (Breivik et al., 2001). This has been done in a continuous global record using American satellite microwave radiometers since the 1970ies and MWI will ensure the continuation of this unique climate data record (CDR).

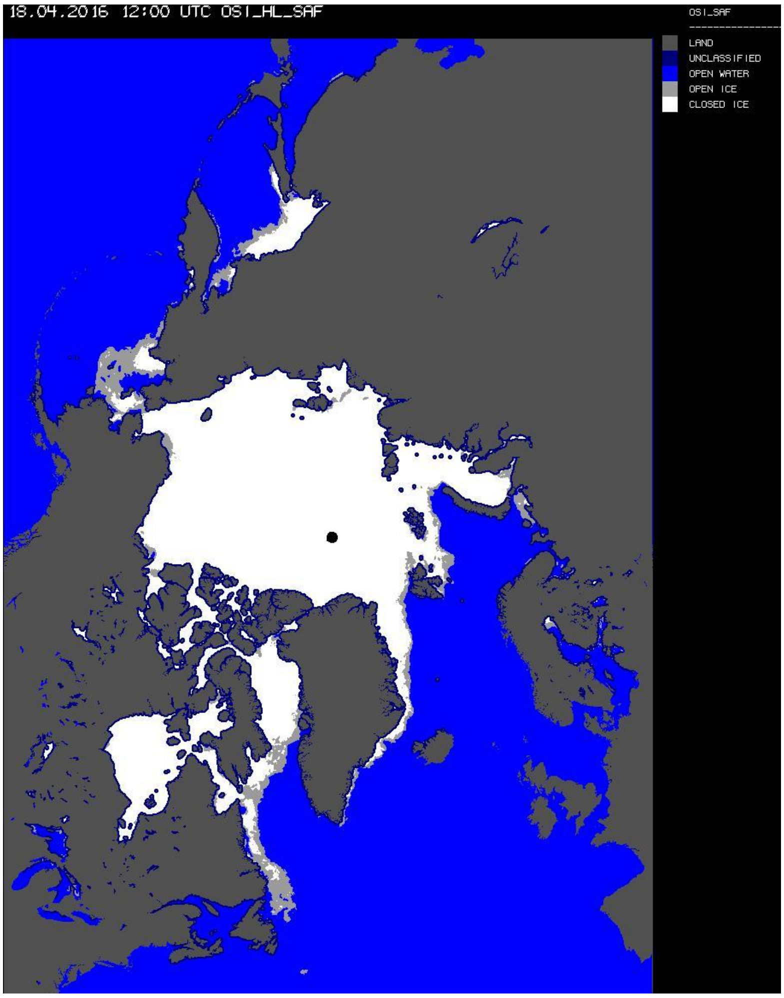

Figure. 6.2.2. The EUMETSAT OSI SAF sea ice edge product 18. April, 2016 based on radiometer and scatterometer data.

There are over 20 different empirical or semiempirical algorithms each one of them using different channels, the polarisation signature, the spectral gradient or combinations of these parameters to compute the sea ice concentration given the measured brightness temperatures (Ivanova et al., 2014; 2015). However, each of these 20 algorithms can be categorised into four different types according to the combination of channels that they use etc. Each of them are having different sensitivity to geophysical atmospheric and surface and instrument noise (Ivanova et al., 2015). The sea ice concentration is used operationally as input to atmospheric and ocean models and for estimating the sea ice extent and area dynamics on climate time scales.

The EUMETSAT Ocean and Sea Ice Satellite Application Facility (OSI SAF) state of the art sea ice concentration production chain is using a combination of two algorithms for their operational production, both of them using AMSR and SSMIS microwave channels at 19 and 37 GHz as input (see Figures 6.2.2 and 6.2.3 as an example). The combined algorithm applies a regional error reduction of atmospheric noise using auxiliary information from the ECWMF NWP model while it avoids potential biases from the same model using dynamical tie-points. The dynamical tie-points also adapts to seasonal and interannual changes and even climatological changes in the ocean and sea ice signatures. A forward model for the random geophysical noise propagation is applied to provide spatially and temporally varying uncertainty estimates which are provided along with the ice concentration estimates. The ESA Climate Change Initiative (CCI) project has adopted a similar approach for the processing of historical microwave radiometer data for (sea ice) climate variable retrieval. The next phase of the OSISAF is preparing for the processing of MWI data for sea ice concentration retrieval using a similar methodology from day one after instrument deployment. The methodology is well adapted for introducing new sensors without the prior calibration phase.

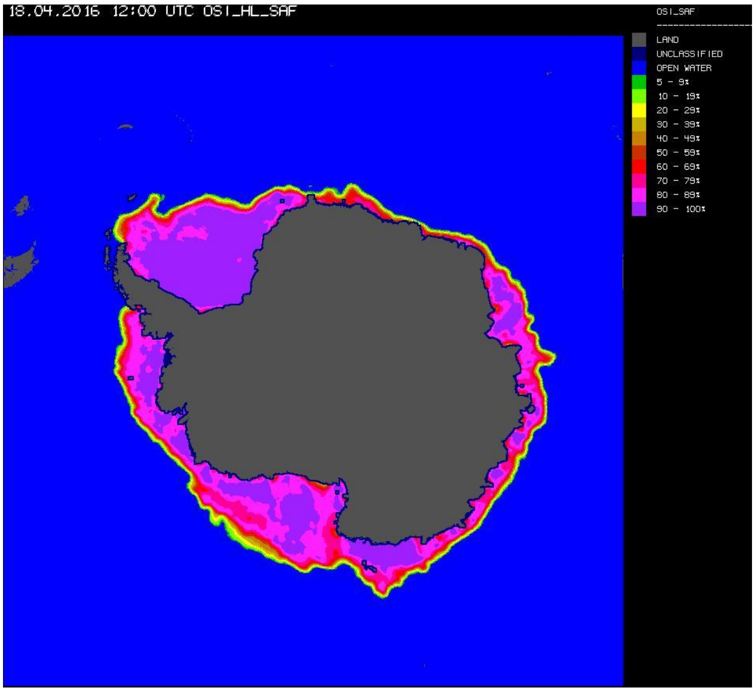

Figure. 6.2.3. The EUMETSAT OSI SAF sea ice concentration for Antarctica on 18. April, 2016 based on SSMIS radiometer data.

Sea Ice type

Two distinct sea ice types can be recognised in microwave radiometer data at 19 and 37 GHz namely: multiyear ice and first-year ice (Rothrock et al., 1988). The ice types are distinct because of different surface permittivity and in particular scattering magnitude and snow cover. First-year ice here including new ice (0-10cm) and young ice (10-30 cm) is sea ice which is formed during the same winter less than a year ago. The level first-year ice is up to 2 m thick and has a relatively high salinity (bulk salinities of about 7 ppt). The formation environment, deformation and snow and ice metamorphosis processes affects its surface roughness. There is normally snow on first-year ice which is dominating the microwave signature variability (Eppler et al., 1992, Ulaby et al., 1986). Multiyear ice is thick old ice which has survived at least one summer melt season. The melt significantly changes the surface of the ice floe and the microwave signatures. The melt processes drains most of the salt away from the surface and a landscape with elevated and rough hummocks with old snow and porous ice and melt ponds with smooth surfaces even after refreezing (Eppler et al., 1992).

These physically distinct ice types have distinct microwave signatures at 19 and 37 GHz and will be observable also at the corresponding MWI frequencies (18.7 and 31 GHz). At higher frequencies (>100 GHz) since only the snow surface layer can be probed (depending on the wavelength) ice types are less distinct. It is clear in this case that snow surface roughness, density and grain size are important factors affecting the emissivity of snow covered surfaces. The OSI SAF is combining microwave radiometer and scatterometer data in operational sea ice type classification (Breivik et al., 2001).

Ice drift

Sea ice drift or displacement over a few days during the cold season can be recorded between consecutive satellite images using the maximum cross correlation of overlapping subsections of the image intensity distribution or wavelet analysis. This is possible because of the brightness temperature intensity distribution in the image subsets which are matched in consecutive images is conserved on the timescale of days during winter (Lavergne et al., 2010). The temporal spacing between images is determined by the resolution of the sensor and the temporal coverage and it does affect the retrieved ice drift vector uncertainty. However, during summer when melt-freeze cycles quickly changes the signature then the correlation breaks down. The window channels on MWI are well suited for deriving sea ice drift and will be ingested in the OSI SAF operational production of sea ice drift from day one after instrument deployment. The sea ice drift analysis will benefit from the coincident SCA and possibly Metimage measurements which can be used for ice drift analysis as well.

Ice emissivity and temperature

The OSI SAF is providing the near 50 GHz sea ice emissivity products for atmospheric temperature sounding applications over sea ice covered surfaces (see Figure 6.2.4). The products are based on a semiempirical model calculation using coefficients derived from 19 and 37 GHz brightness temperature measurements (Tonboe et al., 2013). The emissivity has also been derived at other frequencies even up to 183 GHz for data assimilation applications over ice sheets and sea ice (Karbou et al. 2006; Mathew et al., 2009). For frequencies over 183 GHz the surface emission models are immature, including permittivity and scattering models, theoretical and experimental understanding of the dominant emission processes (see section 5.3.5).

The effective temperature at e.g. 50 GHz is highly correlated with the effective temperature at neighboring window frequencies and also the physical temperature at the snow ice interface (Tonboe et al., 2011). The retrieval of the effective temperature at sounding frequencies is still an open research topic.

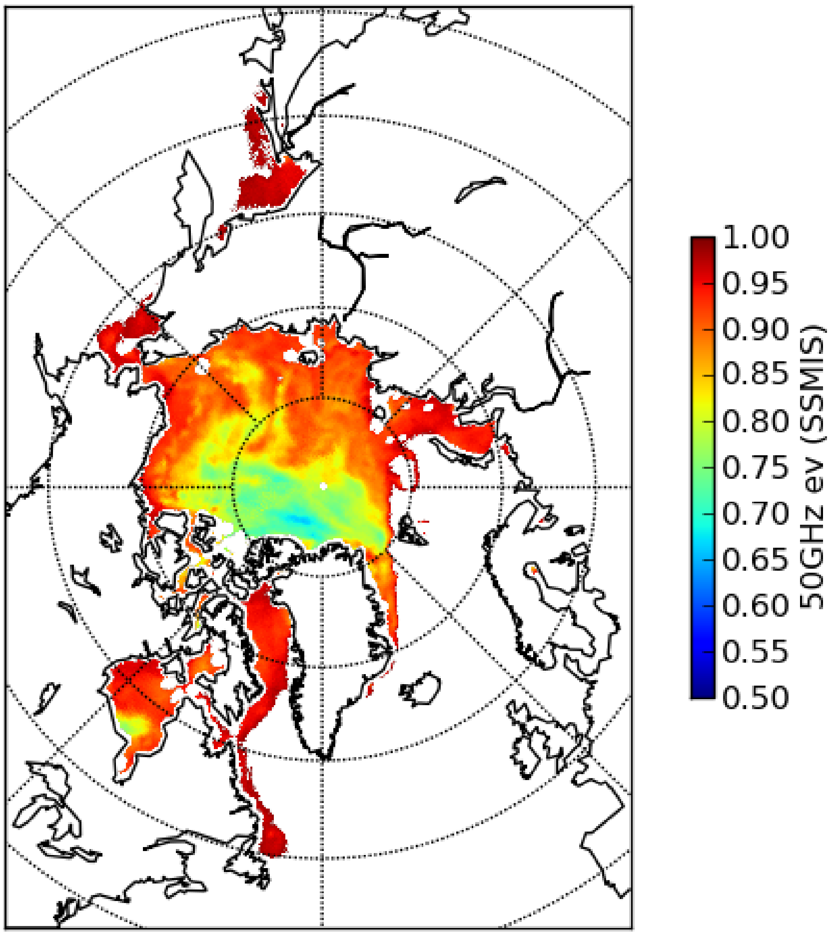

Figure 6.2.4. The EUMETSAT OSI SAF sea ice near 50 GHz emissivity product for the Arctic on 18. March, 2016 using SSMIS radiometer data and a model.

Snow on land and sea ice

Snow on first-year ice has been mapped using empirical relationships between the spectral gradient ratio at 19 and 37 GHz vertical polarisation and the snow depth (Markus and Cavalieri, 1998). The extinction coefficient in dry snow is dominated by scattering and for a given snow grain size and density the scattering increase with frequency and scattering layer depth. The gradient ratio is then related to the scattering magnitude (Comiso et al., 1997) because scattering from the same snow grain size distribution is higher at 37 GHz than at 19 GHz and then the only "free" parameter is then the scattering layer depth or snow depth (Kelly et al. 2003). Penetration into first-year ice beneath the snow at these frequencies is very shallow and the scattering in first-year ice is limited. A product example is provided in Figure 6.2.5.

Of course this empirical relationship is developed for average snow conditions in a specific dataset and in fact it has been shown that layering, density and scattering within the snowpack is very important for the microwave signature (Mätzler et al., 2008, Tonboe, 2010, Kelly et al., 2003). Therefore, for mapping snow on land more sophisticated forward models yet suitable for inversion, retrieval and assimilation such as the HUT model have been developed and used together with microwave radiometer measurements in an model inversion scheme for retrieving snow parameters such as snow water equivalent (SWE: the product of the bulk density and the snow depth) and snow grain sizes (Pulliainen, 2006; Roy et al., 2004). The retrieval of snow over land is further complicated by vegetation and terrain. These more sophisticated models more easily ingest new channels in the retrieval from e.g. MWI. A priori knowledge of snow grain size and density can be used to improve the quality of the retrievals (Pulliainen, 2006) or these parameters are part of the retrieval (Kelly et al., 2003). Such model inversion approaches has not been applied for snow retrieval on sea ice and the retrieval of snow both on land and on sea ice is indeed an open research topic.

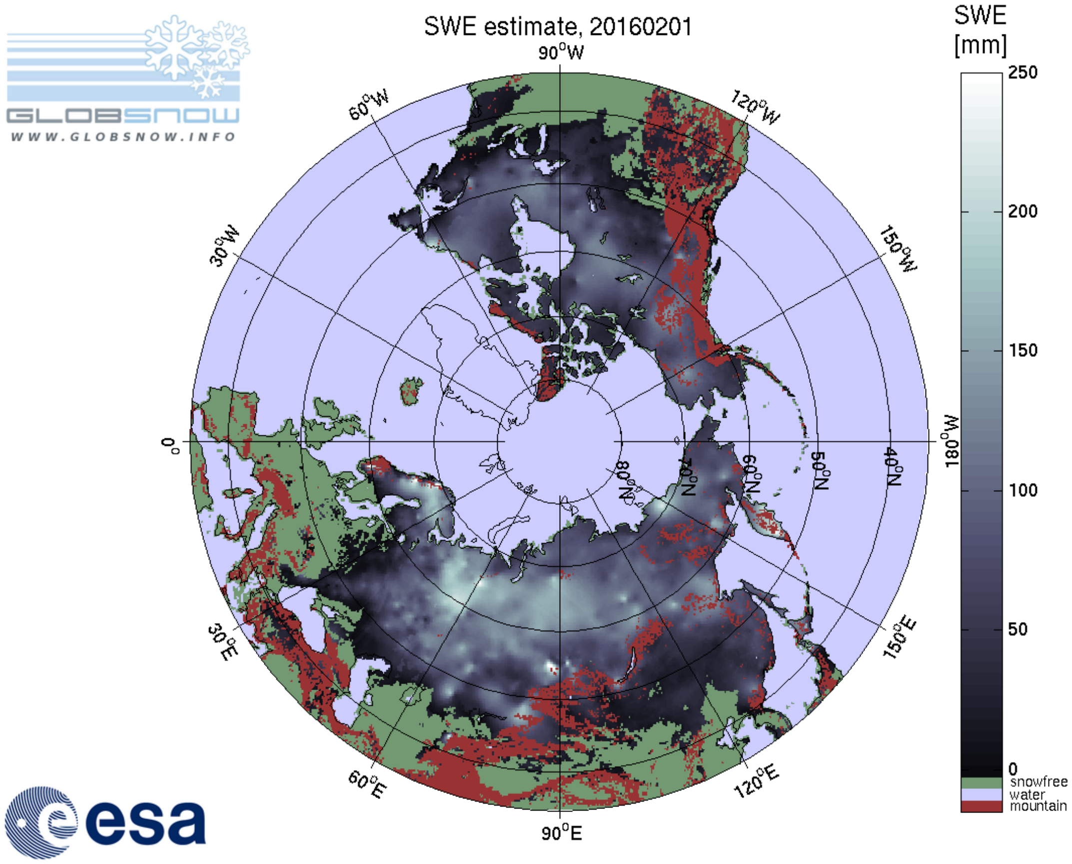

Figure. 6.2.5. The ESA GlobSnow snow water equivalent product on 1. February 2016 covering the northern hemisphere.

6.2.5 Summary of expected impact of MWI-ICI for surface variables

The MWI will be an important continuation of already existing microwave radiometers and will thus provide a continuation of climate time series and operational production of surface parameters in particular for sea ice and snow. The synergy with the SCA will be an asset for both wind retrieval, sea ice drift and the sea ice type and edge classification. The colocation of the MWI conically scanning Tb's at window channels together with the MWI/ICI/MWS sounding channels is expected to be an asset for atmospheric sounding applications. With ICI there is the opportunity to derive detailed ice and water cloud parameters. However, this is still an open research question especially in polar regions and over deserts and the surface emissivity models, if existing, are still immature. ICI is new and applications emerging from the measurements of this instrument are yet to be developed.

6.2.5.1 Error assessment

The OSI SAF sea ice concentration is provided with temporally and spatially varying estimates of uncertainty and other applications are developing methodologies for estimating uncertainties. The total sea ice concentration uncertainty is the combination of two separate and independent components: 1) the resampling uncertainty which is the uncertainty when coarse resolution footprints of the sensor are resampled at a finer resolution grid, and 2) the algorithm uncertainty which includes signature variability around the tie-points caused by atmospheric or surface emissivity variations and instrument noise. The smearing uncertainty dominates at intermediate sea ice concentrations while the algorithm uncertainty dominates where the entire footprint is covered either by open water or 100% ice. The smearing uncertainty can be minimized but not removed by optimizing the resampling grid resolution to match the sensor spatial resolution. High spatial resolution and low noise sea ice concentration is to some extent a trade off because high resolution is achieved with algorithms using the high frequency channels where the atmospheric noise is significantly higher than at the lower frequency channels with coarser resolution. However, for any given frequency there is an optimal grid resolution where the resampling uncertainty is at a minimum.

6.2.5.2 Major scientific challenges

ICI is a new sensor measuring at a frequency range which is unprecedented in space. This requires some fundamental science effort and preparatory studies to fully exploit the data potential in applications such as data assimilation.

6.2.5.3 Overarching research themes

The use of radiances (and backscatter) rather than physical products in data assimilation requires observational operators that consistently combines the measurements from different sensors in Earth system model systems. Research on surface emission models covering the MWI and ICI frequencies especially for snow, sea ice and desert surfaces will benefit a number of applications including sea ice and atmospheric characteristics. The basic overarching science effort includes research on scattering models for snow, dielectric models for pure and saline ice and surface scattering models:

- Permittivity model for freshwater ice at 100 - 700 GHz. A prerequisite for simulating the Earth's surface emissivity is a valid description of the permittivity of the material. Both models for snow scattering and the permittivity of snowpacks use the permittivity of freshwater ice as input.
- A scattering model for Earth surface materials such as snow and desert sands at 100 - 700 GHz. Scattering models such as the improved Born approximation is valid for scattering particles much smaller than the electromagnetic wavelength. This limits its application for natural snowpacks at ICI frequencies. Since scattering is very important for snowpack emissivity in particular for frequencies above 100 GHz it is necessary to find and apply scattering models which are valid for natural snowpacks at ICI frequencies.
- Dedicated validation campaigns in regions with prevailing dry atmospheric conditions and over snow, sea ice and desert regions. The validity of emission models can only be determined by performing in situ measurement campaigns collecting simultaneously

both radiometric and physical parameters. Also the sub-resolution variability can be determined using in situ and campaign data. These are important for tuning models to real world conditions.

- *MWI-ICI Science Plan impact*. The impact of the instruments on surface applications depends on development activities mentioned above. The continuity of the MWI suite of channels will in itself extend the climate time-series and ensure the continuous production of a number of important products such as sea ice concentration, sea ice drift etc. However, if the potential of the ICI should be fully exploited there is a need for conducting the research which is outlined above.

6.2.6 References

Breivik, L.A., S. Eastwood, Ø. Godøy, H. Schyberg, S. Andersen & R. Tonboe. Sea ice products for the EUMETSAT satellite application facility. Can. J. Rem. Sens. 27(5), 403-410, 2001.

Comiso, J. C., D. J. Cavalieri, C. L. Parkinson, P. Gloersen. 1997. Passive microwave algorithms for sea ice concentration: A comparison of two techniques. Remote Sensing of Environment 60(3), 357-384.

Donlon, C. + 25 others. 2007. The global ocean data assimilation experiment high-resolution sea ice surface temperature pilot project. BAMS, DOI:10.1175/BAMS-88-8-1197.

Donlon, C. J., P. J. Minnett, C. L. Gentemann, T. J. Nightingale, I. J. Barton, B. Ward, and M. J. Murray. 2002. Towards improved validation of satellite sea surface skin temperature measurements for climate research. Journal of Climate 15, 353-369.

English, S.J. 2008. The importance of accurate skin temperature in assimilating radiances from satellite sounding instruments. IEEE Trans. Geosci. Rem. Sens. 46(2), 403-407.

Eppler, D. T. + 14 others. 1992. Passive microwave signatures of sea ice , in microwave remote sensing of sea ice. Geophysical Monograph 68, AGU, Edited by F. Carsey, pp. 47-71.

Holmes, T. R. H., R. A. M. De Jeu, M. Owe, and A. J. Dolman. 2009: Land surface temperature from Ka band (37 GHz) passive microwave observations, J. Geophys. Res., 114, D04113, doi:10.1029/2008JD010257.

Ivanova, N., L. T. Pedersen, R. T. Tonboe, S. Kern, G. Heygster, T. Lavergne, A. Sørensen, R. Saldo, G. Dybkjær, L. Brucker, and M. Shokr. 2015. Intercomparison and evaluation of sea ice algorithms: Towards further identification and challenges and optimal approach using passive microwave observations. The Cryosphere 9, 1797-1817.

Ivanova, N., O.M. Johannessen, L.T. Pedersen, and R. T. Tonboe. 2014. Retrieval of Arctic sea ice parameters by satellite passive microwave sensors: A comparison of eleven sea ice concentration algorithms. IEEE Trans. Geosci. Rem. Sens. 52(11), 7233-7246.

Jiménez, C., C. Prigent, S. L. Ermida, and J.-L. Moncet. 2017: Inversion of AMSR-E observations for land surface temperature estimation: 1. Methodology and evaluation with station temperature, J. Geophys. Res. Atmos., 122, 3330–3347, doi:10.1002/2016JD026144.

Karbou, F. E. Gerard, F. Rabier. Microwave land emissivity and skin temperature for AMSU-A and -B assimilation over land. Q. J. R. Meteorol.Soc., 132, 2333-2355, 2006.

Kelly, R. E., A. T. Chang, L. Tsang, J. L. Foster. A prototype AMSR-E Global snow area and snow depth algorithm. IEEE Trans. Geosci. Rem. Sens. 41(2), 230-242, 2003.

Lavergne, T., Eastwood, S., Teffah, Z., Schyberg, H. and L.-A. Breivik (2010), Sea ice motion from low resolution satellite sensors: an alternative method and its validation in the Arctic. J. Geophys. Res., 115, C10032, doi:10.1029/2009JC005958.

Markus, T. and D. J. Cavalieri. 1998. Snow depth distribution over sea ice in the Southern Ocean from satellite passive microwave data. Antarctic Sea Ice: Physical processes Interactions and variability, Antarctic Research Series 74, 19-39, AGU.

Mätzler, C., P.W. Rosenkranz, A. Battaglia and J.P. Wigneron (Eds.), "Thermal Microwave Radiation - Applications for Remote Sensing", IET Electromagnetic Waves Series 52, London, UK, 2006.

Meissner, T. and F. J. Wentz. 2012. The emissivity of the ocean surface between 6-90 GHz over a large range of wind and Earth incidence angles. IEEE Transactions of Geoscience and Remote Sensing 50(8), 3004-3026.

Owe, M., R. de Jeu, and T. Holmes. 2008: Multisensor historical climatology of satellite-derived global land surface moisture, J. Geophys. Res., 113, F01002, doi:10.1029/2007JF000769

Prigent, C., W. B. Rossow, E. Matthews, and B. Marticorena. 1999: Microwave radiometric signatures of different surface types in deserts, J. Geophys. Res., 104(D10), 12,147–12,158.

Pulliainen, J. 2006. Mapping of snow water equivalent and snow depth in boreal and sub-arctic zones by assimilating space-borne microwave radiometer data and ground based observations. Remote Sensing of Environment 101, 257-269.

Rothrock, D. A., D. R. Thomas, A. S. Thorndike. 1988. Principal Component Analysis of satellite passive microwave data over sea ice. Journal of Geophysical Research 93(C3), 2321-2332.

Roy, V., K. Goith, A. Royer, A. Walker, and B. Goodison. 2004. Snow water equivalent retrieval in a Canadian boreal environment from microwave measurements using the HUT snow emission model. IEEE Trans. Geosci. Rem. Sens. 42, 1858-1859.

Saunders, R. W., Martricardi, and P. Brunel. 1999. An improved fast radiative model for assimilation of satellite radiance observations. Q. J. R. Meteorol. Soc. 125, 1407-1425.

Tonboe, R. T. The simulated sea ice thermal microwave emission at window and sounding frequencies. Tellus 62A, 333-344, 2010.

Tonboe, R. T., G. Dybkjær, J. L. Høyer. Simulations of the snow covered sea ice surface temperature and microwave effective temperature. Tellus 63A, 1028-1037, 2011.

Tonboe, R. T., H. Schyberg, E. Nielsen, K. R. Larsen, F. T. Tveter. The EUMETSAT OSI SAF near 50 GHz sea ice emissivity model. Tellus A, 2013, 65, 18380, http://dx.doi.org/10.3402/tellusa.v65i0.18380

Ulaby, F. T., Moore, R. K., and Fung, A. K.: Microwave Remote Sensing. Active and Passive, Norwood, MA: Artech House Inc, 1986.

Weng, F., and N. C. Grody. 1998: Physical retrieval of land surface temperature using the special sensor microwave imager, J. Geophys. Res., 103, 8839–8848.

Wentz, F. J., C. L. Gentemann, D. K. Smith, and D. B. Chelton. 2000. Satellite measurements of sea surface temperature through clouds. Science 288(5467), 847-850.

Wentz, F. J., L. Ricciardulli, K. Hilburn, C. Mears. 2007. How much more rain will global warming bring? Science 317, 233-235.

6.3 Synergetic retrieval with other instruments

The Launch of MWI-ICI will open a very interesting perspective in the synergetic retrieval with other spaceborne instruments. Complementarity of MWI-ICI measurements and products are quite broad and related not only to other space-based microwave radiometric missions, such as NPP, NOAA and GPM, but also to other instruments in LEO platforms, such as rain radars, visible-infrared radiometers and wind scatterometers, and in GEO platforms, such as visible-infrared radiometers.

In the current section are discussed first the possibility of synergetic retrievals of surface variables, while in the following sections atmospheric retrievals are discussed.

6.3.1 Synergetic retrieval of surface parameters with other instruments

Existing synergetic retrievals can be carried out in particular using MWI and scatterometer retrieval combinations e.g. sea ice type, sea ice edge, sea ice drift. In addition, several surface variable retrievals are using auxiliary data which is or can be derived using other satellite sensors e.g. surface temperature (currently from AVHRR and eventually Metimage and IASI NG in future), atmospheric variables such as temperature, humidity and clouds (from microwave sounders (e.g. MWS)and ICI).

6.3.2 Retrieval of geophysical data and parameters using SCA and MWI

Both the sea ice type and the sea ice edge products are retrieved by combining both scatterometer and microwave radiometer data in the analysis. Ocean wind speed and sea ice drift is derived from each sensor separately before they are sometimes combined in a merged product. Yet the use of other products benefits from the coincident acquisition of microwave radiometer data and retrievals and retrievals from other sensors e.g. the retrieval of sea ice surface emissivity and the retrieval of ice surface temperature.

The combination between SCA and MWI is also very promising for evaluating the impact of rainfall fields on sea surface wind retrieval (e.g., Portabella and Stoffelen, 2001; Contrerars and Plant, 2006; Hristova-Veleva et al., 2013). In this respect theoretical models of the ocean backscatter have the big potential of improving a more general and understandable relation between the measured microwave backscatter and the surface wind field than empirical models (Polverari et al., 2015). Even though theoretical models may not help to correct the limit of the current geophysical model functions (GMFs), but they can provide a tool to interpret the ocean response for complex ocean and atmospheric conditions accounting for the effects of both wind and rain. A key point is the extension of sea-wave spectrum models to properly include the ocean surface modifications induced by the impact of the raindrops due to the short wave damping and the generation of the ring waves. By coupling this sea spectrum models with atmospheric radiative transfer, the final goal might be the synergetic retrieval of both sea wind and rainfall intensity using MWI and SCA (Bliven et al., 1997).

6.3.3 Microwave sounding, precipitation missions and multi-platform synergy

We can consider the synergetic approach with the EPS-SG MWS and the GPM core observatory as well as the inter-satellite calibration and LEO-GEO combined method for precipitation tracking and estimation (Kidd and Levizzani, 2011; Levizzani et al., 2007). A major issue to be addressed when combining measurements of different sensors and even on different platforms is the colocation in time and space of their footprint. This may lead to inherent errors that should be taken into account by the combined retrieval algorithm.

6.3.3.1 EPS-SG Microwave Sounder synergetic retrieval

The Microwave Sounder (MWS) provides measurements of temperature and water vapour profiles and in addition information on cloud liquid water along the heritage of AMSU spaceborne instruments. AMSU-like sensors have been also exploited for rainfall retrieval (e.g., Chen and Staelin, 2003; Mugnai et al., 2013). These parameters are key parameters for numerical weather prediction enhancing the meteorological service ability to initialise global and regional NWP models with realistic information on temperature and moisture. The frequent availability of detailed temperature and moisture soundings would also contribute to fulfil other key requirements common to nowcasting and very short range weather forecasting at regional scales. All MWS channels are measured with a single polarisation (QV or QH). MWS will have 40 km footprint at lowest frequencies, whereas footprint at highest frequency channels will be 17 km (the sampling distance on ground is defined by the highest frequency channels). MWS has a non-uniform scanning profile, which maximises the scene viewing time and a quasi-optical system is used to co-locate all channels into one “main beam”. All channels are required to have the same pointing error within 0.1°, whereas the MWS total scan angle will be around ± 49° with respect to nadir with a total pointing knowledge of 0.25°.

MWI-ICI Science Plan impact. These characteristics of MWS are complementary to those of MWI-ICI. The main objective of the MWI is to measure precipitation, but in addition, MWI provides measurements of cloud products, water vapour and temperature profiles and surface imagery. MWI has a moderate antenna size providing on ground footprints ranging from 50 km down to 10 km, depending on frequency. We can expect that a synergy between MWS and MWI-ICI can be exploited for a better temperature profile retrieval in presence of clouds for MWS and for a better first guess of temperature-humidity scenarios for MWI retrieval, but also for a rainfall detection improvement. The strategies to couple the measurements from MWS and MWI-ICI should be carefully analysed in order to over the problem of the different scanning mechanism. In this respect, the science innovation from the MWI-ICI perspective should be mainly focused on numerical studies addressing the combined use of MWS and MWI-ICI as they have been finally designed and implemented in mission Phase B.

6.3.3.2 Global Precipitation Measurement satellite intercomparison

The Tropical Rainfall Measurement Mission (TRMM) was a revolution in terms of how it 'saw' tropical cyclones in terms of size and frequency of occurrence of rain storms in the tropics (e.g., Kummerow et al., 2001). TRMM filled a significant gap in our observations and increased our knowledge about the water cycle and atmospheric circulation over the globe. While small-scale rainstorms occur more frequently in the tropics, large events have a more significant impact on global circulation. The Global Precipitation Measurement (GPM) mission has expanded the TRMM view beyond the tropics, tracking tropical storms as they move into the mid-latitudes and, for the first time, providing a 3-dimensional view of the storms' structural changes as they move towards the poles (Hou et al., 2014). Storms can strengthen as they transition from tropical to mid-latitudes and GPM's improved tracking of the life-cycle of a storm is helping to understand why some, but not all, storms change intensity as they move. GPM precipitation database is also helping scientists to understand regional variations of mesoscale convective systems, and GPM's enhanced instrument sensitivity adds to TRMM's data and improves the understanding of precipitation characteristics in mountainous regions. The GPM Core satellite estimates rain and snow using two instruments: the GPM Microwave Imager (GMI) and the Dual-frequency Precipitation Radar (DPR). The GMI captures precipitation intensities and horizontal patterns, while the DPR provides insights into the three dimensional structure of precipitating particles. Together these two instruments provide a database of measurements against which other partner satellites' microwave observations can be meaningfully compared and combined to make a global precipitation dataset (e.g., Olson et al., 1996; Marzano et al., 1999; Di Michele et al., 2003; Grecu et al., 2004).

MWI-ICI Science Plan impact. The capability of GPM of capturing the 3D nature of precipitation is essential for an inter-comparison with a passive instrument such as MWI-ICI. Indeed, ICI can complement GMI in the observation of icy clouds and, in this respect, CloudSat radar as well can be of interest. The major issue remains the colocation of GPM and MWI-ICI overpasses during a precipitation occurrence, a fact which could limit its overall usefulness. In this respect, the science innovation to be developed after the satellite launch on the MWI-ICI perspective is mainly focused on joint microphysical process analyses and detailed inter-comparisons.

6.3.3.3 MW-IR thermodynamical and cloud combined retrieval

Multispectral infrared radiometers are quite well established instruments installed on LEO and GEO satellites. The most well-known LEO instrument is probably the Moderate Resolution Imaging Spectro-radiometer (MODIS), designed to improve global monitoring of temperature, moisture, and ozone distributions and changes therein (e.g., King et al., 1992; Seemann et al., 2003). MODIS was firstly launched onboard the NASA-EOS Terra and Aqua platforms on 1999 and 2002, respectively and then installed onboard several LEO platforms. The MODIS instrument is a scanning spectro-radiometer with 36 visible (VIS), near-infrared (NIR), and infrared (IR) spectral bands between 0.645 and 14.235 mm. The increased spatial resolution of MODIS measurements delineates horizontal gradients of moisture, temperature, and atmospheric total ozone better than companion instruments, such as the GOES sounder (VIRS, 4-km resolution at nadir), geostationary METEOSAT sounder (SEVIRI, 4-km resolution at nadir), High-Resolution Infrared Radiation Sounder (HIRS; 19-km resolution) and Atmospheric Infrared Sounder (AIRS; 15-km resolution). However, the MODIS broadband spectral resolution provides only modest information content regarding vertical profiles. True sounder radiances with higher- and hyper-spectral resolution, such as AIRS and the Cross-Track Infrared Sounder (CrIS) onboard NPOESS and Interferometric Atmopheric Radiometric Sounder (IASI) onboard Metop satellites, contain more information about the atmospheric vertical distribution of temperature and moisture. Because of the limited spectral resolution of LEO spectro-radiometers, the strength of its retrieved products lies in the resolution of horizontal gradients and the distribution of retrieved quantities in integrated vertical layers (as opposed to vertical profiles). However, near-future European satellites, such as Sentinel-3 and METEOSAT Third Generation (MTG), will also embark new advanced spectro-radiometers.

The wide spectral range, high spatial resolution, and near-daily global coverage of multispectral infrared radiometers enable it to observe the earth's atmosphere and continuously monitor changes. For instance, the advantage of MODIS for retrieving the distribution of atmospheric temperature and moisture is its combination of shortwave and longwave infrared spectral bands (4.4-4.6 and 13.1-14.5 micron) that are useful for sounding and its high spatial resolution that is suitable for imaging (1 km or less at nadir). IR atmospheric and surface parameter retrievals require clear-sky measurements. An operational cloud-mask algorithm is typically used to identify pixels that are cloud free (Seemann et al., 2003). The cloud-mask algorithm determines if a given pixel is clear by combining the results of several spectral threshold tests. A confidence level of clear sky for each pixel is estimated based on a comparison between observed radiances and specified thresholds.

Interestingly, thermal IR (TIR) spaceborne radiometers are also used to discriminate volcanic clouds from water clouds due to refractive index inversion in that spectral region (e.g., Rose et al., 2000). This means that a synergy can be envisaged between TIR and MW radiometers as well.

MWI-ICI Science Plan impact. The optimal combination with MWI-ICI mainly relies, in this respect, on the capability to improve cloud-mask algorithm and to a certain extent, explore the possibility to retrieve temperature and humidity profiles in a cloudy atmosphere. Combination of TIR and MW signatures for volcanic cloud detection should be evaluated as well. The major issue remains the colocation of IR acquisitions and MWI-ICI overpasses but, considering the IR sensor scenario from GEO satellites (e.g., MTG), the optimal combination of MWI-ICI and IR data is a scientific aspect to deepen.

6.3.3.4 LEO-GEO MW-IR precipitation combined retrieval

The problem of using satellite remote sensing data appears to be fairly complicated since presently there is not a single spaceborne platform that can carry all the suitable instruments to ensure a high temporal frequency and spatial resolution for precipitation monitoring (Levizzani et al., 2007). From a meteorological point of view, visible (VIS) and infrared (IR) radiometers can give information on cloud top layers due to their high albedo at optical wavelengths and IR equivalent blackbody brightness temperatures almost equal to cloud physical temperature. On the other hand, microwave radiometers can detect cloud structure and rain rate, since MW brightness temperatures are fairly sensitive to liquid and ice hydrometeors. Regarding platforms, geosynchronous earth orbit (GEO) satellites can ensure a coverage with a high temporal sampling (order of half an hour) from a flight altitude of about 36000 km, while low earth orbit (LEO) satellites have the advantage to fly at a lower altitude (from 400–800 km), thus enabling the use of microwave sensors without losing too much in spatial resolution (order of kilometers to tens of kilometers). The major drawback of LEOs is the low temporal sampling, only twice a day in a given place at mid-latitude. Therefore, LEO–MW and GEO–IR radiometry are clearly complementary for monitoring the earth’s atmosphere and a highly variable phenomenon such as precipitation. Statistical integration of satellite IR and microwave data can be accomplished in several ways (Turk et al., 2000; Ba et al., 2001; Kidd et al., 2004; Marzano et al., 2044; Joyce et al., 2004; Huffman et al., 2007; Kubota et al., 2007; Bellerby et al., 2009).

On one hand, there is a choice of what variables (i.e., predictors) to match in order to provide the final product. A possibility is represented by the direct combination of nearly instantaneous MW and IR data, having the advantage to exploit the observable information without any post-processing and the disadvantage to request IR and MW measurements matched in space and time. However, the latter condition is only satisfied a limited number of times in a given area if few LEO platforms are considered, thus flaring the potentiality of setting up a rapid-updating retrieval algorithm. The feasible approach would be that based on physically based combined retrieval algorithms which, on the other hand, would need a climatological and microphysical tuning. In order to avoid these difficulties, one can resort to approaches that aim to combine IR measurements and MW-based estimates on a statistical basis. By properly choosing a space–time resolution, the ergodicity of the rain process and satellite observations can be invoked. The inversion algorithm, i.e., retrieving rain rate from IR data, can be then derived by using statistical regression or probability matching of the involved variables (or corresponding statistical moments). Even though less physical, the statistical matching exhibits several peculiar features that can be easily exploited for an operational global-scale approach. Indeed, artificial neural networks can be conveniently applied to the same problem dealing with empirically trained algorithms showing comparable performances.

MWI-ICI Science Plan impact. There are several combined LEO-GEO algorithms which ingest both MW and IR data to provide a blended precipitation products such as from EUMETSAT HSAF (Hydrology Satellite Application Facility), EUMETSAT MPE (Multi-sensor Precipitation Estimate), NASA MPA (Multi-satellite Precipitation Analysis), and JAXA GSMap (Global Satellite Mapping). This clearly means that MWI-ICI should certainly contribute to this merged dataset providing a high-quality atmospheric retrieval product. In this respect, the science innovation to be developed from the MWI-ICI perspective is probably limited.

6.3.3.5 Multisatellite microwave radiometric inter-calibration

Spaceborne MW radiometer inter-calibration is an essential component of any effort to combine measurements from two or more radiometers into one dataset for scientific studies (e.g., Ruf, 2000; Kroodsma et al., 2012). One spaceborne instrument in low Earth orbit is not sufficient to perform long-term climate studies or to provide measurements more than twice per day at any given location on Earth. Measurements from several MW radiometers are necessary for analyses over extended temporal and spatial ranges. In order to combine the measurements, the radiometers need to be inter-calibrated due to the instruments having unique instrument designs and calibrations. Inter-calibration ensures that consistent scientific parameters are retrieved from the radiometers. Four methods that use external observations for radiometer calibration are: (1) averaging over-ocean observations for a long period of time to find scan biases; (2) comparisons with other radiometers using co-located observations; (3) deep space manoeuvres; and (4) vicarious calibration using a reference statistic as a virtual cold or warm ‘target’. The latter method relies on deriving a stable statistic of the Earth TB to be used as an external reference point. This is referred to as ‘vicarious’ calibration since the external reference can serve as a calibration point instead of the on-board calibration. Three advantages of vicarious calibration are: it has the ability to be applied to a shorter time period of data than averaging over-ocean observations, it does not require cross-over locations between radiometers, and it is not dependent on a spacecraft manoeuvre. Vicarious cold calibration (VCC) relies on the fact that the coldest stable TBs a microwave radiometer observes are over the ocean with calm surface winds, no clouds, and minimal water vapour (Kroodsma et al., 2012, 2017).

External vicarious calibration single-difference methods can be used to derive calibration offsets between two or more radiometers, thereby inter-calibrating the sensors. Specifically, they are: (1) finding cross-over points between radiometers; and (2) deriving a stable reference statistics with vicarious cold calibration. Inter-calibration is necessary since the absolute calibration of radiometers cannot be assumed to be the same; additionally, the design of most radiometers is not identical. A robust inter-calibration accounts for design differences and derives a calibration offset that is a result of differences in the individual on-board calibrations. The vicarious cold calibration with the single difference method can be also extended by means of double-difference approach, i.e. subtracting the simulated TBs (obtained using a radiative transfer model applied to radiosonde data) to each radiometric measurements (Kroodsma et al., 2012). There are two main advantages to using the vicarious cold calibration double difference (VCC-DD) method over other inter-calibration algorithms. One is that it does not require coincident or near-coincident cross-over points between the two radiometers. The simulated TBs are able to model the natural variability in the observed TBs over time and location, creating a stationary statistic through the single difference. The vicarious cold calibration double difference is able to sufficiently account for design differences between two radiometers including frequency, earth incidence angle, and orbital characteristics.

MWI-ICI Science Plan impact. An objective of the MWI-ICI science plan should be devoted to the estimate of the uncertainty in the intercalibration, taking into account potential errors in the geophysical inputs and improper accounting of seasonal and diurnal variability. Inter-calibration is necessary for achieving consistency in retrieved scientific parameters and the vicarious cold calibration double difference method can be a candidate technique. The intercalibration results should be tested, for example, in terms of possible improvements in parameter retrievals, such as the rain accumulation agreement between the radiometers.

6.3.4 References

Ba, M. B. and Gruber, A.: GOES multispectral rainfall algorithm (GMSRA), J. Appl. Meteorol., 40, 1500–1514, 2001.

Barrett, E. C. and Martin, D. W.: The use of satellite data in rainfall monitoring, Academic Press, London, p. 340, 1981.

Bauer, P.: Over-ocean rainfall retrieval from multisensory data or the Tropical Rainfall Measuring Mission, Part I: Design and evaluation of inversion databases, J. Atmos. Ocean. Techn., 18, 1315–1330, 2001.

Behrangi, A., Hsu, K.-L., Imam, B., Sorooshian, S., and Kuligowski, R.: Evaluating the utility of multispectral information in delineating the areal extent of precipitation, J. Hydrometeorol., 10, 684–700, 2009.

Bellerby, T., Hsu, K.-L., and Sorooshian, S.: MODEL: a satellite precipitation methodology using cloud development modelling, Part I: Algorithm construction and calibration, J. Hydrometeorol., 10, 1081–1095, 2009.

Bliven L. F., P. W. Sobieski, C. Craeye, “Rain generated ring-waves: Measurements and modelling for remote sensing,” Int. J. of Remote Sens., vol. 18, no. 1, pp. 221-228, 1997.

Boukabara S. A., F.Weng, and Q. Liu: Passive microwave remote sensing of extreme weather events using NOAA-18 AMSUA and MHS, IEEE Trans. Geosci. Remote Sens., vol. 45, no. 7, pp. 2228–2246, Jul. 2007.

Boukabara S.-A., K. Garrett, W. Chen, F. Iturbide-Sanchez, C. Grassotti, C. Kongoli, R. Chen, Q. Liu, B. Yan, F. Weng, R. Ferraro, T.J. Kleespies, H. Meng: MiRS: An All-Weather 1D-Var Satellite Data Assimilation and Retrieval System, IEEE T. Geosci. Remote, 48, 3608-3621, 2010.

Casella, D., Panegrossi, G., Sanò, P., Milani, L., Petracca, M., and Dietrich, S.: A novel algorithm for detection of precipitation in tropical regions using PMW radiometers, Atmos. Meas. Tech., 8, 1217–1232, 2015.

Chen, F. W. and Staelin, D. H.: AIRS/AMSU/HSB precipitation estimates, IEEE T. Geosci. Remote, 41, 410–417, 2003.

Contreras R. F., and W. J. Plant, “Surface effect of rain on microwave backscatter from the ocean: Measurements and modeling,” J. Geophys. Res., vol. 111, no. C08019, 2006

Delene, D. J., Rose, W. I., & Grody, N. C.: Remote sensing of volcanic clouds using special sensor microwave imager data. Journal of Geophysical Research, 101(B5), 11579–11588, 1996.

Di Michele S. and P. Bauer: Passive Microwave Radiometer Channel Selection Based on Cloud and Precipitation Information Content Estimation, Q. J. R. Meteorol. Soc., 132, pp. 1299–1323, 2006.

Di Michele S., A. Tassa, A. Mugnai, F.S. Marzano, P. Bauer and J.P.V. Poiares Baptista: Bayesian Algorithm for Microwave based Precipitation Retrieval: description and application to TMI measurements over ocean, IEEE Trans. Geosci. Rem. Sens., ISSN: 0196-2892, vol. 43, pp. 778-791, 2005.

Di Michele S., F.S. Marzano, A. Tassa, A. Mugnai, and P. Poiares Baptista: Physically-based statistical integration of TRMM microwave measurements for precipitation profiling, Radio Sci., ISSN: 0048-6604, vol. 38, n. 4, pp. 8072-8072.17, doi:10.1029/2002RS002636, 2003.

Ebert, E. E., Janowiak, J. E., and Kidd, C.: Comparison of near real- time precipitation estimates from satellite observations and numerical models, B. Am. Meteorol. Soc., 88, 47–64, 2007.

Ferraro, R. R., Smith, E. A., Berg,W., and Huffman, G. J.: A review of screening techniques for passive microwave precipitation retrieval algorithms, J. Atmos. Sci., 55, 1583–1600, 1998

Ferraro, R., Smith, E. A., Berg,W., and Huffman, G. J.: A screening methodology for passive microwave precipitation retrieval algorithms, J. Atmos. Sci., 55, 1583–1600, 1998.

Grecu, M., Olson, W. S., and Anagnostou, E. N.: Retrieval of precipitation profiles from multiresolution, multifrequency active and passive microwave observations, J. Appl. Meteorol., 43, 562–575, 2004.

Haykin S., Neural Networks: A Comprehensive Foundation, 2nd ed. Englewood Cliffs, NJ: Prentice-Hall, 1994.

Hou A.Y., R.K. Kakar, S. Neeck, A.A. Azarbarzin, C.D. Kummerow, M. Kojima, R. Oki, K. Nakamura, and T. Iguchi: The Global Precipitation Measurement Mission, Bull. Am. Met. Soc., 701-722, doi:10.1175/BAMS-D-13-00164.1, May 2014.

Hsu, K., Gao, X., Sorooshian, S., and Gupta, H. V.: Precipitation estimation from remotely sensed information using artificial neural networks, J. Appl. Meteorol., 36, 1176–1190, 1997.

Huffman, G. J., Adler, R. F., Bolvin, D. T., Gu, G., Nelkin, E. J., Bowman, K. P., Hong, Y., Stocker, E. F., and Wolff, D. B.: The TRMM Multisatellite Precipitation Analysis (TMPA): quasi-global, multiyear, combined-sensor precipitation estimates at fine scales, J. Hydrometeorol., 30(8), 38–55, 2007.

Joyce, R. J., Janowiak, J. E., Arkin, P. A., and Xie, P.: CMORPH: a method that produces global precipitation estimates from passive microwave and infrared data at high spatial and temporal resolutions, J. Hydrometeorol., 5, 487–503, 2004.

Kidd C. and V. Levizzani: Status of satellite precipitation retrievals, Hydrol. Earth Syst. Sci., 15, 1109–1116, 2011.

Kidd, C., Kniveton, D. R., Todd, M. C., and Bellerby, T. J.: Satellite rainfall estimation using a combined passive microwave and infrared algorithm, J. Hydrometeorol., 4, 1088–1104, 2003.

King, M. D., Y. J. Kaufman, W. P. Menzel, and D. Tanre´: Remote sensing of cloud, aerosol, and water vapour properties from the Moderate Resolution Imaging Spectrometer (MODIS). IEEE Trans. Geosci. Remote Sens., 30, 2–27, 1992.

Kroodsma, R.A., D.S. McKague, and C. Ruf; Christopher S. Ruf, 2012: Inter-Calibration of Microwave Radiometers Using the Vicarious Cold Calibration Double Difference Method, IEEE J. Sel. Topics Appl. Earth Obs. Rem. Sens., vol. 5, No. 3, 1006-1013.

Kroodsma R. A., D. S. McKague and C. S. Ruf, 2017: Vicarious Cold Calibration for Conical Scanning Microwave Imagers, *IEEE Transactions on Geoscience and Remote Sensing*, vol. 55, no. 2, pp. 816-827.

Kubota, T., Shige, S., Hashizume, H., Aonashi, K., Takahashi, N., Seto, S., Hirose, M., Takayabu, Y. N., Nakagawa, K., Iwanami, K., Ushio, T., Kachi, M., and Okamoto, K.: Global precipitation map using satellite-borne microwave radiometers by the GSMaP Project: production and validation, IEEE Trans. Geosci. Remote Sens., 45, 2259–2275, 2007.

Kummerow C., W. S. Olson, and L. Giglio: A simplified scheme for obtaining precipitation and vertical hydrometeor profiles from passive microwave sensors, IEEE Tran. Geosci. Remote Sensing, vol. 34, pp. 1213–1232, Sept. 1996.

Kummerow, C., Hong, H., Olson, W. S., Yang, S., Adler, R. F., Mc-Collum, J., Ferraro, R., Petty, G., Shin, D.-B., and Wilheit, T. T.: The evolution of the Goddard Profiling Algorithm (GPROF) for rainfall estimation from passive microwave sensors, J. Appl. Meteor., 40, 1801–1820, 2001

Levizzani, V., Bauer, P., and Turk, F. J. (Eds.): Measuring Precipitation from Space: EURAINSAT and the Future, Advances in Global Change Research, Volume 28, Springer, Dordrecht, The Netherlands, 748 pp., 2007.

Lorenc, A. C.: Development of an operational variational assimilation scheme, J. Meteorol. Soc. Jpn, vol. 75, no. 1B, pp. 339–346, 1995.

Marzano F.S. and G. Visconti, Eds., Remote sensing of atmosphere and ocean from space: models, instruments and techniques, Advances in Global Change Research series, Kluwer Acad. Plub., Dordrecht (NL), ISBN 1-4020-0943-7, pp. 246, 2002

Marzano F.S., D. Cimini, T. Rossi, D. Mortari, S. Di Michele and P. Bauer: High-repetition Millimeter-wave Passive Remote Sensing of Humidity and Hydrometeor Profiles from Elliptical Orbit Constellations, J. Appl. Meteor and Climat., ISSN: 1558-8424, DOI: 10.1175/2010JAMC2329.1, vol. 49, pp. 1454–1476, 2010.

Marzano F.S., G. Rivolta, E. Coppola, B. Tomassetti and M. Verdecchia: Rainfall Nowcast from Multi-Satellite Passive Sensor Images using Recurrent Neural Network, IEEE Trans. Geosci. Rem. Sensing, ISSN: 0196-2892, n. 45, pp. 3800-3812, 2007.

Marzano F.S., M. Lamantea, M. Montopoli, M. Herzog, H. Graf. And D. Cimini: Microwave remote sensing of Plinian eruption due to the Grímsvötn Icelandic volcano on May 2011, ISSN: 0034-4257, Rem. Sens. Env., vol. 129, pp. 168–184, 2013.

Marzano, F. S., Mugnai, A., Panegrossi, G., Pierdicca, N., Smith, E. A., and Turk, F. J.: Bayesian estimation of precipitating cloud parameters from combined measurements of spaceborne microwave radiometer and radar, IEEE Trans. Geosci. Remote Sens., 37, 596–613, 1999.

Marzano, F. S., Palmacci, M., Cimini, D., Giuliani, G., and Turk, F. J.: Multivariate statistical integration of satellite infrared and microwave radiometric measurements for rainfall retrieval at the geostationary scale, IEEE Trans. Geosci. Remote Sens., 42, 1018–1032, 2004.

Montopoli M., D. Cimini, M. Lamantea, M. Herzog, H. Graf and F.S. Marzano, “Microwave radiometric remote sensing of volcanic ash clouds from space: model and data analysis”, IEEE Trans. Geosci. Remote Sens., ISSN: 0196-2892, vol. 51, n. 9, pp. 4678-4691, 2013.

Mugnai A., E.A. Smith, G. J. Tripoli, B. Bizzarri, D. Casella, S. Dietrich, F. Di Paola, G. Panegrossi, and P. Sanò: CDRD and PNPR satellite passive microwave precipitation retrieval algorithms: EuroTRMM/EURAINSAT origins and H-SAF operations, Nat. Hazards Earth Syst. Sci., 13, 887–912, 2013.

Mugnai, A., Smith, E. A., and Tripoli, G. J.: Foundations for statistical – physical precipitation retrieval from passive microwave satellite measurements, Part II: Emission source and generalized weighting function properties of a time dependent cloud – radiation model, J. Appl. Meteor., 32, 17–39, 1993.

Olson, W. S., C. D. Kummerow, G. M. Heymsfield, and L. Giglio, A method for combined passive-active microwave retrievals of cloud and precipitation parameters, J. Appl. Meteorol., 35, 1763–1789, 1996.

Polverari, F., F. S. Marzano, L. Pulvirenti, N. Pierdicca, S. M. Hristova-Veleva, F. J. Turk, “Modeling ocean wave surface to simulate spaceborne scatterometer observations in presence of rain," in 2015 IEEE International Geoscience and Remote Sensing Symposium (IGARSS), pp.1203-1206, Jul. 26 – 31, 2015, Milan, Italy, doi: 10.1109/IGARSS.2015.7325988

Portabella, M., and Stoffelen, A., “Rain detection and quality control of SeaWinds, ” J. Atm. and Ocean Techn., vol. 18, n. 7, pp. 1171-1183, 2001

Prata, A. J., I. J. Barton, R. W. Johnson, K. Kamo, and J. Kingwell: Hazard from volcanic ash. Nature, 354, 25, 1991.

Reed P.M., N.W. Chaney, J.D. Herman, M.P. Ferringer and E.F. Wood: Internationally coordinated multi-mission planning is now critical to sustain the space-based rainfall observations needed for managing floods globally, Environ. Res. Lett., 10, doi:10.1088/1748-9326/10/2/024010, 2015

Rodgers, C.D. 2000 Inverse methods for atmospheric sounding. Theory and practice. Series on Atmospheric, oceanic and planetary physics, Vol. 2. World Scientific, Singapore, New Jersey, London, Hong Kong, pp.238.

Rose, W.I., G. J. S. Bluth, and G. G. J. Ernst, 2000: Integrating retrievals of volcanic cloud characteristics from satellite remote sensors: A summary. Philos. Trans. Roy. Soc. London, A358, 1538–1606, 2000.

Ruf, C.S.: Detection of calibration drifts in spaceborne microwave radiometers using a vicarious cold reference, IEEE Trans. Geosci. Remote Sens., vol. 38, no. 1, pp. 44–52, Jan. 2000.

Seemann S.W., J. Li, W.P. Menzel, and L.M. Gumley: Operational Retrieval of Atmospheric Temperature, Moisture, and Ozone from MODIS Infrared Radiances, J. Appl. Met., vol. 42, 1072-1091, 2003.

Smith, E. A., Mugnai, A., Cooper, H. J., Tripoli, G. J., and Xiang, X.: Foundations for statistical – physical precipitation retrieval from passive microwave satellite measurements, Part I: Brightness temperature properties of a time dependent cloud – radiation model, J. Appl. Meteor., 31, 506–531, 1992.

Sparks, R. S. J., M. I. Bursik, S. N. Carey, J. S. Gilbert, L. Glaze, H. Sigurdsson, and W. Woods: Volcanic Plumes. Wiley and Sons, 574 pp, 1997

Hristova-Veleva, S., P. Callahan, R. Dunbar, B. Stiles, S. Yueh, J. Huddleston, S. Hsiao, G. Neumann, B. Vanhoff, R. Gaston, E. Rodriguez, D. Weissman, “Revealing the winds under the rain. Part I: Passive microwave rain retrievals using a new observation-based parameterization of subsatellite rain variability and Intensity-Algorithm description,” J. Appl. Meteor. Climatol., vol. 52, pp. 2828–2848, 2013. doi: 10.1175/JAMC-D-12-0237.1

Surussavadee, C. and Staelin, D. H.: Global millimeter-wave precipitation retrievals trained with a cloud-resolving numerical weather prediction model, Part I: Retrieval design, IEEE Trans. Geosci. Remote Sens., 46, 99–108, 2008.

Tapiador F.J., C. Kidd, K.L. Hsu, and F.S. Marzano, “Neural Networks in Satellite Rainfall Estimation”, Meteorological Applications, ISSN: 1350-4827, DOI:10.1017/S1350482704001173, vol. 11, pp 83-91, 2004b.

Tapiador, F. J., C. Kidd, V. Levizzani, and F.S. Marzano: A neural networks-based PMW-IR fusion technique to derive half hourly rainfall estimates at 0.1° resolution, J. Appl. Meteor., ISSN: 0894-8763, vol. 43, pp. 576-594, 2004a.

Turk, F. J., Rohaly, G. D., Hawkins, J., Smith, E. A., Marzano, F. S., Mugnai, A., and Levizzani, V.: Meteorological applications of precipitation estimation from combined SSM/I, TRMM and infrared geostationary satellite data, in: Microwave Radiometry and Remote Sensing of the Earth’s Surface and Atmosphere, edited by: Pampaloni, P. and Paloscia, S., VSP Int. Sci. Publ., Zeist, The Netherlands, 353–363, 2000.

Ulaby F.T. and D.G. Long., Microwave Radar and Radiometric Remote Sensing, University of Michigan Press, Ann Arbor (USA), ISBN: 978-0-472-11935-6, pp. 984, 2014.

Viltard, N., Burlaud, C., and Kummerow, C. D.: Rain retrieval from TMI brightness temperature measurements using a TRMM PR– based database, J. Appl. Meteorol. Climatol., 45, 455–466, 2006.

Wilheit, T. T., Chang, A. T. C., Rao, M. S. V., Rodgers, E. B., Theon, J. S., 1977: A satellite technique for quantitatively mapping rainfall rates over the ocean. J. Appl. Meteor., 16, 551-560.

Zehner, C. (Ed.): Monitoring volcanic ash from space. Proceedings of the ESA-EUMETSAT workshop on the 14 April to 23 May 2010 eruption at the Eyjafjoll volcano, South Iceland. Frascati, Italy, 26–27 May 2010. http://dx.doi.org/10.5270/atmch-10-01 (ESA-Publication STM-280), 2010.

6.4 Applications of MWI-ICI

6.4.1 Numerical weather prediction

Microwave imager data have been exploited in numerical weather prediction (NWP) data assimilation systems since 1997 (Gérard and Saunders, 1999), using the 'classical' low frequency imager channels at 19, 22, 37 and 85 GHz from the SSM/I series of instruments (Hollinger et al, 1999). Early schemes relied on a pre-processing step to derive total column water vapour (TCWV) and ocean surface wind speed from measured brightness temperatures (Phalippou et al., 1996). These derived estimates were subsequently assimilated in variational systems. Most current operational schemes assimilate radiances directly, using observation operators in the form of fast radiative transfer models to map between model state and measured brightness temperatures.

6.4.1.1 MWI for Numerical Weather Prediction

The benefits of the imager data for NWP have been both *indirect,* through the provision of analysed sea ice data, and *direct,* through the improvement of wind, temperature and moisture analyses and forecasts resulting from the assimilation of radiance data. The primary impact has been to provide observational constraints on lower tropospheric humidity over ocean, for which the surface emissivity is relatively well characterised, as well as improved analyses of wind fields through tracer advection effects (Peubey and McNally (2009) and Geer et al. (2014)). The evolution of the treatment of '*classical*' microwave imager data, and the impacts on atmospheric humidity analyses is traced in a series of publications based on work at ECMWF during the period 1997-present (Gérard and Saunders (1999), Mahfouf et al. (2005), Anderson et al. (2007), Kelly et al. (2008), Bauer et al. (2010), Geer et al. (2010a, 2014)). These publications chart a steady evolution from the assimilation of derived products (TCWV and ocean surface wind speed) in clear sky skies, through radiance assimilation in clear skies, to the assimilation of derived products in cloudy and precipitating scenes, and eventually to the *all-sky* assimilation of microwave imager radiances.

This application has been the focus of significant effort over the last two decades and increasingly sophisticated systems have been implemented at operational NWP centres. Current *state-of-the-art* is represented by the *all-sky* assimilation of microwave imager radiances at ECMWF. Initial development of the system used low frequency (<37 GHz) channels, but recent work has successfully extended the scheme to 183 GHz water vapour sounding channels available from humidity imager/sounder instruments (MHS and SSMI/S, Geer et al. (2014)), relevant to the planned capabilities of MWI. Key features of the scheme are: a fast radiative transfer model (RTTOV-SCATT, Bauer et al. (2006)) that accounts for absorption and scattering by hydrometeors; linearised moist physical schemes (Janiskova and Lopez (2013)) that map between model prognostic variables and state variables required by the observation operator (*i.e.* hydrometeor mass concentrations); a symmetric observation error model which inflates errors (*i.e.* down weights observations) progressively in scattering scenes (Geer and Bauer, (2011)) ; calling the observation operator at model grid points to avoid interpolation problems with highly spatially variable hydrometeor fields; and the averaging of observations to reduce representativeness errors and data volumes whilst improving noise performance.

Synchronously with these scientific developments, the constellation of satellites providing microwave imager data has grown substantially. In addition to the SSM/I series (F-08 - F-15 spanning 1987-present) new sources of data have become available from the SSMI/S series (F-

16 - F-19, spanning 2003-present); the TMI instrument of the TRMM mission (1997-2015); AMSR-E on NASA's Aqua satellite (2002-2011); AMSR-2 on JAXA's GCOM-W mission (2012-present); GMI forming part of Global Precipitation Mission (2014-present); Winsdat on the Coriolis mission (2003-present); and MWRI on the FY-3 series (2008-present). Most of these new sources of data have been exploited at NWP centres (Bell et al. (2008), Kazumori et al. (2014), Geer et al. (2008)). The field remains active and research continues with the aim to extract further benefit from the imager data, both through improvements in spatial-temporal coverage and by more sophisticated use of the data over land, and in cloudy and precipitating scenes.

Considering the larger channel set available from MWI, the closest available analogue is the SSMI/S series of instruments which include a suite of temperature sounding channels in the 50-60 GHz range, with sensitivities spanning the troposphere to mesosphere, a suite of three humidity sounding channels centred on 183 GHz, and an additional window channel at 150 GHz. Efforts to fully exploit the SSMI/S data - by extending schemes to use data over land; to explore synergies between sounding and imaging channels; to exploit the dual polarisation of the imager channels; and to exploit the data in cloudy and precipitating areas, have been hampered by the complex bias characteristics of the data (more below), nevertheless significant progress has been made. Geer et al. (2014) report large benefits from the extension of the *all-sky* scheme, initially developed for classical imager channels, to 183 GHz humidity sounding channels for both imaging and sounding instruments. Baordo et al. (2012, 2013, 2016) report progress on a scheme for assimilating SSMI/S data over land using a dynamic estimation of emissivity. Progress has also been reported on using physically based retrievals (1D-Var) of land surface emissivity for temperature sounding channels prior to the main assimilation – initially tested for 50 GHz channels from cross-track sounders (Newman et al., 2015), but extendable to observations from conical scanning instruments, and to higher frequencies.

Recent work at the Met Office and Météo-France on the assimilation of 183 GHz observations from the Megha-Tropiques SAPHIR mission (Chambon et al. (2015)) has highlighted the synergistic benefits of sounding and imaging channels (Newman et al., 2015), and continued studies on this instrument is expected to further improve the science base for the exploitation of MWI.

The exploitation of the 118 GHz channel suite is less mature. These observations have been available from the FY-3C Microwave Humidity Sounder-2 (MWHS-2) since 2013, and observations at 118 (and 183) GHz were introduced into the ECMWF operational model in April 2016, using the *all-sky* approach (Lu et al., 2015). Significant progress is expected in the exploitation of 118 GHz channels, over land and ocean, prior to the launch of Metop-SG MWI.

To date, many microwave imaging instruments have suffered from brightness temperature biases resulting from a variety of mechanisms. These have included: reflector emission effects for SSMI/S (Bell et al. (2008), TMI (Geer et al., 2008), AMSR-E and SSM/I; solar intrusion effects on the warm calibration load; and radio frequency interference. Consequently, new features designed to mitigate these biases have been incorporated into more recently launched imagers, including the GPM-GMI. The detailed evaluation from this mission should yield new insights into current *state-of-the art* performance which will serve as a baseline for MWI, and inform the development of bias correction strategies to support the exploitation of MWI at NWP centres.

Biases in first guess departures can also arise from errors in the forward modelling of observed radiances. Despite the apparent simplicity of clear sky radiative transfer in the 19-183 GHz region of the microwave spectrum, several improvements have been made in recent years to the underlying spectroscopy of O_2 and H_2O at 50 GHz and 22 GHz (Tretyakov (2009) and Lillegren et al (2005)) respectively. The accuracy of spectroscopic parameters, and indeed of current line shape models, for line absorption at 183 GHz has been brought into question recently (Brogniez et al., 2016) and progress is expected in this area in the near future. The accuracy of radiative transfer and spectroscopy of the 118 GHz O_2 line remains to be critically evaluated, although initial studies indicate airmass dependent biases in the FY-3C MWHS-2 118 GHz channels, consistent with deficiencies in spectroscopic parameters (Lu et al., 2015). These issues are discussed in more detail in Section 5.1.

6.4.1.2 Developing the MWI science base for NWP

Developments of MWI science base for NWP will be rather straightforward given the strong heritage of similar instruments that have been assimilated operationally in weather centres. As stated in the previous section new instruments are becoming available (GMI on GPM-Core, MWHS-2 on FY-3C, AMSR-2 on GCOM-W1, …) that will help to prepare the use of MWI in data assimilation systems by examining challenging issues that remain to be addressed (increased usage over land, sea-ice and snow; improved extraction of cloud information from the high frequency channels such as 118 and 183 GHz, …).

6.4.1.3 ICI for Numerical Weather Prediction

The ICI instrument has no heritage in terms of use for NWP. As a consequence, efforts should be put on it to examine how to extract useful information for improving numerical forecasts. First, a version of the fast radiative transfer model RTTOV needs to be adapted to the new frequencies of ICI. Information content studies need to be undertaken in the NWP context to confirm the interest of this new instrument for atmospheric and surface parameters. The absence of a similar spaceborne instrument will require to perform OSSEs experiments (Hoffman and Atlas, 2016) and to use airborne instruments (like ISMAR) in order to examine the impact of ICI in the NWP context.

The sensitivity of this instrument to cloud ice requires progress regarding the assimilation of all-sky radiances in NWP models, not only in global systems but also in regional ones. Indeed, microphysical properties and dynamical motions are resolved with much more details in non-hydrostatic convective scale models. The level of details regarding the description of hydrometeor properties (number of species, number of prognostic variables for the moments of the particle size distribution) in the cloud scheme has to be compatible with the one given in the radiative transfer model chosen to simulate the TBs. The differences between the satellite pixel (16 km) and the grid mesh of convective scale models (1 km) need to be addressed in the observation operator, projecting the model information into the observation space, in order to address the aggregation/disaggregation processes in a consistent manner (Duffourg et al., 2010). In terms of geographical locations, emphasis could be put on high latitudes where the satellite revisit will increase, and where the scientific community will focus in the coming years (WWRP PPP and YOPP). Regarding the developments of NWP assimilation schemes themselves, although all major NWP centres currently use variational schemes, to solve the solve the analysis problem, work in underway to use ensemble based assimilation schemes (such as Ensemble Kalman Filters (EnKF) or Ensemble Variational (EnVar)) in order to compute flow dependent error statistics of the a priori information (short-range forecast)

(Desroziers et al., 2014). Ensemble techniques should allow the extension of the control vector, in order to initialise on top of temperature, wind, pressure and water vapour, cloud and precipitation condensates (Chambon et al. 2013). This shall lead to an implicit coupling between the model prognostic variables (in particular between hydrometeor concentrations and dynamical variables) and also to extract in a more natural way the information contained in all-sky microwave TBs, in particular the ones from ICI.

6.4.2 Climate

The ice water path is an essential climate variable that is highly uncertain. No observations exist to date from which is possible to derive accurate global estimates of this climate variable which hinders the ability of numerical climate models to fully represent the radiative and dynamic effects of ice clouds (Buehler et al. 2012). ICI will provide this kind of observation with global coverage and therefore improve the initialization of three-dimensional clouds.

The expected improvements in representation of the atmospheric processes from use of ICI observations will contribute to refine climate modelling, in particular the Earth radiative balance. Thus, a particularly important aim of ICI is the provision of measurements related to ice cloud products, supporting the validation of the representation of ice clouds in climate models. This is not only relevant from the hydrological point of view, but is also very relevant for their impact on the Earth’s radiation budget.

6.4.3 Hydrology

Precipitation is a major component of the global water and energy cycle, helping to regulate the climate system. Moreover, the availability of fresh water is vital to life on Earth. Measurement of global precipitation through conventional instrumentation uses networks of rain (or snow) gauges and, where available, weather radar systems. However, the global distribution of these is uneven: over the land masses the distribution and density of gauges is highly variable with some regions having “adequate” coverage while others have few or no gauges. Over the oceans few gauges exist, and those located on islands might be subject to local influences and therefore not representative of the surrounding ocean. The availability of historical precipitation data sets can also be problematic, varying in availability, completeness and consistency as well availability for near real-time analysis.

The usability of satellite-derived products relies upon the data being available in real time (or very near real time). Precipitation products, such as the Global Precipitation Climatology Project (GPCP) monthly precipitation analysis (e.g. Adler et al. 2003), have been used for a range of applications including flood and landslide prediction and drought monitoring. The effective use of satellite precipitation estimates for hydrological and water resource applications (e.g. Sorooshian et al., 2009; Hossain and Anagnostou, 2004). It is very much dependent upon the type of application and the accuracy, spatial resolution, temporal resolution and latency of the estimates: different applications have different data requirements (Levizzani et al., 2007).

Hydrological requirements for precipitation estimates can be divided into two main categories: high resolution/short-duration estimates and lower resolution/ longer term estimates. Flash flood events, with rapid catchment response necessitate fine spatial and temporal scales together with timely delivery of the estimates. The availability of observations at 4×4 km every 15 min is available from some of the GEO satellites, with the potential for 1×1 km, 1 min imagery in rapid scan mode. However, due to the indirect nature of the cloud-top to surface rainfall relationship such estimates are subject to error (e.g., Scofield and Kuligowski, 2003). In this respect, both MWI and ICI are expected to provide more accurate and frequent precipitation estimates to be coupled with GEO satellite infrared passive measurements (e.g., Marzano et al., 2004) and to be ingested into runoff models with their uncertainty (e.g., Hossain and Huffman, 2008).

Fluvial flooding and water resources are characterised by relatively long lead times, therefore satellite derived precipitation products can be of great benefit. Static surface parameters (e.g., geology, soil type, relief), dynamic surface parameters (e.g., soil moisture, vegetation, groundwater) as well as the precipitation (satellite and surface) and meteorological/climatological conditions can be brought together on a global scale to provide a comprehensive hydro-meteorological data base where MWI and ICI products can play a relevant role due to the operational planning of the EPS-SG missions over more than a decade.

6.4.4 References

Adler, R., G. Huffman, A. Chang, R. Ferraro, P. Xie, J. Janowiak, B. Rudolf, U. Schneider, S. Curtis, D. Bolvin, A. Gruber, J. Susskind, P. Arkin, and E. Nelkin, 2003: The Version-2 Global Precipitation Climatology Project (GPCP) Monthly Precipitation Analysis (1979–Present). J. Hydrometeor., **4**, 1147–1167, doi: 10.1175/1525-7541(2003)004<1147:TVGPCP>2.0.CO;2

Andersson, E., E. Holm, P. Bauer, A. Beljaars, G. A. Kelly, A. P. McNally, A. J. Simmons, J.-N. Thepaut, and A. Tompkins (2007). Analysis and forecast impact of the main humidity observing systems. Quart. J. Roy. Meteorol. Soc. 133, 1473–1485.

Baordo, F., A. J. Geer, and S. English (2012). SSMI/S radiances over land in the all-sky framework: one year report. EUMETSAT/ECMWF Fellowship Programme Research Report No. 27, available from http://www.ecmwf.int.

Baordo, F., A. J. Geer, and S. English (2013). All-sky assimilation of SSMI/S humidity sounding channels over land: second year report. EUMETSAT/ECMWF Fellowship Programme Research Report No. 30, available from http://www.ecmwf.int

Baordo, F. and Geer, A. J. (2016), Assimilation of SSMIS humidity-sounding channels in all-sky conditions over land using a dynamic emissivity retrieval. Q.J.R. Meteorol. Soc., 142: 2854-2866. doi:10.1002/qj.2873

Bauer, P., A. J. Geer, P. Lopez and D. Salmond (2010), Direct 4D-Var assimilation of all-sky radiances. Part I: Implementation, Quarterly Journal of the Royal Meteorological Society, Volume 136, Issue 652, pages 1868–1885, October 2010 Part ADOI: 10.1002/qj.659.

Bauer, P., E. Moreau, F. Chevallier, and U. O'Keeffe (2006). Multiple-scattering microwave radiative transfer for data assimilation applications. Quart. J. Roy. Meteorol. Soc. 132, 1259–1281

Bell W, Candy B, Atkinson N, Hilton F, Baker N, Bormann N, Kelly G, Kazumori M, Campbell W, Swadley S. 2008. The assimilation of SSMIS radiances in numerical weather prediction models. IEEE Trans. Geosci. Remote Sensing 46: 884–900.

Brogniez H., English S., Mahfouf J.-F., Behrendt A., Berg W., Boukabara S., Buehler S. A., Chambon P., Gambacorta A., Geer A., Ingram W., Kursinski E. R., Matricardi M., Odintsova T. A., Payne V. H., Thorne P. W., Tretyakov, M. Y., Wang J., 2016. A review of sources of systematic errors and uncertainties in observations and simulations at 183 GHz, Atmos. Meas. Tech., 9, 2207-2221. doi:10.5194/amt-9-2207-2016.

Buehler, S. A., E. Defer, F. Evans, S. Eliasson, J. Mendrok, P. Eriksson, C. Lee, C. Jimenez, C. Prigent, S. Crewell, Y. Kasai, R. Bennartz, and A. J. Gasiewski, "Observing ice clouds in the submillimeter spectral range: the CloudIce mission proposal for ESA's Earth Explorer 8", Atmos. Meas. Tech., 5, 1529–1549, (2012).

Chambon, P., S. Q. Zhang, A. Y. Hou, M. Zupanski, and S. Cheung, 2013: Assessing the impact of pre-GPM microwave precipitation observations in the Goddard WRF ensemble data assimilation system. Quart. J. Roy. Meteor. Soc., 140, 1219-1235. Doi: 10.1002/qj.2215

Desroziers, G., J.-T. Camino, and L. Berre. 2014: 4DEnVar: link with weak-constraint 4D-Var and different possible implementations. Quart. J. Roy. Met. Soc.,140, 2097–2110, 2014

Duffourg F., Ducrocq V., Fourrié N., Jaubert G., Guidard V., 2010. Simulation of satellite infra-red radiances for convective-scale data assimilation over the Mediterranean. J. Geophys. Res. Atmos. doi :10.1029/2009JD012936

Geer AJ, Bauer P, Bormann N. (2008). Solar biases in microwave imager observations assimilated at ECMWF. IEEE Trans. Geosci. Remote Sens. 48: 2660–2669.

Geer, A. J. and F. Baordo (2014). Improved scattering radiative transfer for frozen hydrometeors at microwave frequencies. Atmos. Meas. Tech. 7, 1839–1860.

Geer, A. J. and P. Bauer (2010): Enhanced use of all-sky microwave observations sensitive to water vapour, cloud and precipitation. Published simultaneously as ECMWF Technical Memoranda 620 and ECMWF/EUMETSAT fellowship reports 20.

Geer, A. J. and P. Bauer (2011). Observation errors in all-sky data assimilation. Quart. J. Roy. Meteorol. Soc. 137, 2024–2037.

Geer, A. J., F. Baordo, N. Bormann and S. English (2014), All-sky assimilation of microwave humidity sounders, ECMWF Technical Memorandum 741, November 2014, http://www.ecmwf.int/sites/default/files/elibrary/2014/9507-all-sky-assimilation-microwave-humidity-sounders.pdf

Geer, A. J., P. Bauer, and C. W. O'Dell (2009). A revised cloud overlap scheme for fast microwave radiative transfer. J. App. Meteor. Clim. 48, 2257–2270.

Geer, A. J., P. Bauer, and P. Lopez (2010). Direct 4D-Var assimilation of all-sky radiances: Part II. Assessment. Quart. J. Roy. Meteorol. Soc. 136, 1886–1905.

Gérard, E. and R. Saunders (1999). Four-dimensional variational assimilation of Special Sensor Microwave / Imager total column water vapour in the ECMWF model. Quart. J. Roy. Meteorol. Soc. 125, 3077–3102.

Hoffman R. N., and R. Atlas, 2016: Future Observing System Experiments. Bull. Amer. Met. Soc., 97,1601-1616, doi:10.1175/BAMS-D-15-00200.1

Hollinger J. P., J. L. Peirce, and G. A. Poe, "SSM/I instrument evaluation", IEEE Trans. Geosci. Remote Sensing, vol. 28, pp. 781-790, 1990

Hossain, F., Anagnostou, E. N., and Dinku, T.: Sensitivity analyses of satellite rainfall retrieval and sampling error on flood prediction uncertainty, IEEE T. Geosci. Remote, 42, 130–139, 2004.

Hossain, F. and Huffman, G.: Investigating error metrics for satellite rainfall data at hydrologically relevant scales, J. Hydrometeorol., 9, 563–575, 2008.

Janiskova, M. and P. Lopez (2013). Linearized physics for data assimilation at ECMWF. In Data Assimilation for Atmospheric, Oceanic and Hydrologic Applications (Vol. II), pp. 251–286. Springer

Kazumori, M., A. J. Geer, and S. J. English (2014). Effects of all-sky assimilation of GCOM- W1/AMSR2 radiances in the ECMWF system. Quart. J. Roy. Meteorol. Soc., in preparation, available as ECMWF technical memorandum 732.

Kazumori, M. and S. J. English (201). Use of the ocean surface wind direction signal in microwave radiance assimilation. Quart. J. Roy. Meteorol. Soc., , 141, 1354-1375. Doi:10.1002/qj.2445

Kelly, G. A., P. Bauer, A. J. Geer, P. Lopez, and J.-N. Thépaut (2008). Impact of SSM/I observations related to moisture, clouds and precipitation on global NWP forecast skill. Mon. Weather Rev. 136, 2713–2726.

Levizzani V., P. Bauer, and F. J. Turk, Eds., Measuring precipitation from space – EURAINSAT and the future. Springer, 2007.

Lu,Q., H. Lawrence, N. Bormann, S. English, K. Lean, N. Atkinson, W. Bell, F. Carminati, An evaluation of FY-3C satellite data quality at ECMWF and the Met Office, ECMWF Tech Memo 767, November 2015.

Mahfouf, J-F, Bauer P and Marécal V (2005). The assimilation of SSM/I and TMI rainfall rates in the ECMWF 4D-Var system. Q. J. R. Meteorol. Soc. 131: 437 – 458, doi: 10.1256/qj.04.17

Marzano F.S., M. Palmacci, G. Giuliani, D. Cimini, and J. Turk, "Multivariate statistical integration of satellite infrared and microwave radiometric measurements for rainfall retrieval at the geostationary scale", IEEE Trans. Geosci. Rem. Sens., ISSN: 0196-2892, vol. 42, n. 4, pp. 1018-1032, 2004.

Newman, S, and W. Bell (2015), Enhanced use of AMSU-A over land, ITSC-20, Wisconsin, https://cimss.ssec.wisc.edu/itwg/itsc/itsc20/program/PDFs/30Oct/session10b/10p_04_newman.pdf

Peubey, C. and A.P. McNally (2009). Characterization of the impact of geostationary clear-sky radiances on wind analyses in a 4D-Var context, Quarterly Journal of the Royal Meteorological Society, Volume 135, Issue 644, pages 1863–1876, October 2009 Part A.

Phalippou, L. (1996). Variational retrieval of humidity profile, wind speed and cloud liquid-water path with the SSM/I: Potential for numerical weather prediction, Quarterly Journal of the Royal Meteorological Society, Volume 122, Issue 530, January 1996 Part B, Pages: 327–355, Article first published online : 15 DEC 2006, DOI: 10.1002/qj.49712253002

Scofield, R. A. and Kuligowski, R. J.: Status and outlook of operational satellite precipitation algorithms for extreme precipitation events, Weather Forecast., 18, 1037–1051, 2003

Sorooshian, S., Hsu, K.-L., Coppola, E., Tomassetti, B., Verdecchia, M., and Visconti, G.: Hydrological Modelling and the Water Cycle: Coupling the Atmospheric and Hydrological Models, Springer, Berlin, 291 pp., 2009.

6.5 List of Acronyms

Acronym	Meaning
AMSR-E	Advanced Microwave Scanning Radiometer - Earth Observing System
AMSU	Advanced Microwave Sounding Unit
ANN	artificial neural network
APD	A Priori Database
ATOVS	Advanced TIROS-N Operational Vertical Sounder
ATMS	Advanced Technology Microwave Sounder
BEAMCAT	Bernese Atmospheric Multiple Catalogue Access Tool
BRDF	bidirectional reflectance distribution function
Cal/Val	Calibration/Validation
CCA	Canonical Correlation Analysis
CCI	Climate change initiative
CMEM	Community Microwave Emission Modeling
CRTM	Community Radiative Transfer Model
DA	Data Assimilation
DDA	Discrete Dipole Approximation
DFS	Degrees of Freedom for Signal
DEIMOS	Airborne microwave radiometer (23.8 GHz and 50.3 GHz)
DEM	Digital Elevation Model
DMSP	Defence Meteorological Satellite Program
DTH	Dynamical thermodynamical hydrological
EarthCARE	Earth Clouds, Aerosol and Radiation Explorer
ECR	Essential Climate Record
ECMWF	European Centre for Medium-Range Weather Forecasts
EOF	Empirical Orthogonal Function
EPS	EUMETSAT Polar System
EPS-SG	EUMETSAT Polar System – Second Generation
ER	Entropy Reduction
ESA	European Space Agency
EUMETSAT	European Organisation for the Exploitation of Meteorological Satellites
EURD	EPS-SG End Users Requirements Document
FAAM	Facility for Airborne Atmospheric Measurements
FASTEM	FAST microwave Emissivity Model
FY	Feng Yun
GCOM-W	Global Change Observation Mission – Water (SHIZUKU)
GCOS	Global Climate Observing System
GDAS	Global Data Assimilation System
GEO	Geostationary Orbit
GMI	Global precipitation mission Microwave Imager
GNSS	Global Navigation Satellite System
GPM	Global Precipitation Mission
GRUAN	GCOS Reference Upper-Air Network
GSICS	Global Space-based Inter-Calibration System
HAMP	Microwave package on the High Altitude and LOng range research aircraft
HITRAN	High-resolution transmission molecular absorption database
HPBW	Half Power Beam Width

H-SAF	Hydrology Satellite Application Facility
HUT	Helsinki University of Technology
HyMEx	HYdrological cycle in the Mediterranean EXperiment
IASI	Infrared Atmospheric Sounder Interferometer
ICI	Ice Cloud Imager
IFOV	instantaneous-field-of-view
IOP	Intensive Operation Period
ISMAR	International Sub-millimetre Airborne Radiometer
IR	Infrared
IWP	Ice Water Path
JAXA	Japan Aerospace Exploration Agency
JPSS	Joint Polar System Satellite
LEO	Low Earth Orbit
LWP	Liquid Water Path
MADRAS	Microwave Analysis and Detection of Rain and Atmospheric Structures
MARSS	Microwave Airborne Radiometer Scanning System
MEMLS	Microwave Emission Model of Layered Snowpack
MHS	Microwave Humidity Sounder
MTG	Meteosat Third Generation
MPA	Multisatellite Precipitation Analysis
MWHS	Microwave Humidity Sounder
MWI	Microwave Imager
MWS	Microwave Sounder
MWRI	Microwave Radiation Imager
NASA	National Aeronautics and Space Administration
NCEP	National Center for Environmental Prediction
NOAA	National Oceanic and Atmospheric Administration
NRT	Near Real Time
NWC	Nowcasting
NWP	Numerical Weather Prediction
NWC SAF	Nowcasting Satellite Application Facility
NWP SAF	NWP Satellite Application Facility
OSI SAF	Ocean and Sea Ice Satellite Application Facility
OZA	Observation Zenith Angle
PDF	Probability Distribution Function
PSD	Particle Size Distribution
RFI	Radio Frequency Interference
RT	Radiative Transfer
RTM	Radiative Transfer Model
RTTOV	Radiative Transfer for TOVS
SAF	Satellite Application Facilities
SAG	Scientific Advisory Group
SAPHIR	Sounder for Probing Vertical Profiles of Humidity
SCA	Scatterometer (on EPS-SG platforms)
SIOV	Satellite In-Orbit Verification
SNO	Simultaneous Nadir Overpass
SSM/I	Special Sensor Microwave / Imager
SSMIS	Special Sensor Microwave Imager / Sounder

SMOS	Soil Moisture and Ocean Salinity (ESA mission)
SWE	Snow water equivalent
TB	Brightness Temperature
TCWV	Total Column Water Vapour
TESSEM2	Tool to Estimate Sea Surface Emissivity from Microwave to sub-Millimeter waves - 2
TELSEM2	Tool to Estimate the Land Surface Emissivity in the Microwaves - 2
TIGR	Thermodynamic Initial Guess Retrieval
TIR	Thermal Infrared
TMI	TRMM Microwave Imager
TOA	Top of Atmosphere
TPW	Total Precipitable Water
TRMM	Tropical Rainfall Measuring Mission
VCC	Vicarious cold calibration
VIS	Visible
WMO	World Meteorological Organization
WCRP GEWEX	World Climate Research Programme Global Energy and Water Cycle Experiment
WWRP PPP	World Weather Research Program - Polar Prediction Project
YOPP	Year of Polar Prediction